MATHEMATICAL OPTIMISATION OF DIVER ASCENT PROFILES AT A CONSTANT RISK OF DECOMPRESSION ILLNESS

A thesis submitted in partial fulfilment

of the requirements for the

Degree of Doctor of Philosophy

in

Computational and Applied Mathematics

by

B. J. Horn

University of Canterbury

2003

To my parents
for encouraging a love of learning

Acknowledgements

I wish to thank my supervisors Professor Graeme Wake (University of Canterbury) and Gavin Anthony (QinetiQ Alverstoke) for their encouragement and always being available for discussion, information and advice. I would also like to thank Dr. Chris Price for discussing the finer points of optimisation with me and Dr. Britta Basse for being a sounding board for ideas and sharing her MATLAB knowledge.

I would also like to gratefully acknowledge the research grant and information provided by QinetiQ Alverstoke that made the research possible.

This thesis would not have been completed without the never ending support and proof reading ability of my husband Clive who could always pick out the areas that needed clarification. As well as my kids who provided some light relief from the challenges of research.

Finally I would like to acknowledge the ladies of the UCSA Crèche, who welcomed my family into the crèche community and provided a supportive, safe and fun environment for my daughters that allowed me to finish this research.

Abstract

Divers use decompression schedules that provide a stepped ascent to the surface from their maximum depth to help prevent the occurrence of decompression illness. The risk of decompression illness resulting from these schedules varies across different dives and the models used to generate them. The diver is unaware of this variance in risk.

This thesis describes an investigation into the feasibility of producing optimised iso-probabilistic decompression schedules that minimise the time it takes for the diver to reach the surface from maximum depth. In particular, 1.3 bar constant partial pressure of oxygen in helium dives are considered. The US Linear Exponential Multi-gas (LEM) model is used to describe the risk of decompression illness for a given dive. The Sequential Quadratic Programming (SQP) method is used to minimise the ascent time given non-linear risk constraints and a maximum dive time constraint.

Two approaches to describing the ascent profile have been investigated. The first scheme finds the stop times at each possible stop depth to produce optimised schedules. The total time for decompression is a function of the sum of the stop times. The second scheme defines the ascent profile as a three parameter hyperbolic tangent equation. The SQP method finds the three parameters that produce optimised decompression schedules once the curve is converted to a schedule of decompression stops.

The schedules produced by the SQP method, using a curve to describe the ascent profile, show that it is feasible to produce optimised iso-probabilistic tables that are operationally practical given an acceptable physiological risk model. Comparison with the QinetiQ 90 tables with a nominal 2% operational risk of decompression illness show that the method could provide reductions in the ascent time subject to manned testing.

Table of contents

THIS PAGE IS INTENTIONALLY BLANK

Chapter 1

Introduction

1.1 Research aim

Underwater divers are subjected to changes in ambient pressure during dives that may result in decompression illness. To reduce the risk of occurrence of decompression illness specified ascent profiles are taken from the maximum depth of the dive to the waters surface. These ascent profiles are called decompression schedules. Traditionally decompression methods are not based on the risk of decompression illness. The decompression schedules resulting from these methods cover a wide range of risk values that are unknown to the diver using them.

The aim of this research is to test the feasibility of producing optimised decompression schedules where the definition of an optimised dive is:

A dive profile with the quickest ascent from maximum depth to the surface that will result in a specified risk of decompression illness.

A set of optimised decompression schedules would provide the diver with an iso-probabilistic decompression table set to a known risk of decompression illness.

The Diving and Life Support Systems Group at QinetiQ Alverstoke, UK, sponsored this research as part of their work on the production of decompression schedules. In particular this research is aimed at decompression schedules for rebreather breathing apparatus providing a constant 1.3 bar of oxygen in helium gas mix to the diver.

1.2 Diving terminology

Consider a typical dive. The diver leaves the surface and descends through the water. As the diver descends the weight of water above him increases the ambient pressure on the diver by approximately 1 bar for every 10 msw (metres of sea water) he descends. To maintain the divers lung volume, the pressure of the gas breathed by the diver must be equal to the ambient pressure exerted on the diver.

A diver breathes a mixture of gases under the water. The oxygen that is required by the body may be toxic at pressures greater than 1.6 bar [US Navy 1996a] so a diluent is used to ensure oxygen stays at a safe pressure. Common diluents are nitrogen and helium. Both these gases are not used in any body process when breathed in by the diver. The term *carrier* will be used to describe any nitrogen and/or helium present in the breathing loop or diver's body that originated from the diver breathing it in.

If the diver descends to his *maximum depth* for a given time and then ascends to the surface, without descending again, the dive is called a *bounce dive*. The time taken from leaving the surface at the start of the dive to starting to ascend from the maximum depth is called the *bottom time*. However if the bottom time of the dive is conducted over more than one depth once the initial descent is complete, the dive is called a *multi-level dive*. This work concentrates on bounce dives.

1.3 Decompression illness

"Decompression illness (DCI)", "decompression sickness (DCS)", "malady of the deep" and "the bends" are all names that have been given to illnesses resulting from a person undergoing a reduction in ambient pressure following a period of time at a higher pressure. Examples of this scenario are:

- A diver ascending from the maximum depth of a dive.
- A pilot flying an unpressurised aircraft.

- A tunnel or caisson worker who works in a pressurised environment during their shift and returns to surface pressure at the end of the shift.

The symptoms of decompression illness are wide ranging [Elliot & Moon 1995a, Francis & Gorman 1995]. From pain only symptoms such as skin rashes and joint, muscle or lymph gland pain to symptoms involving the nervous, respiratory and circulatory systems. The later symptoms include; fatigue, amnesia and personality changes, visual and hearing disturbances, paralysis or weak muscles and in extreme cases complete circulatory collapse, loss of consciousness and death.

Most cases of decompression illness can be treated to complete resolution by timely pressurisation in a hyperbaric chamber or by returning to the ground in the case of aviators. The many physiological drivers behind these varied symptoms are still being researched in an attempt to better understand them. However, it is generally accepted that excess carrier levels in the body on decompression are the cause. The formation of bubbles in the tissues and circulatory system drive some of the symptoms. Long term implications of compression and decompression such as hearing and bone problems have also been observed [McCallum & Harrison 1995, Elliot & Moon 1995b]. It is important to minimise the decompression stress on people to avoid both the short and long term results of decompression.

It is not possible to predict whether a given individual on a given day will result in decompression illness from a dive. There is variability in the incidence of decompression illness across people, time and dive type [Berghage et al 1974]. The same person may do a dive profile safely many times and then develop decompression illness from the same dive profile.

1.4 Reducing the risk of decompression illness

The safest way to prevent decompression illness is to not to subject people to a reduction in pressure. When this is not possible, the rate of decompression should be chosen to keep the decompression stress on the body at a safe level.

Consider the diver example in more detail. At sea level the ambient pressure exerted on the body by the air above it is approximately one bar. When a diver descends through a column of water the ambient pressure increases. According to Henry's Law the amount of gas that will dissolve in a liquid is directly proportional to the partial pressure of the gas. To see how the gases in the body tissues change during a dive consider the example air dive shown in Figure 1.1. The area of the outlined boxes at the bottom of the diagram represents the partial pressure of the carrier in a tissue when at equilibrium with the breathing gas at given depth. The grey area represents the current partial pressure of the carrier in solution in the tissue.

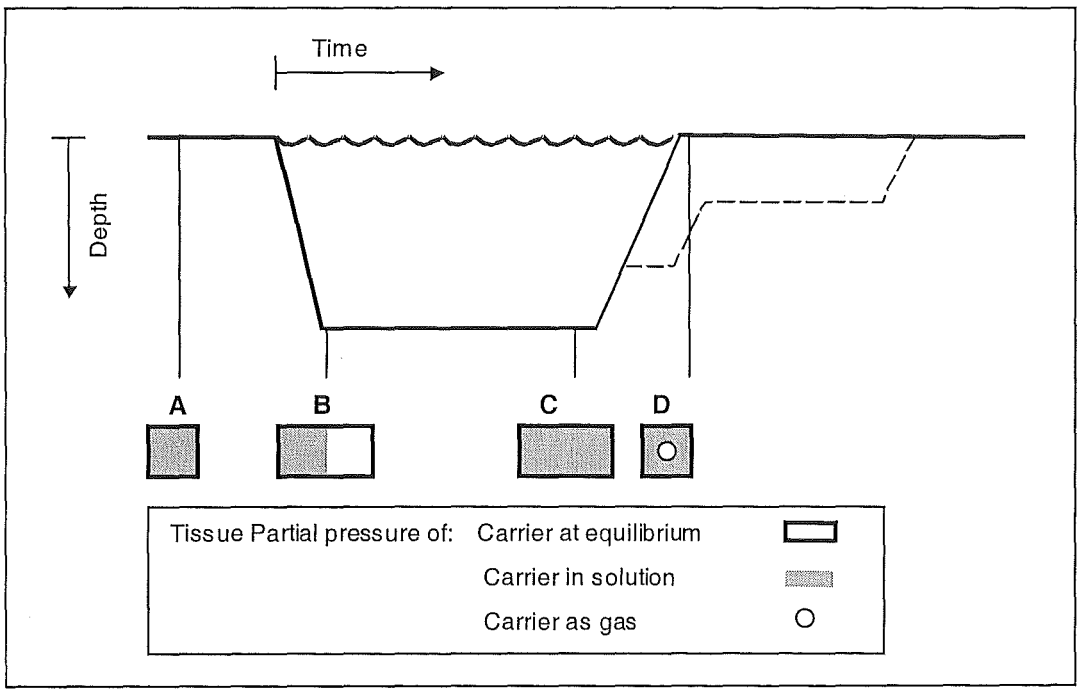

Figure 1.1 *Example of partial pressure of carrier in a tissue during a bounce dive. The dashed line represents an ascent profile containing decompression stops.*

Before the dive {A}, the carrier nitrogen in the body tissues of the diver is equilibrated with the amount of nitrogen supplied by the blood and all the nitrogen will be in solution.

When the diver descends in the water to his maximum depth {B}, the partial pressure of nitrogen in the breathing gas and therefore the arterial system will be higher than at the surface. The pressure gradient between the blood and the tissue along with Henry's Law means that more nitrogen can go in to solution in the tissue. If the diver stays at maximum depth long enough {C}, the nitrogen in the tissue will again equilibrate with the nitrogen in the arterial system.

If the diver then ascends to the surface {D} the ambient pressure is reduced, reversing the carrier pressure gradient between the blood and the tissues. The excess nitrogen in the tissues moves back into the blood stream where it can be removed from the body via the lungs. If the diver ascends at a rate at which the blood cannot remove the excess nitrogen, some of the excess nitrogen in the tissue may come out of solution in the form of bubbles.

To reduce the decompression stress and therefore the risk of decompression illness for the diver, the diver must ascend at a sufficiently slow rate that allows the excess nitrogen to be removed by the blood. Operationally this is accomplished by ascending to the surface in a number of steps called decompression stops, as shown by the dashed line in Figure 1.1. Divers obtain details of the required stops from a printed table of decompression schedules or from a dive computer that calculates the stops in real time and is carried by the diver.

1.5 Why are new decompression methods required for constant partial pressure of oxygen in helium apparatus?

New technologies are continually being introduced to the diving arena resulting in new underwater breathing apparatus. One example is rebreather apparatus that maintains the level of partial pressure of oxygen within a given small range of values during the dive. The advantages of maintaining a constant partial pressure of oxygen as opposed to breathing a constant fraction of oxygen are:

- A reduction in the risk of oxygen toxicity. This can result in convulsions and unconsciousness. A diver with these symptoms while under water would be in extreme danger. A constant fraction of oxygen will result in a partial pressure of oxygen that increases with depth. Apparatus that maintain a constant partial pressure of oxygen independent of the depth prevent the partial pressure of oxygen becoming too high.

- The higher the partial pressure of oxygen in a gas mix, the lower the partial pressure of the carrier will be.

  — During the bottom time of the dive, a lower partial pressure of carrier reduces the amount of carrier that will dissolve in the body tissues and therefore the excess levels of carrier during the ascent.

  — During decompression a lower partial pressure of carrier will increase the rate of washout of any excess carrier in the tissues.

Some of the current tables [Thalmann 1985, Nishi 1987] based on a constant fraction of oxygen in the gas mix or a lower partial pressure of oxygen could provide a safe decompression regime for 1.3 bar oxygen in helium dives. However the safety margin would be overly conservative. The decompression required for a given time at the bottom would be unnecessarily long.

Current table design involves a component of guesswork. A typical decompression table may contain decompression schedules for a hundred or more dive profiles. Such a number of schedules is impossible to test to any level of significance. The

tables are tested for a subset of dives for the specific equipment and dive types likely to be used. Parameters of the underlying model are tweaked if a dive trial is indicating high levels of decompression stress for some of the dive profiles. This means the models become specific to the dive type they are tested on and may not be applicable to equipment with different breathing gas characteristics, different diving environments or different maximum depths.

Ideally the risk boundary for a diver getting decompression illness or not getting decompression illness should be known. The lack of understanding of the mechanisms that cause the symptoms, the variability in dive outcomes and the ethical constraints on dive trials means that the risk boundary is not well defined. Until a general risk boundary can be defined, new decompression models must be generated for new equipment and diving scenarios. A new decompression model can be generated from existing models with new parameters or be a new model.

1.6 Scope of thesis

This thesis is written in two parts. Part one considers decompression models and their use in the generation of decompression schedules. Chapter 2 provides a brief overview of physiological and risk models that have been applied to decompression modeling in the past.

The only model available to the author that had been calibrated on constant 1.3 bar oxygen in helium dives was the US Linear Exponential Multiple gas model (LEM). This model is described and evaluated in chapter 4 using the data described in chapter 3.

In chapter 5 the LEM model is used to indicate the distribution of risk of decompression illness across published models applied to rebreather dives. This chapter highlights the need for constant risk decompression tables and discusses the question of what is an acceptable level of risk?

Part two of the thesis describes and evaluates methods to produce optimised decompression schedules using LEM for the underlying physiological risk model. Chapter 6 introduces the Sequential Quadratic Programming (SPQ) method for constrained optimisation and how it can be applied to the production of optimised decompression schedules.

Chapters 7, 8 and 9 describe two different implementations of the SQP method and the associated results. The best of these results are then compared to the latest 1.3 bar oxygen in helium decompression tables produced by QinetiQ Alverstoke. The comparisons are given in Chapter 10 along with the implications for producing an automated system for the production of iso-probabilistic decompression schedules.

1.7 Notation

Due to the range of disciplines and models the research covers, a large amount of notation is introduced. To help clarify the notation each chapter will start with a list of the notation used within it.

1.8 Caution

The decompression schedules given in this thesis have been produced to test the feasibility and possible advantages of optimised decompression methods. The schedules and associated methods have NOT been tested and SHOULD NOT BE USED FOR DIVING OPERATIONS without comprehensive testing.

Chapter 2

Decompression methods

2.1 Notation

ata	Atmospheres absolute	K	Gas exchange time constant
DCI	Decompression illness	P_{amb}	Ambient pressure
DT	Total dive time	P_j	Partial pressure of carrier j
msw	Metres of sea water	$\breve{P}_j$	Equivalent carrier partial pressure if all forced into solution
$P(DCI)$	Probability of decompression illness	P_{CO_2}	Partial pressure of carbon dioxide
SAC	Safe ascent criteria	P_{H_2O}	Partial pressure of water vapour
SAD	Safe ascent depth	P_{O_2}	Partial pressure of oxygen
$\#^A$	... in the blood supply	dQ/dt	Blood flow per unit tissue volume
$\#^T$	... in the tissue	r,z	polar coordinate axes
α	Solubility of carrier	R	Rate of arterial carrier partial pressure change
A,B	Gas flow constants	$\Re$	Instantaneous decompression stress dose
a	Radius of blood vessel	S	Measure of decompression stress
b	Radius of tissue cylinder	t	Time
c	Carrier concentration	Thr	Carrier pressure above ambient that is required form a bubble in tissue
C	Critical quantity of dissolved carrier	v_i	Logistic descriptive variables
d	Depth	V	Velocity of blood through capillary
D	Diffusion coefficient	$n, k, \beta, \gamma, \omega, \varphi, \phi$	Model constants

2.2 Introduction

This chapter introduces some published mathematical approaches for modelling the effect of decompression on divers during oxygen in helium dives and the resulting risk of decompression illness. Chapter 2 is included in the thesis to provide a brief background on decompression modelling for readers unfamiliar with diving research.

2.3 Overview of decompression methods

The aim of a decompression method is to bring divers to a reduced ambient pressure safely. A generic scheme for a decompression method is shown in Figure 2.1.

On the left side of Figure 2.1 is a list of possible inputs to the method. Some of these inputs are quantities that can be monitored in real time during the dive. Other inputs are not quantifiable or are historical in nature such as previous injuries to the diver.

The implementation of the methods described in the following sections use a subset of the possible inputs; time-pressure profile and the breathing gas. There is insufficient knowledge to include factors such as temperature, physical characteristics and stress into a decompression method in a realistic manner. Flook [1997] has researched the incorporation of exercise into a decompression model. Dive computers and tables may incorporate user instigated safer decompression profiles when the risk of decompression illness is thought to be increased by one or more of the possible inputs given in Figure 2.1 [Bühlmann 1995; Sunnto 1994]. One example is the US Navy [1996a] rule that states: "If the divers are exceptionally cold during the dive or if the workload is relatively strenuous select the next longer decompression schedule than the one that would normally be selected."

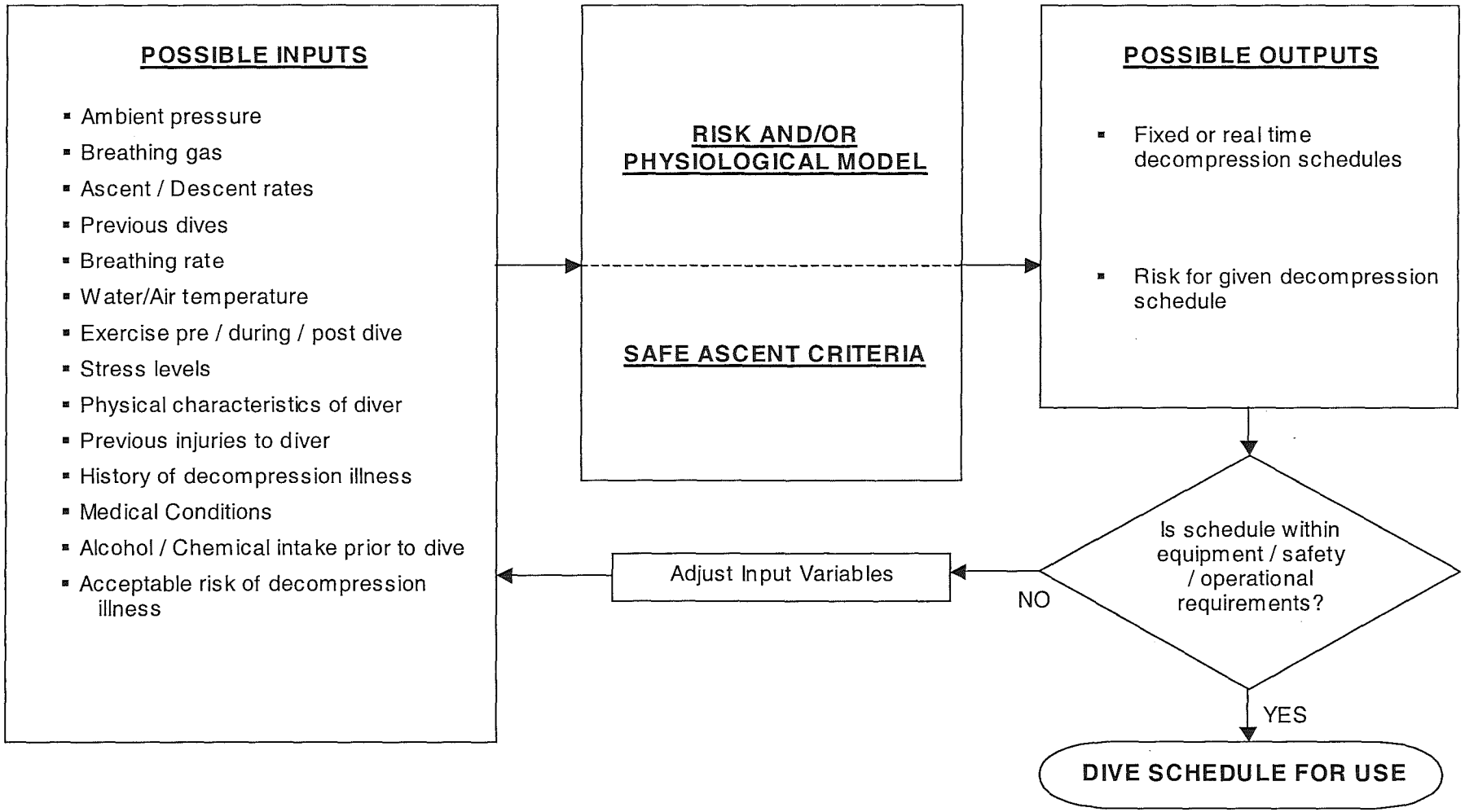

Figure 2.1 General schematic for decompression methods

The input data is used by the decompression model to develop a description of the decompression stress on the diver. Secondly, ascent rules are used to design the decompression depth-time schedule to be used for the divers decompression. The ascent rules are commonly called Safe Ascent Criteria (SAC). These methods have two possible outputs; the decompression schedule and an estimate of the risk of the diver getting decompression illness from the given dive schedule.

When a decompression schedule has been suggested it is important that the schedule is assessed to see that it meets the requirements of the diving situation. For example, a very safe dive schedule will be no good if the breathing apparatus will not provide enough gas to complete it.

2.4 Representing the dive

Consider a typical bounce, no decompression stop dive as shown by the solid line in Figure 2.2. The depth of the diver will vary during the dive, in turn changing the partial pressure of the gases the diver breathes. For the decompression model to process this information, the depth and gas profiles must be simplified. Two levels of simplification are currently used depending on whether a decompression table or dive computer is to be used.

A decompression table will provide the decompression schedule for a single maximum depth and bottom time, as represented by the dotted line in Figure 2.2 (a). This means the model will be assuming the diver stays at the maximum depth for the whole of the bottom time, which is unlikely to be true. Hence the tables tend to give a margin of safety due to the profile simplification. Sometimes the descent time to bottom depth for table calculation is taken to be near to zero time, to ensure all possible descent rates are included by the schedules time-depth profile.

Alternatively a dive computer will log the depth of the dive at short intervals during the dive and treat the dive as a series of steps. These can be linear splines as indicated by the dotted line in Figure 2.2 (b) or steps of constant depth. This means

the simplified profile could increase or reduce the margin of safety depending on the shape of the depth time profile and the depth sampling frequency.

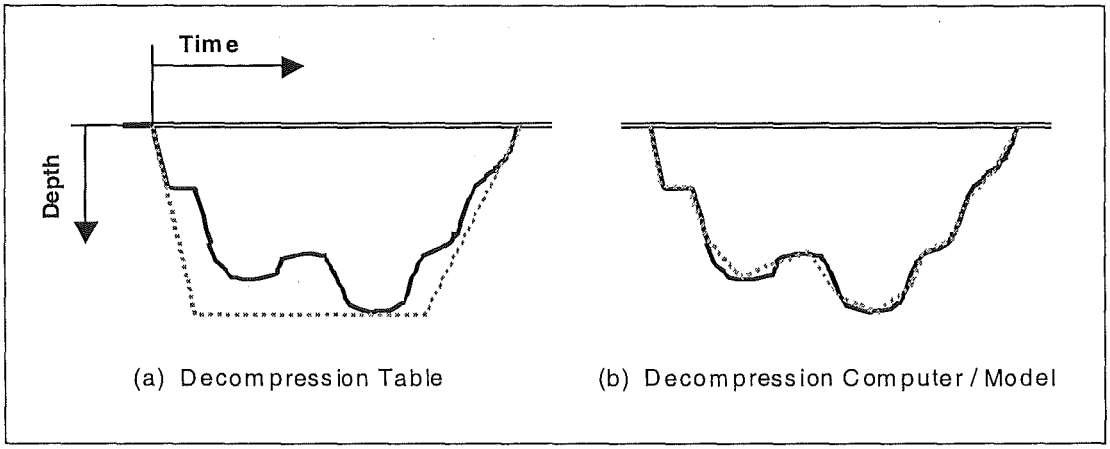

Figure 2.2 *Dive depth-time profile (solid line) and simplified profile used in (a) dive tables and (b) dive computers and model calculations.*

Many numerical descriptions of decompression in divers use a function of the partial pressure of carrier in the body tissues to define the risk of decompression illness. To describe the partial pressure of carrier in the tissue you must be able to describe the partial pressures of the gases the diver breathes throughout the dive. For a fixed percentage gas mix this is linked to the changing ambient pressure, but for rebreathers the partial pressures will depend on the control system in the breathing apparatus.

An example of a partial pressure of oxygen profile for a rebreather dive to 81 msw [Gay et al., 1997] is shown in Figure 2.3.

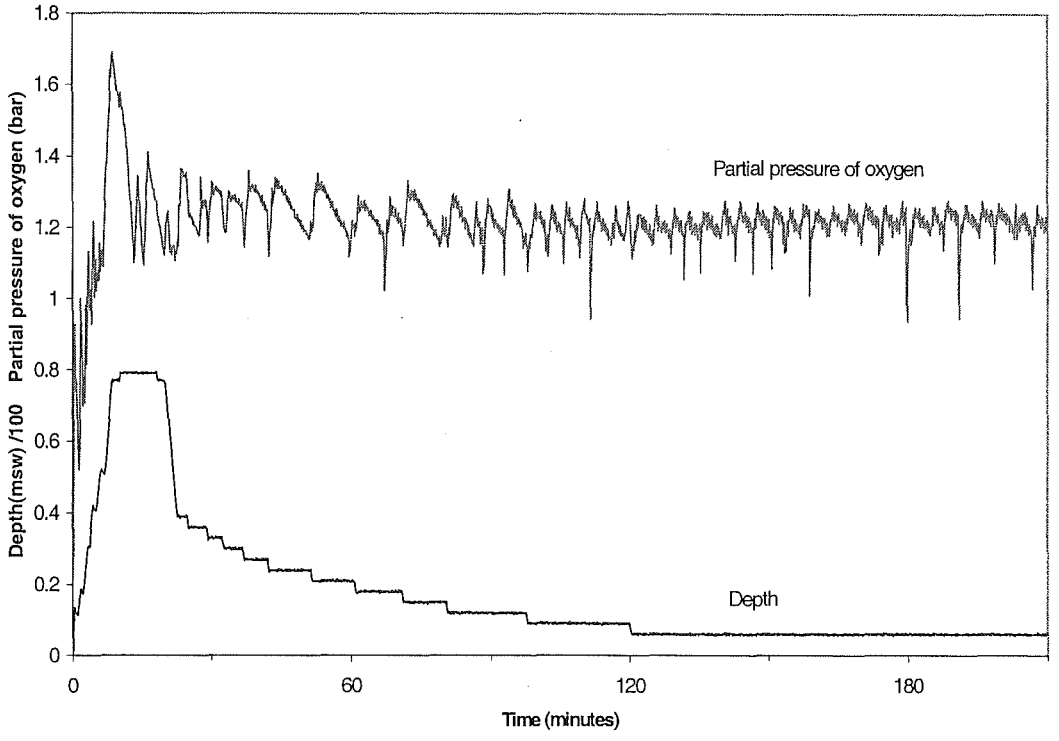

Figure 2.3 *Depth and partial pressure of oxygen breathed by a diver using a rebreather during a dive to 81 msw [Gay et al., 1997]*

For the example given in Figure 2.3, averaging over time the partial pressure allows the dive to be described by 30 data points compared to the 1440 used to plot Figure 2.3. In the development of the Canadian Underwater Mine counter measures Apparatus (CUMA) HeO_2 Tables, decompression profiles were based on a constant partial pressure of oxygen of one bar [Nishi & Warlow, 1997]. During the trials the time weighted average partial pressure of oxygen was higher than one bar used to generate the tables. The real time partial pressure of oxygen was not used as input to the decompression algorithm as it varied between dives and the tables needed to be safe for all dives.

2.5 Physiological models

Studies into the effects of changes of ambient pressure on animals and the human body have been carried out since the seventeenth century. In the seventeenth century Von Guericke constructed the first device to alter ambient pressure in a controlled manner. In 1670 Robert Boyle used a similar device to decompress a viper and noted a bubble moving in the waterish humour of one of its eyes. This was the first documented case indicating that a rapid reduction in pressure could lead to bubbles forming in the tissues of the body.

An understanding of the mechanisms of decompression illness was limited until Bert [1878] conducted a series of experiments on blood and respiration at pressures above and below ambient pressure at sea level. He concluded that more serious decompression illness was provoked by the presence of free gas as bubbles in the body and these bubbles consisted mainly of nitrogen.

Since the nineteenth century there has been a large number of models proposed for describing the physiological effects of decompression on a diver. A good summary of the history of decompression models and procedures is given in Bennett and Elliot's book [1995]. While there are a large number of models in the published literature there are only a few that have been sufficiently tested on humans under controlled conditions. The lack of or insufficient testing is due to the prohibitive cost, ethical restrictions of running manned trials and difficulties in measuring blood and tissue gas pressures during dives. Results determined from animals may not cross over directly to human physiology.

The body is made up of a large number of interconnected tissues and blood vessels. Attempting to model the complete body geometry and chemistry would be an enormous computational task that would be impractical at this time. Decompression methods are designed to be applicable to a general population of divers. For this population a highly complicated and computationally expensive model is unlikely to produce better results than simpler models can currently produce. In the future it may be possible to model individual characteristics and decompression physiology in

a complex manner and produce more accurate personalised decompression schedules.

The decompression models of the last hundred years all use a simplified representation of the diver's blood flow and tissues. Figure 2.4 shows a number of geometries that have been suggested in the past.

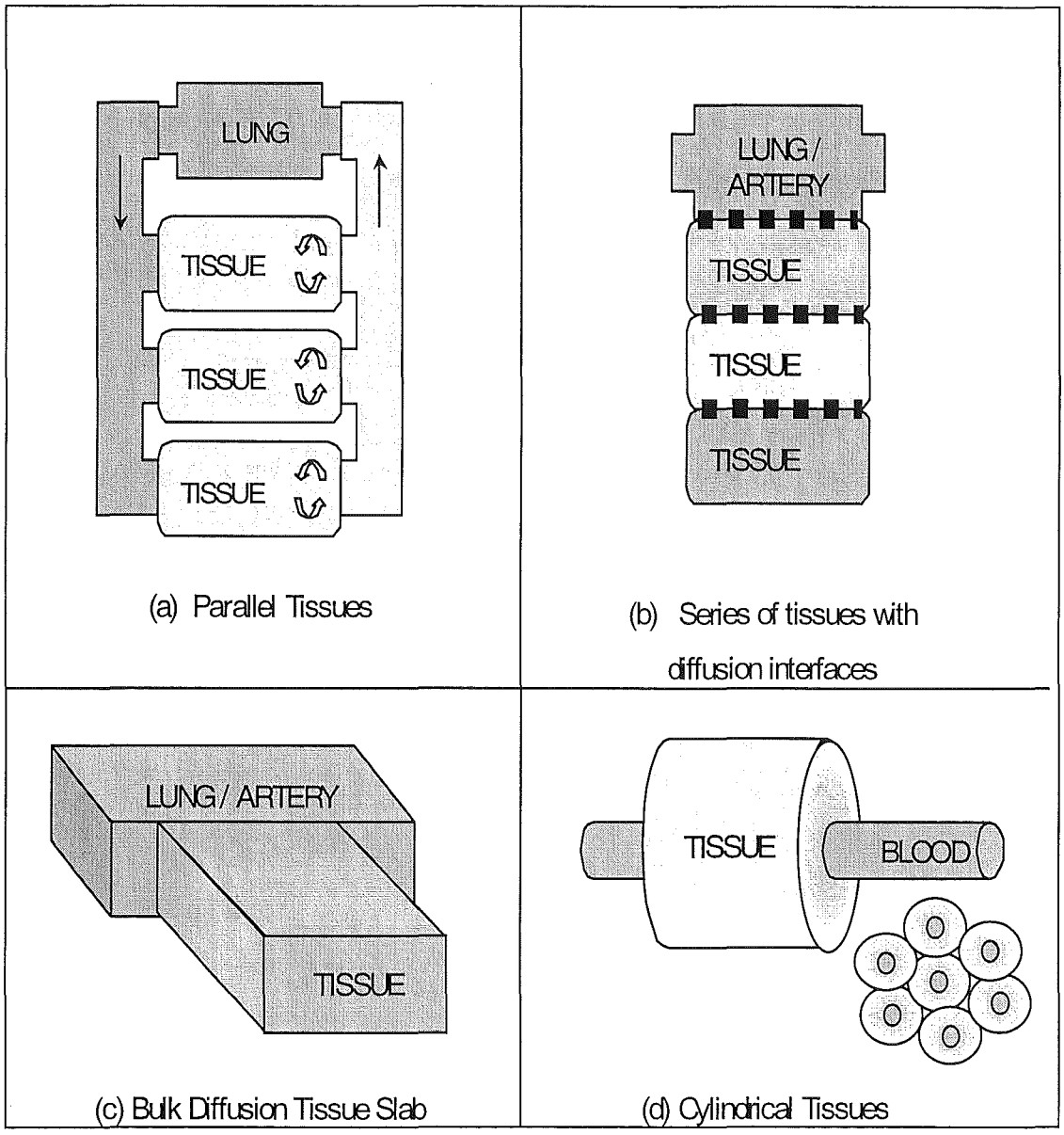

Figure 2.4 Geometries used to model decompression stress on divers.

The most popular geometry used today for oxygen in helium decompression tables and computer algorithms is a series of parallel tissues [Bühlmann, 1995; Schreiner & Kelly, 1971; Tikuisis et al., 1985] as shown in Figure 2.4(a). Each tissue is supplied with blood from the lungs that contains the same partial pressure of carrier. The blood flow per unit volume of tissue is different for each tissue and the tissue is assumed to be well stirred so no diffusion gradient of carrier exists.

The model eliminates the need to define tissue and capillary sizes. The partial pressure of the carrier gases in the blood leaving the tissue is assumed to be equal to the partial pressures in the tissue.

The number of independent tissues varies from three in the US LEM model [Thalmann et al., 1997] to 16 in Bühlmann's ZH-L16A model [Bühlmann, 1995]. This type of model is known as a perfusion limited model. Perfusion is a measure of the blood supply to the tissue.

The rate of change of carrier partial pressure in a tissue is governed by the gradient between the partial pressure of carrier in the arterial blood, P^A, and in the tissue, P^T, scaled by a tissue dependant gas exchange constant, K.

$$\frac{dP_j^T}{dt} = K\left(P_j^A - P_j^T\right) \tag{2-1}$$

The ZH-L16A model solves equation (2-1) by splitting the dive into a number of short steps, t_i to t_{i+1}, during which there is no change in depth or breathing gas. Therefore the partial pressure of the carrier gas in the arterial blood entering the tissue is assumed to be constant for the time step. The gas exchange constant, K, is defined as the natural logarithm of 2 divided by the gas half-time for carrier in the tissue, t^{HLFTM}.

The ZH-L16A update equation for the partial pressure of carrier gas j, in the tissue, P^T_j, is given by,

$$P_j^T\left(t_{i+1}\right) = P_j^T\left(t_i\right) + \left(1 - 2^{-(t_{i+1}-t_i)/t_j^{HLFTM}}\right)\left(P_j^A\left(t_i\right) - P_j^T\left(t_i\right)\right). \tag{2-2}$$

The change in partial pressure of the carrier in the tissue is proportional to the carrier pressure gradient between the arterial blood and the tissue. When more than one carrier gas is present in the blood and tissues the partial pressures of the carrier gases are calculated separately and summed.

The ZH-L16A model uses nitrogen half-times of 4-5 minutes up to 635 minutes. These values where chosen from examining trials data breathing nitrogen mixes. The half-times for helium were taken to be 2.65 times smaller than the half-times for nitrogen. This ratio comes from the diffusion rates of the two gases which are inversely proportional to the square root of their molecular weights. Note that Bühlmann is using a diffusion concept which has no relevance to a parallel tissue perfusion model. Incorporating a diffusion component into the model suggests that diffusion and perfusion are important in modelling decompression illness.

A similar model called the E-E or Exponential-Exponential model was used by the US Navy to develop air tables [Thalmann, 1985: Appendix A]. Their model uses equation (2-1) to determine an update in carrier partial pressure for constant pressure steps or linear pressure changes. For a rate of carrier partial pressure change in the arterial blood of R_j, the tissue update equation becomes,

$$P_j^T(t_{i+1}) = P_j^T(t_i) + \left(1 - e^{-K\delta t}\right)\left(P_j^A(t_i) - P_j^T(t_i)\right) + R_j\left(\delta t - \tfrac{1}{K}\left(1 - e^{-K\delta t}\right)\right)$$

where $\delta t = t_{i+1} - t_i$ (2-3)

The gas exchange constant is dependant on the solubility of the carrier in the tissue, α^T, and in the blood α^B, and the blood flow per unit volume of tissue, $\frac{dQ}{dt}$,

$$K = \frac{dQ}{dt}\left(\frac{\alpha^B}{\alpha^T}\right) \quad . \tag{2-4}$$

However in the computer implementation of equation (2-3) the gas exchange constant was set equal to the natural logarithm of 2 divided by the gas half-time for the tissue. With this substitution, the E-E model solution to the governing equation

given by equation (2-1) with the carrier partial pressure in the arteries held constant over the time step is the same as Bühlmann's ZH-L16A model with different values of the gas exchange constants.

The gas exchange constants for real non-fatty tissues are not different for nitrogen and helium. 'For all tissue except fat the ratio of solubility of gas in tissue over the solubility in blood is equal to one for helium and nitrogen, within the limits of measurement techniques' [V. Flook, pers.comm.]. For a purely perfusion model this means the value of the gas exchange constant K for nitrogen and helium should be the same for the same tissue. Similar to Bühlmann's models, the US Navy parallel tissue models use shorter half-times for helium than nitrogen, suggesting the need for a diffusion component in the physiological model.

The US Navy developed this model further to create decompression tables for their Mark 15/16 0.7 ata fixed partial pressure of oxygen breathing apparatus [Thalmann, 1985]. The new model is known as the E-L or Exponential Linear model. Only a single carrier gas was assumed to be present at a time. The three main differences from the E-E model were:

- A reduction of the partial pressure of the carrier in the arterial blood by taking into account the metabolic gases of carbon dioxide and water vapour,

$$P_j^A = P_{amb} - P_{O_2}^A - P_{CO_2}^A - P_{H_2O}. \tag{2-5}$$

- A linear tissue gas exchange when a gas phase is formed.

- A different half-time for saturating or de-saturating tissues.

No super saturation of the carrier gas in the tissue was allowed. Once the total pressure in the tissue exceeds ambient the excess carrier will form a bubble. Accordingly a bubble will form when;

$$P_j^T + P_{O_2}^T + P_{CO_2}^T + P_{H_2O} > P_{amb}. \tag{2-6}$$

Modelling the bubble and setting the internal pressure of the bubble equal to the ambient hydrostatic pressure gives the following linear carrier update equation for a constant inspired partial pressure of oxygen,

$$\breve{P}_j^T(t_{i+1}) = \breve{P}_j^T(t_i) + \left(P_{O_2}^T + P_{CO_2}^T - P_{CO_2}^A - P_{O_2}^I\right) K\left(t_{i+1} - t_i\right) \qquad (2\text{-}7)$$

where $\breve{P}^T$ is the partial pressure of carrier in the tissue that would exist if all the carrier was forced into solution.

The partial pressure of oxygen and carbon dioxide in the tissue and blood is assumed to remain constant due to metabolic and respiratory processes, so the update equation becomes independent of depth. The reduction in carrier in the tissue is proportional to the length of the step and inversely proportional to the tissue half-time.

The linear removal of carrier from a tissue when bubbles are present was also noted by Van Liew [1993].

The E-L model uses equation (2-3) when no gas phase is formed and equation (2-6) is false. When a bubble is formed on ascent and equation (2-6) is true then equation (2-7) is used to update the partial pressures of carrier j in the tissues.

Decompression tables for 0.7 ata oxygen in helium breathing apparatus [US Navy, 1996b] were generated using the physiological model given by equations (2-3) to (2-7). The diver was assumed to be saturated with helium instead of nitrogen at the beginning of the dive and the model was not used once the diver reached the surface at the end of the dive. No attempt was made to model the combined gas exchange of helium and nitrogen between the tissue, bubble or blood. The E-L model used six tissues for oxygen in helium dives covering a range of tissue gas exchange constants. The helium gas exchange half-times ranged from 5 to 120 minutes for tissue helium uptake and between 5 and 145 minutes for tissue helium removal.

The last model in this series of models from the US Navy, further developed the E-L model to include more than one carrier gas. The main changes were:

- Oxygen is allowed to contribute to total gas tissue pressure and bubbles.

- While no bubbles have formed the partial pressures of the carrier gases are calculated independently from each other.

- Once a bubble forms then any or all of the carrier gases can contribute to the bubble volume and the equations for partial pressure update for carrier gases become linked and have to be solved numerically.

- The model could be used to model the diver physiology at the surface post dive. Most decompression illness symptoms become evident post dive, rather than while the diver is still in the water.

- The properties of each tissue are described by 5 parameters. The metabolic gas partial pressures are assumed constant across all three tissues.

A review and detailed description of this Linear Exponential Multi-gas (LEM) model is given in Chapter 4.

An alternative to the Haldanian geometry described above is a diffusion model developed by Stubbs and Kidd [1965] as shown in Figure 2.4(b). The model was built as an pneumatic analogue computer in 1960s. One configuration of the computer consisted of four compartments in series. The gas could flow between the volumes through pneumatic resistors. The volume of each compartment was the same, as was the resistance to gas flow between the compartments.

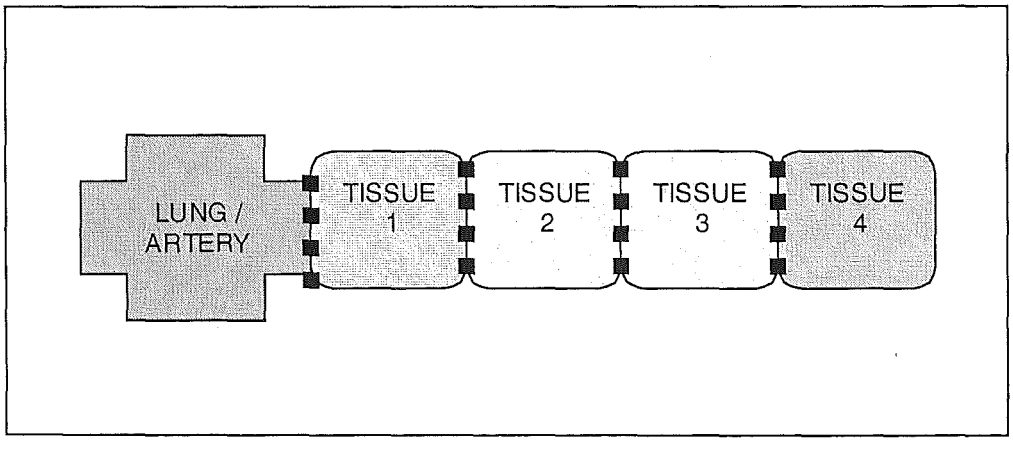

Figure 2.5 Kidd Stubbs four tissue model.

The pneumatic model shown in Figure 2.5 can be described by a set of four non-linear differential equations for the pressure P_i in the ith compartment:

$$\begin{aligned}
\frac{dP_1}{dt} &= A\left[(B + P_{amb} + P_1)(P_{amb} - P_1) - (B + P_1 + P_2)(P_1 - P_2)\right] \\
\frac{dP_2}{dt} &= A\left[(B + P_1 + P_2)(P_1 - P_2) - (B + P_2 + P_3)(P_2 - P_3)\right] \\
\frac{dP_3}{dt} &= A\left[(B + P_2 + P_3)(P_2 - P_3) - (B + P_3 + P_4)(P_3 - P_4)\right] \\
\frac{dP_4}{dt} &= A\left[(B + P_3 + P_4)(P_3 - P_4)\right]
\end{aligned} \tag{2-8}$$

where A and B are gas flow constants and P_{amb} is ambient pressure [Nishi & Lauckner, 1984]. The rate of change of pressure in each of the compartments is related to the pressure differences across the pneumatic resistors to the neighbouring tissue compartments. The pressure differences are weighted by the sum of the pressures in the two adjoining compartments.

The first compartment has access to ambient pressure and is equivalent to a fast half-time tissue. The fourth compartment is only connected to the third compartment and exterior ambient gas changes must travel through all the other compartments before reaching the fourth compartment. The fourth compartment is equivalent to a slow half-time tissue.

The half-time equation for a single compartment over the time interval t_i to t_{i+1} is given by,

$$T_{HLFTM} = \frac{\ln\left(2 - \frac{P(t_{i+1}) - P(t_i)}{B + P(t_{i+1}) + P(t_i)}\right)}{A\left(B + 2P(t_{i+1})\right)} \tag{2-9}$$

where A and B are the constants of equation (2-8). Note that the half-time for carrier uptake is shorter than for elimination and the constant B controls the asymmetry and non-linearity of carrier exchange.

This simple model for air dives has only two parameters to be determined; the gas constants A and B. The model described by equation (2-8) was modified by Nishi to

account for using helium as the carrier gas and a set of decompression tables have been produced for use with 1.0 ata constant partial pressure of oxygen in helium breathing apparatus. The modifications have not been published, but the resulting tables have been tested by diving trials [Nishi & Warlow, 1997] and are in use by the Canadian Navy.

Another geometry considered for modelling gas uptake and elimination arose from observations that many of the less serious cases of decompression illness resulted in pain in or around a joint. Some parts of a joint are very poorly perfused and mainly rely on diffusion for supplies. Hempleman [1995] suggested that cartilage tissue could be modelled as a slab of avascular tissue with one face of this slab well perfused by a network of blood vessels, as shown in Figure 2.4(c). From Ficks law of diffusion, at some distance x from the blood tissue interface the concentration of carrier gas, c, can be described by,

$$\frac{\partial c}{\partial t} = D\frac{\partial^2 c}{\partial x^2} \tag{2-10}$$

where D is the diffusion coefficient. The solution of this equation is dependent on the boundary and initial conditions chosen.

Since the early 1900s people have tried to model body tissues using a geometry closer to human physiology such as considering a tissue with capillaries running through it [Popel, 1989]. The simplest representation of this is by considering the capillary as a cylinder surrounded by an annulus of tissue, with cylindrical symmetry as shown in Figure 2.4(d) and Figure 2.6.

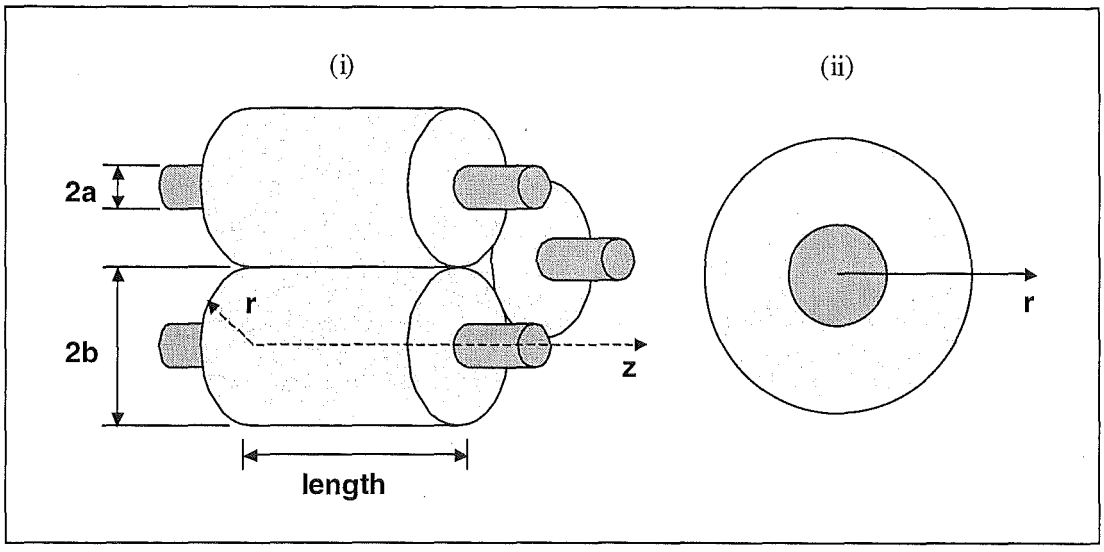

Figure 2.6 *The geometrical tissue-capillary model: (i) Cylinder with tissue/capillary length effects and (ii) the infinite thickness model with angular symmetry.*

Hennessy [1974a] produced a cylindrical model which allowed both nitrogen and/or helium to be a carrier. The blood was assumed to be well stirred and the cylinder was treated as an infinitely long cylinder with the same carrier in the blood along the length of the capillary. The carrier is allowed to radially diffuse into and out of the tissue from the blood.

When the combined partial pressures of the carrier and metabolic gases exceeded ambient pressure plus an extra quantity to account for elasticity and surface tension of a bubble, a bubble was assumed to have formed. The diffusion of the two carrier gases becomes linked once the bubble is formed.

Hennessy solved the governing equations for the above model using a finite difference formula with a mesh in the radial direction. The solutions to the governing equations for this geometry are more complicated than the other geometries considered and usually require a numerical solution technique to be applied.

The complexity of the above model can be increased by considering the continual loss or gain of carrier as the blood travels down the capillary. Hennessy [1974b] defined the partial pressure of a carrier at a point in the tissue to be the solution of,

$$\frac{\partial P^T(r,z,t)}{\partial t} = \frac{D^T}{r}\frac{\partial}{\partial r}\left(r\frac{\partial P^T}{\partial r}\right) + D^T\frac{\partial^2 P^T}{\partial z^2} \quad (2\text{-}11)$$

= Radial diffusion of carrier in tissue cylinder + Diffusion of carrier along the tissue cylinder

which is dependent on the blood carrier partial pressure along the capillary as defined by

$$\frac{\partial P^A(z,t)}{\partial t} = -V\frac{\partial P^A}{\partial z} + \frac{2D^T\left(\alpha^T/\alpha^A\right)}{a}\left(\frac{\partial P^T}{\partial r}\right)_{r=a} \quad (2\text{-}12)$$

= Transport and diffusion of carrier along capillary + Flux of carrier across capillary / tissue boundary

where V is the blood flow rate, D^T is the diffusion coefficient of carrier gas in the tissue and r,z and a are as shown in Figure 2.6. The radial coordinate is constrained to be less than or equal to a in equation (2-12) and between a and b in equation (2-11). Solutions to the above equations require the length of the cylinder as well as boundary and initial conditions.

2.6 A perfusion, diffusion or bubble limited process?

There has been much debate over whether perfusion or diffusion controlled models should be used to model tissue gas kinematics [Hennessy, 1974b; Wienke, 1989; Hempleman, 1995].

In reality one or both mechanisms may control the distribution of carrier in tissues and between the tissues and the blood. Well perfused tissues may be better modeled by perfusion, while poorly perfused tissues may be better modeled by diffusion. Tikuisis et al. [1985] suggested that diffusion limiting approaches have merit in

modeling the finer details of gas exchange between tissue and blood, but perfusion limiting approaches are better for analysis of whole body gas exchange.

In the body, tissues are not isolated objects they are connected to other tissues. Consider a well perfused tissue attached to a sparsely perfused tissue. After a decrease in pressure, the well perfused tissue with a short half-time will equilibrate quickly with the arterial blood. However, the poorly perfused tissue with a longer half-time will eliminate the excess carrier at a slower rate. This will result in a pressure gradient across the interface of the two tissues which may cause diffusion of the carrier into the well perfused tissue. The diffusion of carrier from the poorly to the well perfused tissue would produce the equivalent of a tissue with two half-times.

The Stubbs and Kidd [1965] model incorporates a simple representation of this tissue interface diffusion. The parallel tissue models of Thalmann [1985] and Bülhmann [1995] could be said to incorporate this idea by using a large number of tissues with different half-times. The more complicated LEM model uses only three tissues so will be less able to represent the inter-tissue diffusion.

The occurrence of decompression illness when flying a week after a dive, suggests that perfusion is not the only controlling factor. The half-time of the tissue would have to be much longer than currently accepted to be possible. Arguments have been given that the delay in decompression illness is due to the presence of bubbles in the tissues which reduce the rate of washout of carrier gas from the tissue. The washout of carrier can be slowed by bubbles obstructing blood vessels or the reduction in the partial pressure of carrier gas in the tissue, as the carrier diffuses into the bubble.

While models like the E-L model use a very simple representation of a bubble, other researchers have tried using a more detailed model of the bubble itself, or indeed a set of bubbles [Gault, 1992; Tikuisis et al., 1991; Ball et al., 1995].

Van Liew & Burkard simulated the competition for carrier between the blood, tissue and bubbles [Van Liew & Burkard, 1993; Burkard & Van Liew, 1995]. They found that if enough bubbles were present in the tissue, it is possible for enough carrier to diffuse into the bubbles to reduce the partial pressure of carrier in the tissue to a

lower level which becomes clamped. The pressure gradient between the tissue and blood has been reduced and the carrier removed by the blood can be replaced by diffusion out of the bubbles. The removal of excess carrier from the tissue and bubbles follows a straight line course.

Which ever approach is taken, perfusion or diffusion limiting, the research suggests the need for:

- More than one tissue or one tissue with multiple half-times.
- A slower carrier washout if bubbles have formed.

2.7 The contribution of oxygen to decompression illness risk

At sea level breathing air most of the oxygen in the blood is bound to haemoglobin or carbon dioxide. Only a small fraction is dissolved in the blood. Tissue oxygen extraction ranges from 1% to 10% (ml/100ml of blood) [Folkow & Neil, 1997].

Most decompression methods assume that oxygen is not directly connected to the risk of decompression illness and only acts to reduce the amount of carrier gas in the blood or tissue. Hyperbaric trials with goats [Donald, 1955] indicated that higher partial pressures of oxygen did affect the risk of decompression illness. However, most of the goats recovered spontaneously on returning to sea level, suggesting that the excess is quickly used by the body once normal ambient pressure is achieved.

The researchers at NMRI also found that their most successful probabilistic models were under predicting the risk of decompression illness in oxygen in nitrogen dives that included a period that the diver breathed a high fraction of oxygen. Parker et al. [1998] considered two possible additions to their basic E-L model:

- A decrease in nitrogen uptake / elimination due to the ability of the partial pressure of oxygen to alter the circulation. This was achieved by scaling down the nitrogen tissue half-time once the partial pressure of oxygen reaches a critical value.

- A component of the partial pressure of oxygen in the tissue was allowed to contribute to the carrier to test for bubble existence and growth.

Each of the above modifications improved the models capability to predict decompression illness for dives using high partial pressure of oxygen.

100% oxygen hypobaric (altitude) exposures have been modelled using a single tissue E-E model to describe the partial pressure of nitrogen and oxygen in the tissue. Logistic regression was used to relate the partial pressure of nitrogen or nitrogen plus oxygen in the tissue to the presence of bubbles [Foster et al., 1998]. The partial pressure of oxygen contributing to the risk of decompression illness was treated as a constant during the time at altitude. The results showed that the model incorporating a constant partial pressure of oxygen in the risk calculation gave the closest fit to the data.

The above research suggests that models can be improved by including a mechanism for oxygen to contribute to the risk of decompression illness as well as the carrier gases. This improvement comes at the cost of extra parameters to be determined. In the case of the LEM model, 2 extra parameters are required for each tissue.

2.8 Decompression illness risk models

While there have been many approaches to modelling the effects of decompression on a diver, all researchers agree that individual responses to decompression is highly variable in nature. The same dive profile can produce a range of outcomes, from no decompression illness symptoms to different types of decompression illness.

Most decompression methods ignore the variability in decompression illness outcome which exists at our current level of understanding of decompression physiology. These methods use a safe or not safe step function. No account is taken of the probability of decompression illness from a dive profile.

In 1974 Berghage et al. conducted a series of hyperbaric trials on mice and found the decompression illness outcomes could be described by a binomial distribution. They suggested that dose response curves should be fitted to a parallel tissue model (Figure 2.4(a)) to provide an estimate of risk of decompression illness for a dive.

The function chosen to convert carrier tissue pressures into a probability of decompression illness must be able to predict a zero risk value when no decompression occurs and a smooth increasing risk with the severity of the pressure drop and dive profile.

The researchers at the US Naval Medical Research Institute (NMRI) continued the previous research and tested two different risk functions on saturation dives with a single pressure drop from the bottom depth to the surface [Weathersby et al., 1984]. The first formulation followed the Hill's equation,

$$P(DCI) = \frac{S^n}{S^n + (S_{50})^n} \tag{2-13}$$

where S is dose of decompression stress, S_{50} is the dose corresponding to a 50% incidence of decompression illness and n is a constant which controls the steepness of the dose-response curve. The parameters S_{50} and n must be determined from dive data.

The second risk function considered is taken from survival analysis [Kleinbaum, 1996] and is of the form,

$$P(DCI) = 1.0 - \exp(-kS^n) \tag{2-14}$$

where k and n are constants determined from the data.

In both functions the decompression stress dose, S, could be a number of quantities taken as a maximal value or integrated over time such as;

- bubble nucleation rate,
- total or maximum bubble volume,

- number of bubbles formed,
- ambient pressure reduction or
- partial pressure of carrier gas in tissue above that in the blood.

The saturation dives consisted of a dive to raised pressure for a period of at least 24 hours, followed by a single reduction in pressure. The size of this reduction in pressure was used as the decompression stress dose. Parameters were estimated using the maximum likelihood method.

Similar maximum likelihood results were obtained from the two risk functions given by equations (2-13) and (2-14) for human dives using oxygen in helium breathing gas.

Further work at NMRI looked into the form of the decompression stress dose and how the time of occurrence of decompression illness could be used to improve parameter estimation for the physiological model [Burkard & Van Liew, 1995]. In a later paper [Thalmann et al., 1997] they suggested that integrating the sum of the instantaneous decompression stress doses, $\Re^T$, over the duration of the dive, DT, and the following 24 hours gave the best results of oxygen in nitrogen dives with a E-L physiological model,

$$P(DCI) = 1 - \exp\left(- \int_0^{DT+24hrs} \sum_{tissue\ T} A^T \Re^T \, dt \right). \tag{2-15}$$

The instantaneous decompression stress dose for each tissue, $\Re^T$, was calculated as a relative super saturation above a tissue dependent threshold value, Thr,

$$\Re^T(t) = \frac{\breve{P}^T_{carrier}(t) + P_{metabolic} - P_{amb}(t) - Thr^T}{P_{amb}(t)} \tag{2-16}$$

where the instantaneous dose is constrained to be equal to or greater than zero. When the dose is negative, the value is taken to be zero.

This risk model has been further developed for more than one carrier by substituting the single burden for the sum of the carrier burdens for nitrogen, helium and oxygen if included [NMRI , 1995, 1996] .

An alternative decompression stress dose that can be physically measured is the bubbles in a diver during and following decompression. Doppler ultrasound scans can detect moving bubbles [Horn, 1998; Eatock & Nishi, 1986]. These bubbles can be graded depending on signal amplitude and bubble frequency. The Kisman-Masurel (K-M) bubble grades (BG) range from 0 to IV. A risk model is suggested by Gault [1992] which uses the maximum predicted bubble radius, r, to fit the probability of the maximum bubble grade occurring,

$$P(BG=i)=\frac{\left(\frac{r}{\beta}\right)^{i\gamma}\left(1-\frac{r}{\beta}\right)^{(4-i)\gamma}}{\sum_{j=0}^{4}\left(\frac{r}{\beta}\right)^{j\gamma}\left(1-\frac{r}{\beta}\right)^{(4-j)\gamma}} \qquad i=0 \text{ to } 4 \tag{2-17}$$

where γ and β are parameters to be estimated from the data. This probability model did not fit the intermediate bubble grades well. The best fit to the oxygen in nitrogen dives considered was obtained when the bubble grades were grouped into two sets and a third scaling parameter, ω, was added.

$$\begin{aligned} P(BG=0,1 \text{ or } 2) &= [P(BG=0)+P(BG=1)+P(BG=2)](1-\omega)+\omega/2 \\ P(BG=3 \text{ or } 4) &= [P(BG=3)+P(BG=4)](1-\omega)+\omega/2 \end{aligned} \tag{2-18}$$

The third parameter ω, adds a constant probability factor to all the bubble grade outcomes. For the dives and bubble model considered by Gault, this parameter was estimated to have a value of 2.1%. As equations (2-17) and (2-18) are only dependent on bubble radius, these equations could be applied to bubbles generated by more than one carrier gas with out modification.

Another approach to predicting the risk of DCI using bubble dynamics has been proposed by Foster et al. [2000] for exercising at altitude. They suggest that "the instantaneous probability of symptom onset at time t is proportional to the expected

total volume of bubbles from a region of tissue at time t" and " the probability of ever experiencing DCI during a decompression is directly related to the cumulative volume of bubbles formed."

The last risk model that shall be considered does not use an underlying physiological model. Logistic regression [Hosmer & Lemeshow, 1989; Leffler, 2001] can fit a set of descriptive continuous, discrete or categorical variables to the outcome of decompression illness. Examples of descriptive variables are maximum depth, ascent profile descriptors and oxygen decompression use (YES/NO). The outcome of decompression illness is the occurrence of decompression illness symptoms or not. The logistic model can be extended to cover multiple outcomes, such as including a marginal decompression illness category.

The probability of decompression illness, P(DCI), occurring from a dive described by N independent variables, v_j, is given by the relationship

$$P(DCI) = \frac{1}{1+e^{-g(v)}} \qquad \textbf{where} \qquad g(v) = \beta_0 + \sum_{j=1}^{N} \beta_j v_j \tag{2-19}$$

and β_j are model parameters to be determined from dive data.

It can be argued the logistic model does not have a physiological basis so can not be applied to dive types different from the dives used to calibrate the model parameters. However, the production of decompression tables based on oversimplified physiological models all end up being specific to the dive types they are tested on. With today's models, all decompression tables should be restricted for use with dives similar to those used for testing the tables.

2.9 Safe Ascent Criteria

The previous sections have described some of the physiological and risk models that have been published. The next step is to be able to turn these models into rules for

the safe decompression of divers. There are two approaches to providing safe ascent rules; deterministic approaches or risk based probabilistic approaches.

Most deterministic approaches use a series of depth and tissue dependent, critical partial pressures of the carrier which should not be exceeded on ascent. Most methods [Workman 1965; Bülhmann 1995; Thalmann 1985] use a linear function to define the safe ascent depth (SAD) for a given partial pressure of carrier, $\boldsymbol{P^T}$,

$$SAD^T = \phi\left(P^T - \varphi\right) \tag{2-20}$$

where ϕ and φ are tissue dependent constants estimated from trials data.

A decompression schedule is created in the following way. When the diver leaves the bottom depth he will have a certain partial pressure of carrier in each of his tissues. Equation (2-20) is used to determine the tissue dependent safe depths to which the diver can ascend to. The deepest safe depth will either be sea level or a depth which will indicate the first decompression stop depth. The diver then ascends to this stop depth and will stay there until all his tissues allow him to progress to the next shallower stop depth. The time he spends at the stop depth is the decompression stop time.

In the decompression tables developed by Thalmann [1985], only one carrier is considered. So for oxygen in helium tables only the partial pressure of helium contributes to equation (2-20). In contrast, Bühlmann [1995] summed the partial pressures of nitrogen and helium to give the partial pressure of carrier in a tissue, $\boldsymbol{P^T}$. The parameters φ and ϕ were changed according to the fraction of nitrogen in $\boldsymbol{P^T}$.

Values of safe ascent depth parameters from different implementations of equation (2-20) have not been given here. The parameters have been derived using their associated physiological models fitted to dive data, not real physiological data. Hence it is not possible to directly compare safe ascent depth equations.

Bubble models could also provide the basis for a safe ascent rule, where the radius or volume of the bubble or bubbles must be kept below a critical value [Foster 1998].

An alternative deterministic ascent rule which works reasonably well for single carrier, short bottom time, bounce dives was derived from the slab tissue diffusion model (Figure 2.4(c)) [Hempleman 1995]. While the carrier gas diffusing into and out of the tissue slab is not affected by the opposite end of the slab, the quantity of carrier diffusing into the tissue is proportional to the square root of the time. For a dive to depth, d, for a time, t, there will be a fixed quantity, Ω, of carrier such that,

$$\Omega = d\sqrt{t} \quad \text{or} \quad \Omega = d_1\sqrt{t_1} = d_2\sqrt{t_2} \,. \tag{2-21}$$

So if a diver goes to depth d_1 for time t_1, or depth d_2 for time t_2 the diver should be reasonably safe if the above relationship is followed. Setting Ω equal to 500 gives no decompression stop dives close to the US Navy [1996a] Air Tables.

The above deterministic examples of safe ascent rules all have a decompression illness or no decompression illness step function dependent on the partial pressure of the carrier in the tissues as shown in Figure 2.7. The variability in decompression illness outcome for a dive suggests that a better way to both fit model parameters and to construct decompression schedules is to use a probabilistic approach. The safe ascent rule becomes, the diver must ascend such that the probability of decompression illness occurring is equal to or below a chosen value. The dashed line in Figure 2.7 shows one possible probabilistic definition of risk.

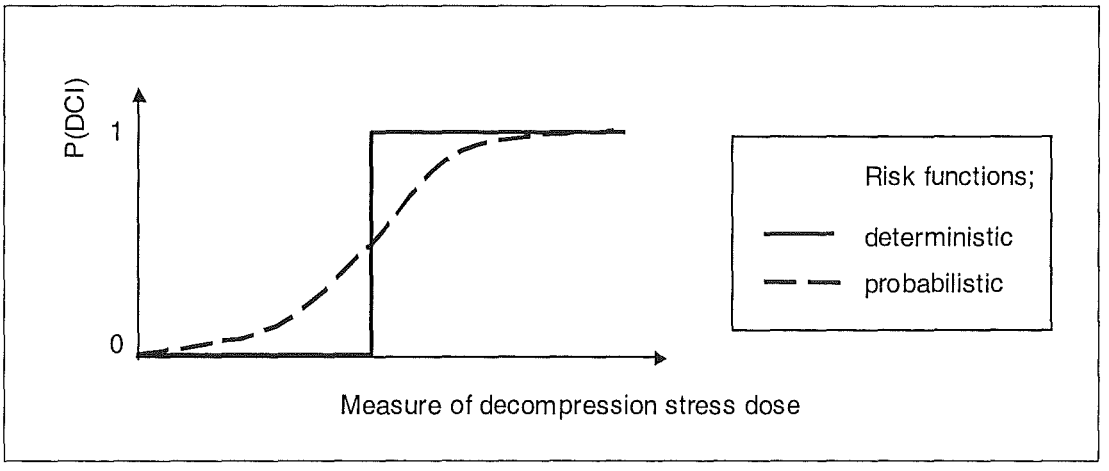

Figure 2.7 *Probabilistic and deterministic approaches to estimating the probability of decompression illness*

Weathersby et al. [1985] noted there are a large number of possible ascent paths that a diver can take which result in the same probability of decompression illness. The researchers at NMRI proposed a method to be able to produce a decompression schedule in real time for oxygen in nitrogen dives using the LEM physiological model [Survanshi et al., 1994]. The LEM model has analytical solutions for carrier exchange between the blood and tissues and tissues and blood.

To avoid large, time consuming searches for the shortest decompression path with a risk of decompression illness below the chosen value, a local search method was used. Instead of waiting until the end of the bottom time of the dive to start calculating the ascent path, a small number of candidate ascent paths are considered several times a minute as the dive progresses. As the time intervals between update calculations are short, the last optimum ascent path will always be a good starting point for calculating the new ascent path. Completing a series of small local searches for the duration for the dive provides close results to those obtained by a global search method [Parker et al 1994], but for much reduced computational resources

2.10 Conclusions

This chapter has described a number of approaches to producing decompression schedules for divers. While there are a large number of models in the published literature there are only a few that have been sufficiently tested on humans under controlled conditions, especially when considering oxygen in helium rebreather dives.

The DCIEM 1.0 ata constant partial pressure of oxygen in helium decompression tables have been tested and are used by the Canadian Navy. The US 0.7 ata constant partial pressure of oxygen in helium tables were tested and have been in service for a number of years. Both these tables were developed from basic models with the parameters tweaked during trials to provide safe tables. The Bühlmann model is

widely used, but to the author's knowledge the model parameters have not been calibrated against oxygen in helium bounce dives.

The addition of helium and oxygen gases to nitrogen as carriers adds to the complexity of the models and in some cases changes the solution methods from analytical to numerical solutions.

The models that have been developed in the last century have varied in complexity. If the physiological mechanisms leading to decompression illness could be modelled correctly, the variability in decompression outcomes would be reduced and a single model should be able to predict the risk of decompression illness for all types of dives. However at our current level of understanding the simpler models with a couple of parameters seem to provide as safe decompression as more complicated models of 20 or more parameters when calibrated to specific dive types.

Chapter 3

Data

3.1 Introduction

This chapter describes the data used to review the probabilistic LEM model in Chapter 4. The data come from an international military dive trial database that provides data for a wide range of dives in a common format.

3.2 The nature of dive trial data

The best data for training models to predict decompression illness would contain an even number of dives resulting in decompression illness symptoms and asymptomatic dives over a random distribution of possible dives.

All the data described in this chapter were recorded during dive trials conducted under controlled environmental conditions using fit military divers. Some of the trials were designed to test new equipment while other trials were designed to test decompression procedures.

Because dive trials and decompression tables are ethically designed to minimise the risk of injury to divers, the trials to validate decompression schedules are biased on the side of safety. If dives result in unacceptable cases of decompression illness, the decompression model is usually modified to create safer tables, resulting in safer dives being conducted for the rest of the trial. This process means dive profiles are biased away from the region of higher risk of decompression illness.

While the above approach is good for ensuring safe decompression tables are used, the biasing of the data is not helpful for producing optimised tables.

Another important feature of trial data is the number of repetitions of a single dive profile during a trial. The financial cost of running trials prevents testing of a single dive profile enough times to provide a statistically significant value of the probability of decompression illness for the profile. To use the data to develop models a number of different profiles must be considered together. This may result in a good estimation of overall risk, but may mask the inability of a model to predict the risk of some profiles when incorrect risks cancel each other out.

Factors both physiological and environmental (Figure 2.1) may influence the occurrence of decompression illness from a dive. Not all this information may be recorded or available from a dive trial. One example of an environmental factor affecting the decompression stress on the diver is the clothing of the diver. A diver in a dry chamber may experience gas transfer through the skin as well as through the circulation.

3.3 Dive trial database

The dive database has a common format for recording all the dive profiles. All depths are measures in units of feet of sea water (fsw) and all periods of time are measured in units of minutes.

The following information is recorded for each man dive:

- A unique dive label.
- The time, depth and breathing gas profile at coordinates throughout the dive and for twenty four hours after the end of the dive (forty eight hours after saturation dives). Linear changes in depth occur between the coordinates.
- The dive decompression illness outcome; no symptoms, marginal decompression illness or full decompression illness (Type I or II).

- The time interval that decompression illness symptoms first appeared if decompression illness was diagnosed.

A wide range of dives are included in the database, including; bounce dives, surface decompression dives, saturation dives and submarine escape dives, breathing different combinations of oxygen, nitrogen and helium.

Dives were chosen from the database with the following characteristics:

- Single bounce dives with a single maximum depth.
- Dives that continually descend from the surface to the maximum depth. This avoids the cases when the diver conducts a small ascent on the descent to help clear their ears.
- Dives that continually ascend from maximum depth to the surface.
- Dives that did not contain a shallow pre-dive before the main dive.
- No surface decompression dives.
- The diver had not dived in the 24 hours previous to the dive starting.
- Helium was breathed for at least part of the dive.
- No missing data in the dive record.

The subset of dives defined by the above characteristics contained 3455 dives including 155 cases of decompression illness and 39 cases diagnosed with marginal decompression illness.

Figure 3.1 shows the distribution of the data as defined by the maximum depth, bottom time, total time for decompression and partial pressure of oxygen, PO_2, at the maximum depth. The banding of the partial pressure of oxygen occurs because the partial pressure is recorded to one decimal place.

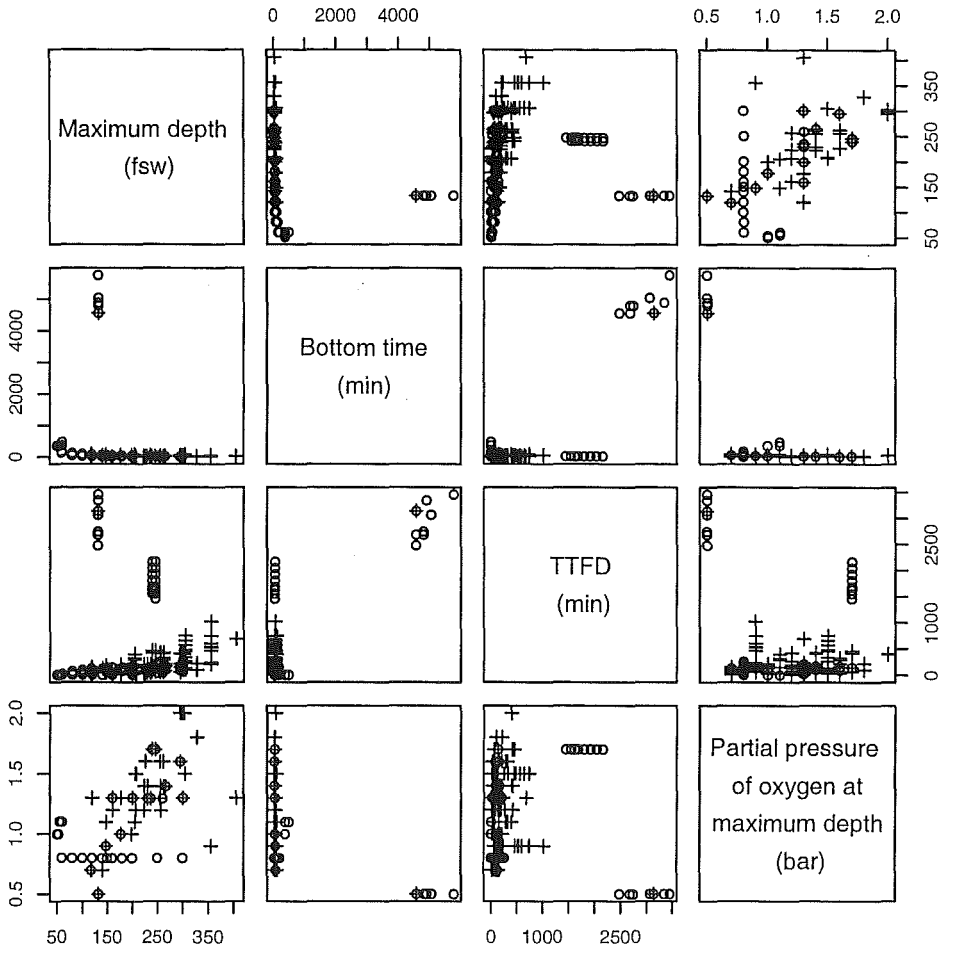

Figure 3.1 *Distribution of dive summary variables in combined bounce dive and outlier dive data sets. (+) represent dives where the diver breathes close to 100% oxygen during part of the ascent, and (o) represent dives where the diver does not breath close to 100% during the ascent.*

Figure 3.1 shows there are some outlying values of both bottom time and total time for decompression in the data. These values correspond to dive durations that are much greater than the 240 minute duration of the rebreather equipment this thesis is considering. To aid in future analyses, the dive data were split into two sets. The 351 outlying values where put into a set called the "outlying dive" data set and the remaining 3104 dives into a set called the "bounce dive" data set. The percentage of dives resulting in decompression illness in the bounce dive data was 4.4% compared to 7.4% in the outlying dive data.

Dive trial name	Reference	# man dives	# cases of DCI (Marg)	Depth range (fsw)	Bottom time range (min)	TTFD range (min)	# dives using 100% oxygen	Bottom PO_2 (Bar)	Wet / Dry
DC8416D	Nishi 1987	430	14 (2)	118 - 328	9 -100	8.3 - 218.3	367	0.7 – 1.8	Dry
DC8416S		91	7			8.3 – 217.5	81		
DC8416W		178	4			8.3 – 217.5	159		Wet
DRATMXA	Alverstoke	66	1	223 - 256	13 – 27	37 - 288	61	1.2 – 1.7	Dry
DRATMXW		131	8	230 - 263	14 – 27	37 – 288	121	1.3 – 1.7	Wet
EDU185S	?	1562	56 (2)	60 - 300	10 – 180	2 – 257	0	0.75	
EDUHE70	Thalmann 1985?	152	13 (2)	141 - 355	15 – 60	35 – 290	152	0.7 – 1.5	
NMR9404	Survanshi 1998	462	26 (22)	119 - 300	9 – 32	5 – 205	161	1.3	Wet
NMR9404o	Survanshi 1998 Flynn 1998	32	1	300	25	226 – 232	32	1.3	Wet

Table 3.1 *Bounce dive dataset summary by dive trial.*

Dive Trial Name	Reference	# man dives	# cases of DCI (Marg)	Depth range (fsw)	Bottom time range (min)	TTFD range (min)	# dives using 100% oxygen	Bottom PO_2 (Bar)	Wet / Dry
DRATMXA	Alverstoke	27	0	239 - 256	24 – 26	408 - 2160	20	1.4 – 1.7	Dry
DRATMXW		58	2 (10)	246 - 263	14 – 28	325 - 2160	42		Wet
DCHELONG	?	27	0	295 - 303	55 – 60	395 – 405	27	2.	
EDUHE70	Thalmann 1985?	110	18 (1)	205 - 405	20 – 90	320 - 1019	110	0.9 – 1.5	
NMR86H6	?	60	1	50 - 60	360 – 480	1.2 – 2.5	0	1 – 1.1	Dry?
NSMTMX	?	69	4	132	4559 – 5760	2473 - 3451	1	0.5	Dry ?

Table 3.2 *Outlier dive dataset summary by dive trial.*

A summary of these two data sets separated by dive trial is given in Tables 3.1 and 3.2. Where reports on the dive trials have been located, the reference number is given in the second column of the table.

The NMR9404 and NMR9404o trials represent the closest breathing mix to the target 1.3 bar oxygen in helium rebreather dives. The trial was designed to explore if increasing the partial pressure of oxygen to 1.3 bar from 0.7 bar would reduce decompression time. " A sequential dive trial was designed in which the outcome of dives at each step dictated the selection of a profile for the next test. Excessive decompression sickness (DCS) outcome resulted in selection of a safer next profile. Conversely low DCS outcome resulted in selection of a riskier profile." [Survanshi et al., 1998]. The divers were in wet suits in water temperatures from 45 to 67 °F.

The DC8416 trials [Nishi 1987] were conducted using fixed 16 % oxygen in helium mix at maximum depth. The decompression illness outcomes and dive profiles for the divers wearing drysuits and fully immersed in water (DC8416W), standby divers in drysuits (DC8416S) and dry participants (DC8416D) are recorded.

The largest trial data base is the EDU185S data. This trial covered a range of dive depths and bottom times. All the dives use a constant partial pressure of 0.75 bar oxygen in helium in the breathing mix at maximum depth.

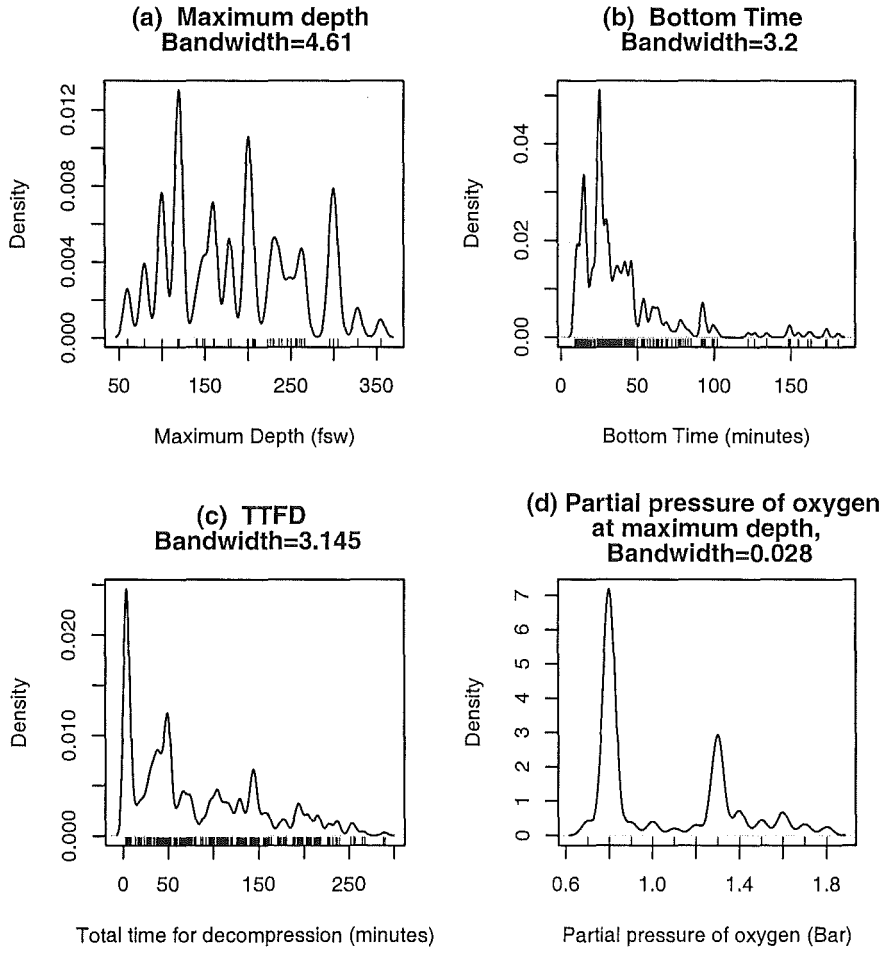

Figure 3.2 *Distribution of maximum depth, bottom time, total time for decompression and partial pressure of oxygen at maximum depth for dives in the bounce dive data set*

The data given in the bounce dive data set are summarised in Figure 3.2. The data density is plotted using smoothing kernels with standard deviation equal to the bandwidth indicated on each plot.

The four density plots show that there is a good distribution of dives over the depths from 60 fsw to 355 fsw, while the length of the bottom times for most of the dives is less then an hour.

The total time for decompression has a group relating to dives with no decompression stops and then a steadily decreasing numbers of dives with increasing total time for decompression.

The partial pressure of oxygen breathed by the divers has two noticeable groups; one at 0.75 bar (EDU185S trial) and one around 1.3 bar. The rest of the partial pressure of oxygen values are spread across the range between 0.7 and 1.8 bar.

To see if the four variables plotted in Figure 3.2 acted as discriminatory predictor factors for the outcome of decompression illness in a dive the maximum depth, bottom time, total time for decompression and partial pressure of oxygen in the breathing mix were plotted in Figure 3.3 for dives resulting in no symptoms of decompression illness. A similar plot is given in Figure 3.4 for dives that resulted in full or marginal cases of decompression illness. Visually comparing Figure 3.3 and 3.4 shows there is no discernable difference in dive outcome over this range of predictor values.

These figures also show the biasing of dive profiles present in the trial database to ensure minimal decompression illness outcomes; increasing maximum depth corresponding to decreasing bottom time, increasing total time for decompression and some increasing of partial pressure of oxygen.

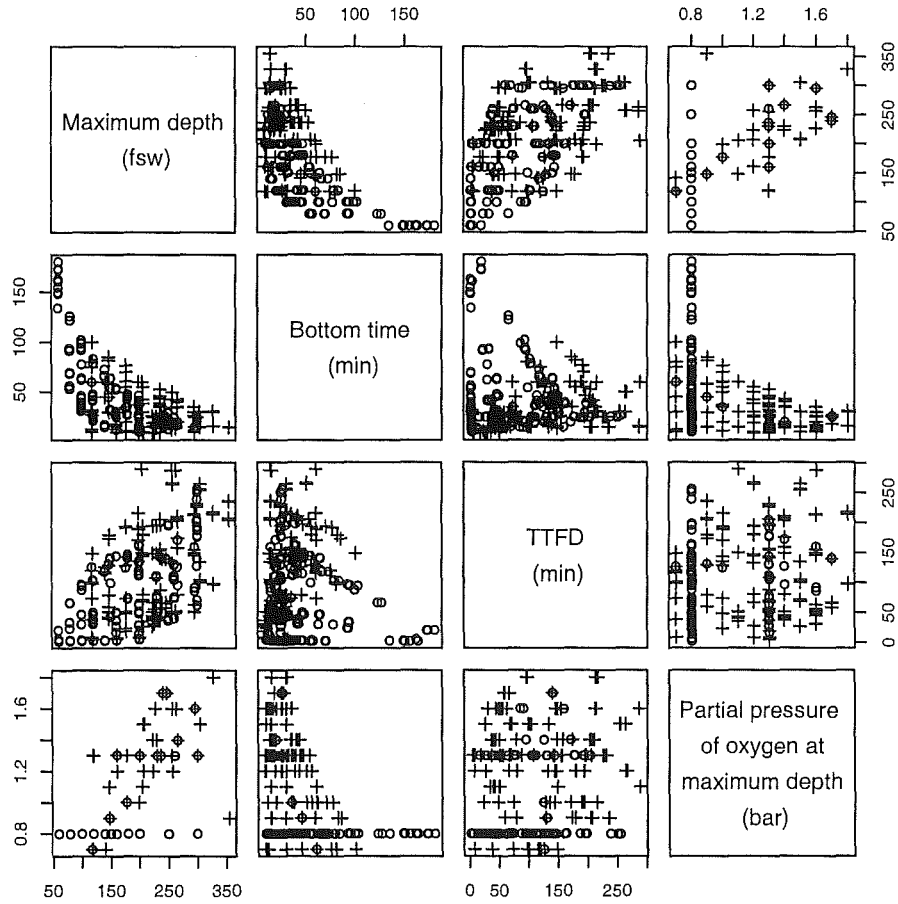

Figure 3.3 *Distribution of maximum depth, bottom time, total time for decompression and partial pressure of oxygen values for asymptomatic dives in the bounce dive data set. (+) represents dives which use close to 100% oxygen during part of the ascent, (o) represents dives which do not.*

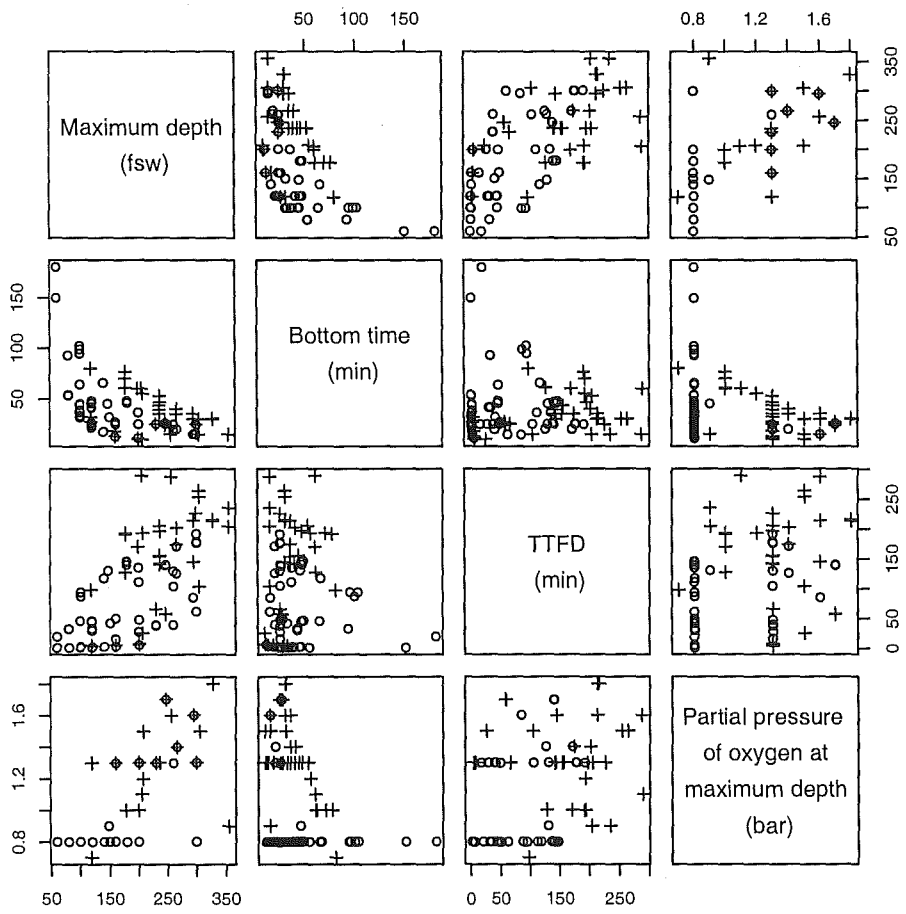

Figure 3.4 *Distribution of maximum depth, bottom time, total time for decompression and partial pressure of oxygen values for dives in the bounce dive data set that resulted in full or marginal decompression illness. (+) represent dives using close to 100% oxygen for part of the dive ascent and (o) represent dives which do not..*

3.4 Comparison of model predictions with trial data

Trial data provide the number of cases of decompression illness for the dive profiles considered in the trial. Due to time and financial constraints most dive profiles are tested by a small number of dives. If decompression illness incidence seems high, then testing of the profile is generally halted biasing the collection of data on the profile.

In terms of comparing model estimates of the risk of decompression illness with the trials data, the trial design poses the following problems:

- The trial results for a particular dive profile can only be compared against the model prediction if sufficient numbers of identical dives were completed. The smaller the number of dives the larger the confidence interval representing the likely number of observed cases of decompression illness during subsequent dives on this profile.
- The variability of decompression illness between man dives on the same profile cannot be quantified due to the small numbers of dives using the same depth and gas profile.

While the ability of a model to predict the probability of decompression illness cannot be tested for single profiles. The model can be looked at in terms of groups of dives.

A common method for examining the fit of models with a binary outcome is to use classification tables. A user defined cut point, P_c, in the model probability of decompression illness could be used to decide whether the outcome is equivalent to 1 or 0. An example of a classification table for the diving data is shown in Table 3.3.

The argument is commonly made that if the model predicts the data group membership by having high values of a and d relative to b and c, then there is evidence that the model fits the data. However the truth of this statement is dependent on the variability of DCI outcome in the data.

		Data	
		DCI	No DCI
Model	$P(DCI) \geq P_c$	a	c
	$P(DCI) < P_c$	b	d

Table 3.3 *Classification table for decompression illness outcome for a series of dives.*

Consider the data shown in Figure 3.5. Both graphs show the distribution of DCI outcome for an imaginary variable W with the same group mean values of W but different variances. While a cut point for W can be found for graph (a) which will lead to good classification results, the large variability in decompression illness as shown in graph (b) will always lead to seemingly poor classification of the data. The cut point classification procedure is also sensitive to the relative sizes of the two groups of data.

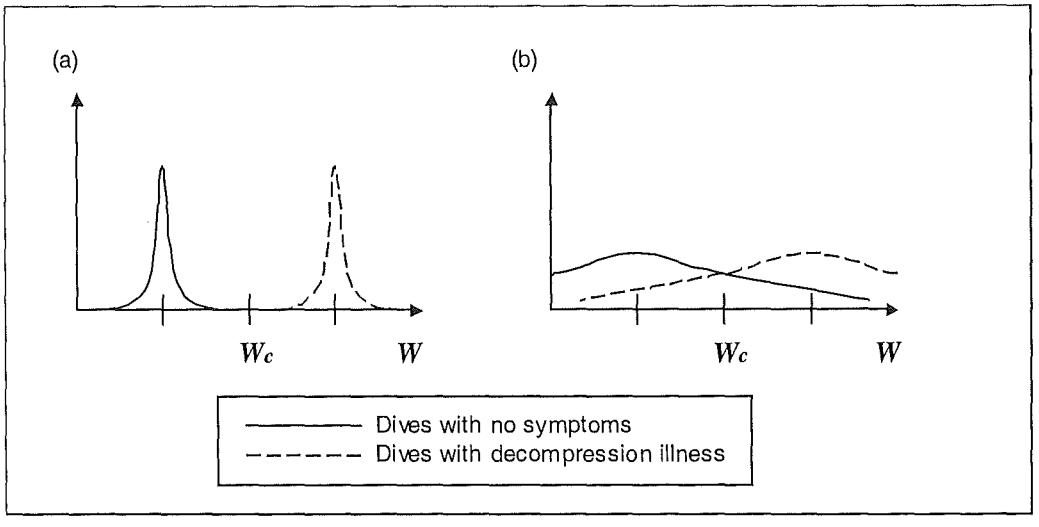

Figure 3.5 *Comparison of classification of data with small and larges variances.*

Reducing the continuous probability of decompression illness from the model to a binary outcome also over simplifies the description of the data. Consider two dive

profiles resulting in model estimates of probabilities of decompression illness of 0.048 and 0.052. In terms of the model these dives have a similar risk of decompression illness. If these dives were classified using a cut point of 0.05, the first dive profile would be considered as symptom free and the second dive as resulting in decompression illness.

Following from the above discussion, 2x2 classification tables will NOT be used to examine the fit of different models to the data.

3.5 Conclusions

The international data set provides a range of dives recorded in a common format. The bounce dives where the diver breathes oxygen in helium for part or whole of the dive have been selected for analyses in the following chapters. Dives with total dive durations which are remote from the values associated with the 240 minute duration of the 1.3 bar oxygen in helium rebreather dives have been put into a separate data set called 'outlier dives'.

The information provided does not include all the variables that may affect the decompression illness of a dive, such as ambient temperature, clothing or exercise.

Most of the data from dive trials are biased towards the safety of the diver and avoiding dives that result in decompression illness.

Plots of the dive summary variables show there is no simple relationship between decompression illness outcome and the maximum depth, bottom time, total time for decompression, partial pressure of oxygen or the use of oxygen decompression in the bounce dive data set.

Chapter 4

Review of the US Probabilistic Linear Exponential Multi-gas Model

4.1 Notation

A^T	Tissue risk weight	P_{XO}^T	Tissue bubble factor
P_{amb}	Ambient pressure (fsw)	P(DCI)	Probability of decompression illness
P_j^A	Arterial partial pressure of carrier j	$r(t)$	Hazard Function at time t
P_j^{Insp}	Inspired partial pressure of carrier j	$r^T(t)$	Tissue component of Hazard Function
P_j^T	Partial pressure of carrier j if dissolved in tissue	R_j^A	Rate of arterial partial pressure change in carrier j
$\overline{P}_j^T$	Total partial pressure of carrier j in tissue volume.	V^T	Proportional to bubble volume per unit tissue volume for given tissue
PO_2^{SET}	Offset for partial pressure of oxygen used for metabolic processes	σ_j^B	Solubility of carrier j in blood
P_{thr}^T	Tissue risk threshold factor	σ_j^T	Solubility of carrier j in tissue

4.2 Introduction

The American decompression modelling team, who until recently were based at the Naval Medical Research Institute (NMRI) at Bethesda developed a probabilistic model for predicting the risk of decompression illness associated with a dive [NMRI, 1995, 1996]. The last model developed by the NMRI team uses up to three of the following breathing gases: Oxygen, nitrogen and helium and will be called the probabilistic Linear Exponential Multi-gas model (LEM). Subject to the choice of model parameters all three gases can contribute to the risk of decompression illness.

This chapter first describes the LEM model and some of the assumptions made in its development. A study into the sensitivity of the model to fluctuations in the partial pressure of oxygen characteristic of rebreathers is then described. The chapter concludes by assessing the decompression illness prediction results of the LEM model as produced by the PROB3 program.

The LEM model was chosen to be the physiological – risk model for the optimisation work in Chapters 7 and 9 because it was the only model available to the author that was specifically calibrated for constant 1.3 bar oxygen in helium dives. However, due to the lack of published or confirmed details about parts of the development of the model, this may not be a precise replication of the US model.

The model described in this section has been implemented in a C software program called PROB3 [Horn, 1999a]. All the LEM results given in this thesis were produced using the PROB3 program.

4.3 LEM model overview

The risk of decompression illness predicted by the LEM model is a function of:

1. **The dive time, depth and breathing gas profile.**

2. **The physiological model** provides a simplified model of pressure dependent gas exchange between the body tissues, venous and arterial

systems and lungs. Exponential gas exchange kinetics are used when a gas phase is absent and a bubble model is used when a gas phase is present.

3. **The risk model** that converts the carrier partial pressures in the body tissues into a probability of decompression illness.

The link between the physiological and risk models is the total pressure of the carriers; oxygen, nitrogen and helium plus the metabolic gases in the tissues.

4.4 Physiological model

The physiological model described here is a simplified representation of human physiology and does not attempt to describe the details of the complete physiological system. Some of the assumptions made in the model development are discussed in the next section.

The diver breathes from breathing apparatus where the gas supplied to the diver is free of water vapour. The sum of the partial pressures of the inspired gases, P_j^{Insp}, is equal to the ambient pressure, P_{amb}, at the mouth of the diver. The j in P_j represents one of the possible carrier gases; nitrogen, helium or oxygen that is not used metabolically and will go into solution in the blood or tissue.

The inspired gases enter the airways and lungs of the diver where the inspired gas is mixed with water vapour and carbon dioxide. No account is taken of mixing with any oxygen or carrier already present in the airways. Gas exchange between the lungs and blood is continuous and the blood is fully equilibrated with the lung gases. The partial pressure of nitrogen or helium in the arteries, P_j^A, is proportional to the appropriate inspired carrier partial pressures;

$$P_j^A = P_j^{Insp}\left(\frac{P_{amb} - P_{H_2O} - P_{CO_2}^A}{P_{amb}}\right) \qquad (4\text{-}1)$$

where P_{H_2O} is the partial pressure of water vapour in the arteries or tissues and $P^{A}_{CO_2}$ is the partial pressure of carbon dioxide in the arteries.

The partial pressure of arterial oxygen that will not be metabolised in the body, $P^{A}_{O_2}$, is controlled by the model parameter $PO_2{}^{SET}$. If $PO_2{}^{SET}$ is greater than the partial pressure of inspired oxygen, $P^{Insp}_{O_2}$, all the oxygen inspired is set aside for metabolic processes. If $PO_2{}^{SET}$ is less than the partial pressure of inspired oxygen, a proportion of the difference contributes to the total gas arterial pressure:

$$P^{A}_{O_2} = \begin{cases} \left(P^{Insp}_{O_2} - PO_2^{SET}\right)\left(\dfrac{P_{amb} - P_{H_2O} - P^{A}_{CO_2}}{P_{amb}}\right) & P^{Insp}_{O_2} > PO_2^{SET} \\ 0 & P^{Insp}_{O_2} \le PO_2^{SET} \end{cases} \qquad (4\text{-}2)$$

The arterial blood transports the inspired gases to the tissues of the body. This model represents the body as three tissues of different properties. It is assumed that these three tissues are sufficient to model the processes that result in decompression illness. Each tissue is completely independent of the other two tissues, as shown in Figure 4.1. Depending on the pressure gradient of the partial pressures of the carrier in the arteries, P^{A}_{j}, compared to the tissues, P^{T}_{j}, carrier will transfer in to or out of the tissues.

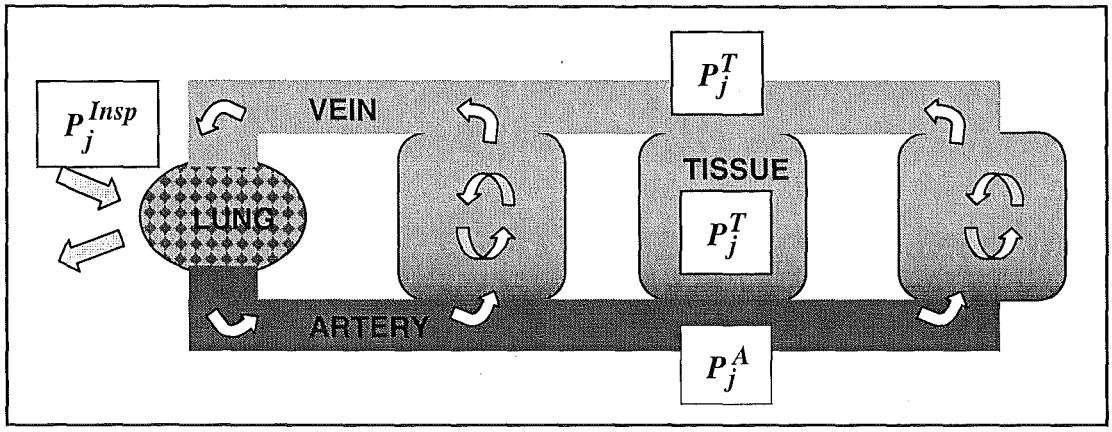

Figure 4.1 Block diagram of physiological parallel tissue model

The tissues can have a number of gases present within them, either dissolved in solution or in a gaseous form in a bubble; nitrogen, $P_{N_2}^T$, helium, P_{He}^T, oxygen that will not be used for metabolic processes, $P_{O_2}^T$, and metabolic gases, $P_{metabolic}$.

The partial pressure of the metabolic gases is assumed to be a constant value for the duration of the dive and is the same for each of the tissues. The early parameter sets used metabolic gas values of;

$$\left.\begin{aligned} P_{H_2O} &= 2.04\ fsw \\ P_{CO_2}^T &= 2.30\ fsw \\ P_{O_2}^{T(met)} &= 2.00\ fsw \end{aligned}\right\} \quad P_{metabolic} = 6.34\ fsw .$$

Later parameter sets defined the partial pressure of the metabolic gases to be zero, arguing that the tissue parameters for oxygen, nitrogen and helium can compensate for the removal of these gases from the model.

When the total pressure in tissue T is less than a small amount P_{XO}^T above ambient pressure,

$$\sum_j P_j^T + P_{metabolic}^T \leq P_{amb} + P_{XO}{}^T \tag{4-3}$$

all the carrier in the tissue is in solution and the gas exchange for oxygen, nitrogen and helium occur independently of the other two gases.

While the gases are in solution, the gas kinetics follow the established exponential formula developed by Thalmann [1985];

$$\frac{dP_j^T}{dt} = K_j \left(P_j^A - P_j^T \right) \tag{4-4}$$

where $K_j = \frac{\sigma_j^B}{\sigma_j^T} \frac{dQ}{dt}$

and σ_j^B is the solubility of gas j in the blood, σ_j^T the solubility of gas j in the tissue and $\frac{dQ}{dt}$ is the blood flow per unit tissue volume.

If the tissue partial pressure of carrier j is known at time t_i, then the tissue partial pressure of gas j at t_{i+1} is given by,

$$P_j^T(t_{i+1}) = P_j^A(t_i) + \left(P_j^T(t_i) - P_j^A(t_i)\right) e^{-K_j \delta t} + R_j^A \left\{ \delta t + (1/K_j)\left(e^{-K_j \delta t} - 1\right)\right\} \tag{4-5}$$

where δt is the time interval between points t_i and t_{i+1} and R_j^A is the rate of arterial partial pressure change with time of carrier j.

To form a bubble in the tissue the partial pressure of the gases present in the tissue must be greater than ambient by a small factor, P_{XO}^T, to over come the effects of surface tension that will try to shrink and collapse a bubble. In other words for a bubble to form in tissue T,

$$\sum_j P_j^T + P_{metabolic}^T > P_{amb} + P_{XO}{}^T \tag{4-6}$$

The total pressure in the tissue can not physically increase more than a small amount over ambient, unless a bubble is formed into which excess gases will flow. To describe this scenario, we need to define two pressures, the physical partial pressure of a carrier in the tissue, $\bar{P}_j^T$, and the partial pressure of carrier j if all the gas was forced into solution, P_j^T. These two pressures are related via the expression,

$$\bar{P}_j^T = \frac{P_j^T \sigma_j^T}{\sigma_j^T + V^T} = \frac{P_j^T}{1 + \frac{V^T}{\sigma_j^T}} \tag{4-7}$$

where V^T is a scaled value of the bubble volume per unit tissue volume, which has the same units as solubility. While a bubble exists the following relationship must hold true.

$$\sum_j \bar{P}_j^T + P_{metabolic}^T = P_{amb} + {P_{XO}}^T \tag{4-8}$$

The gas kinetics with bubbles present is given by,

$$\frac{dP_j^T}{dt} = K_j \left(P_j^A - \bar{P}_j^T \right). \tag{4-9}$$

The numerical solution for gas exchange equation (4-9) for the interval t_i to t_{i+1} is found by iteratively solving two equations. The first equation estimates the partial pressure of each carrier in the tissue,

$$P_j^T(t_{i+1}) = P_j^T(t_i) e^{-\beta_j^T \delta t} + \frac{K_j^T}{\beta_j^T} P_j^A(t_i) \left(1 - e^{-\beta_j^T \delta t}\right) + \frac{K_j^T}{\beta_j^T} R_j^A \left\{ \delta t + \frac{1}{\beta_j^T} \left(e^{-\beta_j^T \delta t} - 1 \right) \right\}$$

where

$$\beta_j^T = \frac{K_j^T}{1 + \frac{V^T(t_{i+1})}{\sigma_j^T}} \tag{4-10}$$

Once the partial pressure of carrier estimates are known a new bubble volume factor, V^T, is calculated from equations (4-7) and (4-8). The iterations continue until the bubble volume factor has converged. Note, the exchange of carriers; oxygen, nitrogen and helium are no longer independent of each other, but are linked via the bubble volume.

4.5 Physiological assumptions

1. *The body and physiological processes can be modelled as three parallel and independent tissues.*

   The body is a complex system of materials and processes. To try to model this in detail is beyond our current knowledge and computing capabilities. A better approach is to start with a simplistic and useable model and add on components as required to fit the model to the trials data. The basic parallel tissue model is trusted in the diving community and forms a proven foundation for more complicated model components.

2. *The carrier concentration through out the tissue is constant, or in other words there is no carrier concentration gradient across the tissue volume.*

   Examination of most tissues reveals a large number of capillaries per unit volume, where intercapillary distance is normally measured in fractions of a millimeter [Curtis & Barnes, 1989]. Accepting normal diffusion coefficients for small gas molecules such as nitrogen and helium it would be impossible to sustain large concentration gradients in well perfused tissues. In tissues which are poorly perfused the saturation and desaturation across the tissue

would be slower. However the concentration gradients across tissues are more likely to be influenced by the control of blood in the capillaries in response to temperature, exercise and carbon dioxide levels.

3. *The partial pressure of carrier in the arterial system arriving at the tissue is in equilibrium with the partial pressure of carrier in the lungs.*

Theory suggests that changes to ambient breathing gas pressure will be instantly transmitted to the alveoli in the lung. It takes approximately 0.01 seconds for dissolved molecules to reach the pulmonary capillaries from the alveoli and a second for the blood to pass the length of the pulmonary capillary. At these time scales the error introduced by this assumption is small.

Hyperbaric experiments on rabbits exposed to sudden changes in inspired carrier [Tikuisis et al., 1985] found that arterial blood was not instantaneously changed in line with the inspired gas. For a sudden change from breathing 10% oxygen in nitrogen to 10% oxygen in helium at ambient pressure of 5 bar, a period of 17 minutes was required to reach 99% Helium saturation. The time taken to reach 99% saturation with nitrogen after a change from breathing a helium mix to a nitrogen mix took 55 minutes. This research suggests the need for a carrier exchange mechanism between the arteries and the lungs in a similar manner as between the arteries and tissues.

4. *The partial pressure of carbon dioxide in the arterial system is constant throughout the dive.*

The partial pressure of carbon dioxide in the arterial system will be fairly constant if the diver is breathing normally and there is no damage or obstructions in the lungs. The lungs are very efficient at removing carbon dioxide from the blood.

Divers sometimes hypoventilate to conserve their breathing gas. Hypoventilation causes carbon dioxide to build up in the tidal volume of the lungs which hinders the removal of carbon dioxide from the blood. This may lead to increased levels of arterial carbon dioxide and a decrease in the carrier transferred from the lungs to the blood from the inspired gas.

5. *The partial pressure of carrier in the venous system is the same as the partial pressure of carrier in the tissues.*

Where the capillary enters the tissue, the partial pressure of carrier in the blood will be equal to that in the artery. This provides the carrier concentration gradient used in the LEM model for carrier exchange. This assumption means that the blood leaving the tissue capillaries is fully equilibrated with the tissue, removing the venous system from the model. However, no effort is made to model the change in blood carrier concentrations as the blood flows through the tissue capillaries. The LEM carrier exchange looks at the greatest rates of carrier uptake and elimination possible by comparing arterial with tissue carrier concentrations, as in the case of a very short capillary.

4.6 Risk model

The probability of decompression illness for a dive can be calculated from the expression,

$$P(DCI) = 1 - e^{-\int r dt} \tag{4-11}$$

where $e^{-\int r dt}$ is the survival function and **r(t)** is the hazard function [Kleinbaum 1996]. The hazard function is defined as the instantaneous potential per unit time for decompression illness to occur given that the diver is free of decompression symptoms up to time t.

The hazard function is dependent on the total tissue pressure of carrier if it was forced into solution, P_j^T, a tissue dependent threshold parameter P_{thr}^T, a tissue dependent gain, A^T and the maximum depth of the dive:

$$r(t) = \mathbf{max\_depth}^{PWR} \sum_{tissue\ T} A^T r^T(t) \tag{4-12}$$

where

$$r^T(t) = \begin{cases} \dfrac{\sum_{gas\ j} P_j^T(t) + P_{metabolic}^T - P_{amb}(t) - P_{thr}^T}{P_{amb}(t)} & \sum_{gas\ j} P_j^T(t) + P_{metabolic}^T > P_{amb}(t) + P_{thr}^T \\ 0 & otherwise. \end{cases}$$

In the model development the PWR parameter was included to incorporate the perception that deeper dives are associated with higher risks of decompression illness. In the parameter sets seen by the author [NMRI, 1995, 1996] the $\mathbf{max\_depth}^{PWR}$ value is one, removing the maximum depth scaling factor. The value of one has been used for these results in this thesis.

The probability of decompression illness is a function of the integral of the hazard function over the whole process of decompression including the surface time following the dive. This means that a dive involving low instantaneous hazard, ***r(t)***, for a long time period may have a similar probability of decompression illness as a dive with very high instantaneous hazard for a short period of time. If the symptoms of decompression illness are related to bubble volume, then short duration - high instantaneous hazard may be more significant than long duration - low hazard.

4.7 LEM Parameter Set

The LEM model uses three tissues. Each tissue is defined by seven parameters:

- Gas exchange half-time between tissue and blood circulation for nitrogen,
- gas exchange half-time between tissue and blood circulation for helium,
- gas exchange half-time between tissue and blood circulation for oxygen,
- partial pressure threshold for non zero risk, P^{THR},
- risk weighting factor, A^{T},
- tissue carrier pressure above ambient over which a bubble exists, P_{xo}, and
- a factor to control the amount of oxygen in the tissue that can act as a carrier instead of being used metabolically, PO_2^{SET}.

The US calibration of parameters for the LEM model was conducted using the Levenberg-Marquardt least squares method [Marquardt, 1963; Bailey & Homer, 1977] to maximise the log likelihood of the model outcome given the trials data. This iterative method was highly sensitive to the choice of starting parameter values, suggesting there are many local solutions to the parameter estimation problem.

The parameter set used for this thesis was produced following the US Human decompression trial [Survanshi et al., 1998] with 1.3 ATA oxygen in helium conducted in 1995-6 (Data set NMR9404) . So these dives would have been included in the data set used for parameter calibration. It is possible that a number of trials where the divers only breathed oxygen in nitrogen gas mixes would have also been included in the calibration data set.

For commercial reasons the parameter values cannot be given in this thesis, instead a general description is given below. The twenty one parameters describe a three tissue model.

The first tissue has the biggest weighting to the risk of DCI, with all three gases having short half-times for gas exchange. Partial pressures of oxygen may contribute to the risk of DCI. The bubble model is initiated close to supersaturation, however a larger threshold pressure above ambient must be reached before contributing to the hazard function than the other two tissues.

Oxygen does not contribute to the total carrier partial pressure for tissues two and three. Tissue two with very short tissue carrier half-times uses the bubble model for supersaturation, however tissue three with the longest tissue carrier half-times is constrained to have both exponential uptake and elimination of nitrogen and helium.

4.8 Sensitivity of LEM model to the format of partial pressure of oxygen input

In an ideal world the gas control system of rebreather apparatus would ensure that the partial pressure of oxygen breathed by a diver would remain exactly at the required value. In the real world this is not yet possible and a cyclic update occurs as shown in Figure 4.2. This leads to two characteristics of rebreather dives:

- The oxygen level is breathed down to a certain point, then extra oxygen is added to the breathing loop until the oxygen level reaches a prescribed level (◆), and so the cycle continues.
- An overshoot in partial pressure of oxygen may occur during the descent of the diver (▼).

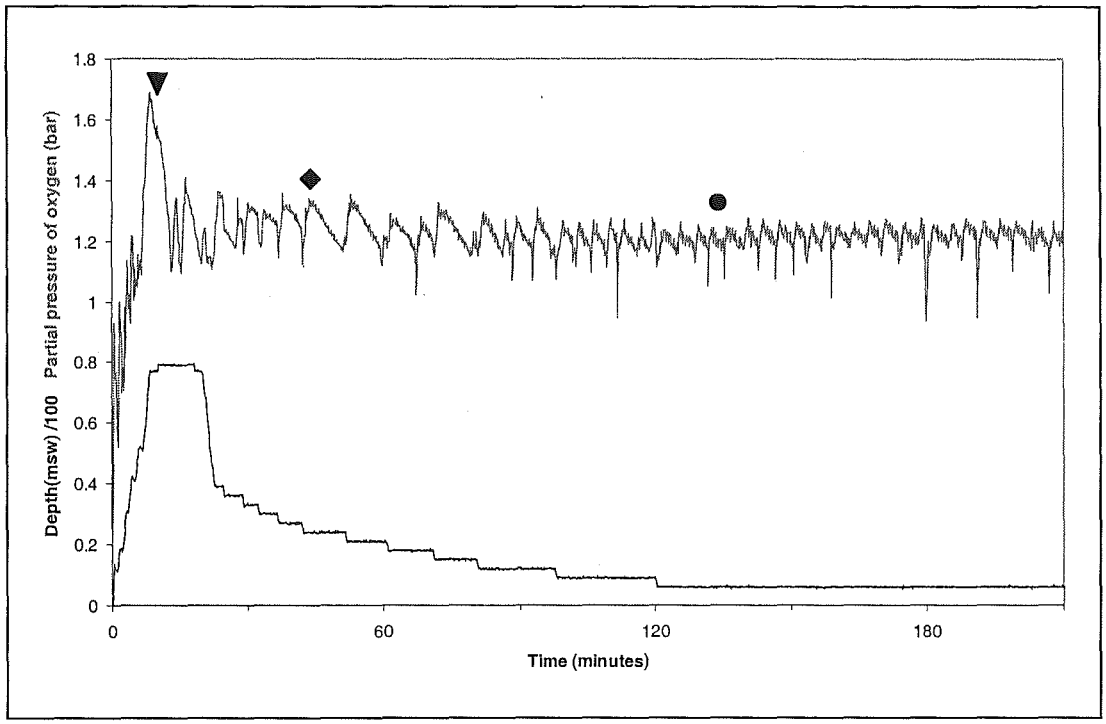

Figure 4.2 *The partial pressure of oxygen breathed by a CDBA diver and time depth profile during a 1.3 bar oxygen in helium dive to 80 msw in 1997 [Gay et al., 1997]. Triangle indicates PO_2 overshoot due to ascent, diamond indicates the start of the 24 msw stop and the circle the start of the 6 msw stop.*

While each dive equipment and diver may provide different profiles, the general features of rebreather oxygen partial pressure profiles are similar. As discussed in chapter two the description of the partial pressures of gases may be simplified to avoid overly large data sets. Individual trial reports should be consulted to see how the database partial pressure of oxygen was defined if rebreathers were used. There does not seem to be a consensus on how the partial pressure of oxygen is defined.

This section compares the PROB3 results using a simplified example of the partial pressure of oxygen breathed by the diver with the constant partial pressures of oxygen used in the trial database. To examine the sensitivity of the model to fluctuations in the partial pressure of oxygen, two sets of simulations were completed.

(a) Partial pressure of oxygen overshoot on descent:

During the descent there is an overshoot in the partial pressure of oxygen, which lasts for a number of minutes, as seen in Figure 4.2. The overshoot in pressure arises from the control system introducing too much diluent into the breathing loop during the rapid increase in ambient pressure on descent. The PROB3 program was run for dive profiles with and without the oxygen spike. The probability of decompression illness for a dive including an oxygen spike was less than for the dive with no oxygen spike. Therefore, designing decompression tables with dive profiles containing no oxygen spikes should be a safe approach. If future parameter sets incorporate greater oxygen effects through their values of PO_2^{SET} and oxygen half-time, the effect of this overshoot should be readdressed, especially for short but deep dives.

(b) Cyclic oxygen partial pressure:

A cyclic component to the oxygen and helium partial pressure was created by imposing saw-tooth noise over the constant pressure value. The saw-tooth noise profile was continually applied to the inspired partial pressure of oxygen and helium while the ambient pressure was greater than sea level. Once the diver removed the set and breathed air the partial pressure of oxygen becomes constant again. For the duration of the dive ambient pressure is maintained in the breathing loop by allowing the inert gas, in this case helium, to compensate for the oxygen as shown in Figure 4.3.

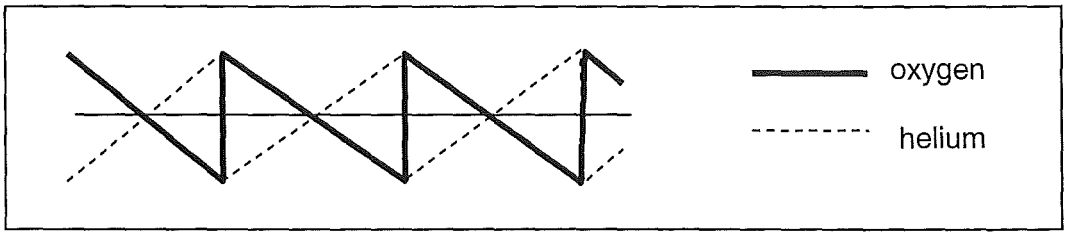

Figure 4.3 Noise profile

The amplitude and period of the saw-tooth profile was chosen to relate to two positions in Figure 4.2. Figure 4.4 shows the two cases considered; Case A (Figure 4.2 ●) based on data at the 6 msw decompression stop and Case B (Figure 4.2 ♦) based on data at the 24 msw to 15 msw stops.

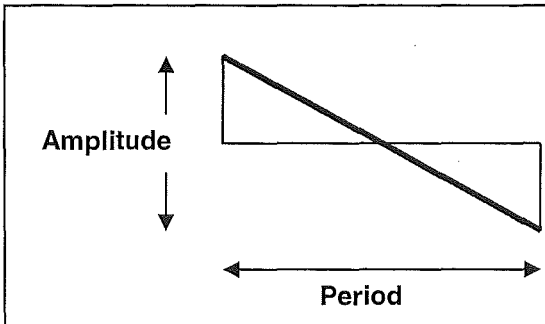

Case	A	B
Amplitude (bar)	0.1	0.21
Period (minutes)	4.0	7.0

Figure 4.4 Sample noise profiles, Case A, B and C.

Two different dive profiles from Interim MCM/EOD LSE Table B [Anthony & Horn, 1997] were considered: A deep dive with a long in water decompression time (81msw/20 minutes) and a shallower dive for the same bottom time but only requiring 6 minutes of in water decompression (36msw/20 minutes). The constant partial pressure of oxygen was set to either 0.4 bar , 0.7 bar or 1.3 bar.

Table 4.1 shows the probability of decompression illness, P(DCI), for the dives described above using a constant partial pressure of oxygen and the difference in P(DCI) for each of saw-tooth cases A and B compared to the constant partial pressure of oxygen value.

Columns 4 and 5 of Table 4.1 show the difference between the P(DCI) of a dive with the saw tooth gas profile and with a constant oxygen partial pressure profile. In all cases the constant partial pressure of oxygen profile under-predicts the probability of decompression illness caused by the rebreather.

Both the 1.3 bar partial pressure of oxygen dives show a very close agreement between the constant and sawtooth gas profiles. While the difference in risk for an

oxygen set point of 0.7 bar is still below one case of decompression illness in a thousand, the difference in risk increases when further reducing the oxygen set point to 0.4 bar.

Profile	PO_2 of breathing mix	P(DCI| constant PO_2)	P(DCI | saw tooth PO_2) – P(DCI | constant PO_2)	
			Case A	Case B
BT: 20 min MD: 81 msw TTFD: 199 min	0.4 bar	0.099478	0.012115	0.031345
	0.7 bar	0.059857	0.000387	0.000975
	1.3 bar	0.016430	0.000001	0.000021
BT: 20 min MD: 36 msw TTFD: 6 min	0.4 bar	0.061142	0.000570	0.001103
	0.7 bar	0.039488	0.000426	0.000778
	1.3 bar	0.010839	0.000106	0.000003

Table 4.1 *Comparison of decompression illness risk for constant and non constant partial pressure of oxygen.*

In summary when using the LEM model;

- The difference between the P(DCI) for constant and saw tooth gas profiles is very small and decreases with increasing median partial pressure of oxygen.
- For a median partial pressure of oxygen of 1.3 bar the effect of ignoring rebreather fluctuations in the partial pressure of oxygen is negligible.
- For a median partial pressure of oxygen of less than 0.7 bar the effect of ignoring the rebreather fluctuations in partial pressure of oxygen causes the LEM model to under predict the risk of decompression illness in a more significant way. For low median partial pressures of oxygen sensitivity analyses should be conducted when using the LEM model for rebreather dives. Including the partial pressure of oxygen over shoot on descent in the dive profile lowers the risk of DCI.

4.9 PROB3 analysis of oxygen in helium dives

The PROB3 program was used to predict the probability of decompression illness for the oxygen in helium dives described in Chapter 3. The US team calibrated the model parameters using some or all of the dives recorded in the database. Therefore, there will be some overlap in the data used to train the model and now being used to test it.

Tables 4.2 and 4.3 shows the prediction capability of PROB3 program to describe the risk of decompression illness associated with a given dive trial from the bounce and outlier dive data. This is a test of the model under different dive types and environmental conditions. The number of dives in each of the trials ranged from 27 to 1562.

Column 3 shows the number of decompression illness cases observed in the data set and column 5 gives the number of decompression illness cases predicted by the PROB3 model. This expected frequency is the sum of the probability of decompression illness of all dives in the data set.

The trial size and number of decompression illness cases for each trial was used to calculate a 95% confidence interval for the number of decompression illness cases in a trial of the same size [Horn, 1999b]. Column 4 gives the estimate of the 95% confidence interval. The marginal cases of decompression illness were given a value of 0.1 for the purpose of calculating the confidence interval. This is an estimate of the confidence interval because the assumption is made that the variability in decompression illness risk is the same for all the dive profiles in the dataset. A measure of the variability in decompression risk for different dive profiles is not known. The table cells shaded grey indicate that the frequency of decompression illness predicted by PROB3 is outside the 95% confidence interval for the trial data.

To remove the data set size factor from the comparisons the last column in Table 4.2 and 4.3 gives the difference between the trial and PROB3 outcomes normalised by the number of dives in the trial. For this calculation a marginal case of decompression illness was given a value of 0.1. The same value as used by the US in

the estimation of parameter sets from the trials data [Parker et al., 1992]. The data sets have been ordered by the difference in expected and observed frequencies of decompression illness as given in the last column of the tables.

Table 4.3 shows the outcome of decompression illness for all the outlier data dives grouped by trial is well predicted by the PROB3 program. The PROB3 program also predicts within the 95% confidence interval for most of the bounce dive trials as shown in Table 4.2.

The NMR9404 trial consisting of 1.3 bar oxygen in helium dives is predicted well by the PROB3 program, which is to be expected as the model parameters were generated after this trial. The predicted frequency of decompression illness is below the trial outcome but well within the 95% confidence intervals for the trial.

(1) Dataset	(2) Man dives	(3) Observed cases of full DCI (marginal DCI)	(4) Trial 95% confidence interval	(5) PROB3 Expected cases of DCI	(6) (Expected - Observed) / Man dives
DC8416W	178	4 (0)	1.1 – 10.1	16.8	+0.072
DC8416D	430	14 (2)	7.7 – 23.2	42.5	+0.066
DC8416S	91	7 (0)	2.9 – 13.8	8.7	+0.019
DRATMXA	66	1 (0)	0 – 5.4	1.9	+0.014
EDU185S	1562	56 (2)	42.5 – 72.3	73.2	+0.011
EDUHE70	152	13 (2)	7.0 – 21.6	12.8	-0.003
NMR9404	461	25 (22)	18.0 – 38.8	22.5	-0.012
NMR9404o	32	1 (0)	0 – 5.2	0.6	-0.013
DRATMXW	131	8 (0)	2.6 – 15.3	5.8	-0.017

Table 4.2 *Observed and PROB3 predicted decompression illness outcomes for dives in the bounce dive data set.*

Dataset	Man dives	Observed cases of full DCI (marginal DCI)	Trial 95% confidence interval	PROB3 Expected cases of DCI	(Expected - Observed) / Man dives
DCHELONG	27	0 (0)	0 – 3.4	1.5	+0.055
DRATMXA	27	0 (0)	0 – 3.4	1.3	+0.048
NMR86H6	60	1 (0)	0 – 5.4	3.8	+0.047
DRATMXW	58	2 (10)	0.6 – 8.3	3.2	+0.003
NSMTMX	69	4 (0)	1.1 – 9.8	3.4	-0.009
EDUHE70	110	18 (1)	11.0 – 27.1	16.2	-0.017

Table 4.3 *Observed and PROB3 predicted decompression illness outcomes for dives in the outlier dive data set.*

In contrast the PROB3 program strongly over predicts the outcome of decompression illness for some of the dives in the DC8416W, DC8416D and EDU185S trials. The DC8416W and DC8416D dives that are over predicted are mainly deep dives to depths of more than 200 fsw and for bottom times in the range 30 to 55 minutes. In contrast, the well fitted NMR9404 trial dives to 200 – 300 fsw had bottom times of 20-25 minutes. The DC8416W and D dives with longer bottom times would absorb more carrier into the slow tissues of the model and correspondingly have more carrier to remove from the tissues on ascent.

It is noticeable the outlier data is well predicted by the PROB3 program, suggesting that at least some of this data was used to calibrate the model. This is a possible reason for the deeper, longer dives in the bounce dive data set producing too great a risk of decompression illness.

The EDUHE70 dives in the outlier data set have maximum depths greater than 200 fsw and for bottom times in the range 20 to 90 minutes. The percentage of dives resulting in decompression illness is 16.45%. Table 4.3 showed that PROB3

predicted the outcome of these dives closely. If these EDUHE70 dives were used in the calibration dataset, the risk could be biased to higher values for longer, deeper dives.

Next, the ability of PROB3 to predict decompression illness risk independently from trial design and size was investigated. The bounce dive data was split into 10 quantiles based on the PROB3 risk of decompression illness for each of the man dives. Table 4.5 shows the observed and predicted decompression illness outcomes for each of the 10 quantiles of data. There are three noticeable features to the results:

1. The number of decompression illness cases estimated by PROB3 is more than or close to the observed trial data. The exception being group four with 16.4 observed cases of decompression illness compared to the 11.7 cases predicted by the PROB3 program. The difference is due to dives from the EDU185S trial. Investigation of the dive profiles has shown no obvious dive profile type leading to this grouping. The intervals of probability values over groups 3 to 7 is small and the 11.7 predicted cases is well within the range of values given by the 95% confidence interval. Therefore, this grouping is likely to be a result of the variability in the decompression illness outcome.

2. Between groups 2 and 8, relating to a probability of between 0.018 and 0.068 there seems to be a slight increase in the dive outcomes. There is a greater increase in the PROB3 outcomes, but they remain within the range given by the 95% confidence interval.

3. Groups 9 and 10 contain the highest risk profiles as defined by the PROB3 program, with associated probability of decompression illness of between 0.068 and 0.44. PROB3, while following the trend of increasing risk as shown by the trial data, over predicts the risk of the decompression illness. Again this discrepancy relates to the DC8416D data where 10.2 decompression illness cases occurred in the data compared to 30.3 predicted by the PROB3 program in quantile 10. Also, DC8416W data provides 3 cases of decompression illness compared to the 11.2 cases predicted by PROB3 in quantile 10.

For most military decompression table design, the acceptable probability of decompression illness will be in the range of 0.005 and 0.05 that corresponds to the first five groups in Table 4.5. The LEM prediction capability for this risk interval is good.

Table 4.4 shows the incidence of decompression illness for dives involving breathing near to 100% oxygen during decompression (oxygen decompression) and those that do not use oxygen decompression. The simpler two-carrier gas, LE model described in Chapter 2, was found to underestimate the risk of decompression illness when near to 100% oxygen was breathed on ascent [Survanshi et al., 1994]. A chi-squared test of Table 4.5 was conducted with the null hypothesis; the number of decompression illness cases allocated to each type of decompression is independent of the actual or predicted results. The resulting chi-square value of 1.147 supports the null hypothesis and indicates the LEM model with current parameters has similar prediction capability for dives using oxygen decompression or not. This may be due to the introduction of oxygen as a carrier in one of the tissues.

	Number of dives	Number of observed cases of decompression illness	Number of PROB3 predicted cases of decompression illness
Oxygen decompression	1134	50.3	81
No oxygen decompression	1970	82.5	103.57

Table 4.4 *Comparison of the number of PROB3 predicted and trial observed cases of decompression illness for dives using oxygen decompression and those not using oxygen decompression.*

Group Number	1	2	3	4	5	6	7	8	9	10
$P(DCI)_{PROB3}$ interval	0.0002 to 0.0178	0.0178 to 0.0278	0.0278 to 0.0345	0.0345 to 0.0396	0.0396 to 0.0484	0.0484 to 0.0549	0.0549 to 0.0614	0.0614 to 0.0683	0.0683 to 0.12	0.12 to 0.44
$P(DCI)_{PROB3}$ group mean	0.0107	0.0228	0.0319	0.0373	0.0430	0.0524	0.0582	0.0645	0.0908	0.183
Number of dives	313	312	306	314	308	317	309	304	310	311
PROB3 estimated cases of DCI	3.4	7.1	9.8	11.7	13.3	16.6	18.0	19.6	28.1	57.2
Observed cases of DCI full (marginal)	2 (0)	8 (3)	6 (4)	16 (4)	8 (3)	11 (0)	11 (1)	13 (2)	21 (7)	34 (4)
Trial 95% confidence interval	0.2 to 7.2	3.5 to 15.6	2.2 to 12.9	9.2 to 25.6	3.5 to 15.6	5.5 to 19.4	5.5 to 19.4	7.0 to 21.9	14.0 to 32.7	23.9 to 46.5

Table 4.5 *Comparison of observed and PROB3 predicted decompression illness frequency for oxygen in helium dives grouped by the PROB3 predicted probability of decompression illness.*

4.10 Conclusions

This section has reviewed the LEM model as implemented in the PROB3 program. When using the PROB3 program the following should be noted:

- For the parameter set used in this chapter, the simplification of rebreather gas mix profiles to a constant partial pressure of oxygen rather than a cyclic partial pressure produces a negligible difference in probability of decompression illness when the partial pressure of oxygen is at 1.3 bar.

- If future parameter sets incorporate greater oxygen effects through their values of PO_2^{SET} and oxygen half-time, the effect of the overshoot in partial pressure of oxygen on descent should be investigated, especially for short but deep dives.

Comparing the frequency of decompression illness predicted by the PROB3 program with the current parameter set and the trials data has shown:

- For most dives in the database listed in Chapter 3, the PROB3 program provides a reasonable risk of decompression illness for a dive. This is true for the 1.3 bar oxygen in helium dive data (NMR9404).

- For dives to depths deeper than 200 fsw for longer bottom times such as 30 minutes or more, PROB3 markedly over predicts the risk of decompression illness.

- The over prediction of the risk for these deep, longer dives could be due to the inclusion of high risk dives from the EDUHE70 trial in the calibration data set which have deep dives with bottom times in the range of 20-90 minutes.

- When the data set is split into dives involving oxygen decompression and not using oxygen decompression, PROB3 over predicts the risk of decompression illness for both groups of dives. The inclusion of oxygen as a carrier in one tissue prevents the under-predicting of risk present in earlier models.

Possible future improvements to LEM include:

- Reformulating the risk model to reflect the correlation between bubble dynamics and different types of decompression illness symptoms. This could include taking into account the maximum hazard function value as well as the integrated hazard over the whole time the diver is decompressing.

- Modelling of gas exchange between the lungs and arteries to incorporate a gradual change in arterial carrier quantities after a breathing gas change.

THIS PAGE IS INTENTIONALLY BLANK

Chapter 5

Are current decompression methods iso-probabilistic?

5.1 Introduction

A decompression model has been developed for the U.S. Navy which provides a numerical value of the risk of decompression for a dive. This Linear-Exponential Multi-gas (LEM) model was described and evaluated in Chapter 4.

In this chapter, a program called PROB3 [Horn, 1999a], which implements the LEM model is used to estimate the variability in the risk of decompression illness associated with published constant partial pressure of oxygen in helium decompression schedules. PROB3 is also used to examine the decompression benefits of breathing a gas mix with a higher partial pressure of oxygen.

The mechanisms that cause decompression illness are not completely understood and no current models can accurately predict the outcome of decompression illness for a single dive. However, the LEM model is useful for making relative estimates of the risk of decompression illness.

5.2 Comparison of risk associated with published decompression tables

One of the published decompression tables for oxygen in helium rebreathers is the US Navy 0.7 ata oxygen in helium tables [US Navy, 1996b]. The table was generated by the EL model with m-value safe ascent criteria [Thalmann, 1985]. The physiological model parameters and safe ascent parameters were chosen and tested using manned diving trials where the diver breathed a partial pressure of oxygen kept in the range 0.6 to 0.8 ata .

A subset of 50 dive schedules was taken from the US 0.7 ata oxygen in helium tables. This subset of dives spanned dives with a maximum depth of 70 to 310 fsw (~21 to 95 msw) and decompression requirements from direct ascents to five hours of in water decompression.

The PROB3 program was used to estimate the risk of decompression illness of 50 schedules with the diver breathing a constant partial pressure of oxygen of 0.7 bar in helium gas mix for the dive and breathing air on surfacing. The actual decompression illness rate for these dives was not available to the author. The unit of 1 bar is approximately equal to 1 ata.

Figure 5.1 shows the estimated probability of decompression illness, P(DCI), for each dive as described by the maximum depth and the total time for decompression, TTFD. Recall the total for decompression is the time from the diver leaving maximum depth to reaching the surface.

Figure 5.1 shows there is a wide range of risk levels ranging from almost zero to seven percent probability of decompression illness across the range of maximum depths and total time for decompression. All the dives involving ascents greater than two hours have a higher risk of decompression illness associated with them.

The shallower short decompression or no stop dives have a longer bottom time than the deeper short decompression dives. For example, the shortest bottom time listed for a depth of 50 fsw is 205 minutes, compared to the 5 minute bottom times listed for maximum depths of 210 fsw and deeper. This explains the step in the risk of decompression illness for the short decompression dives.

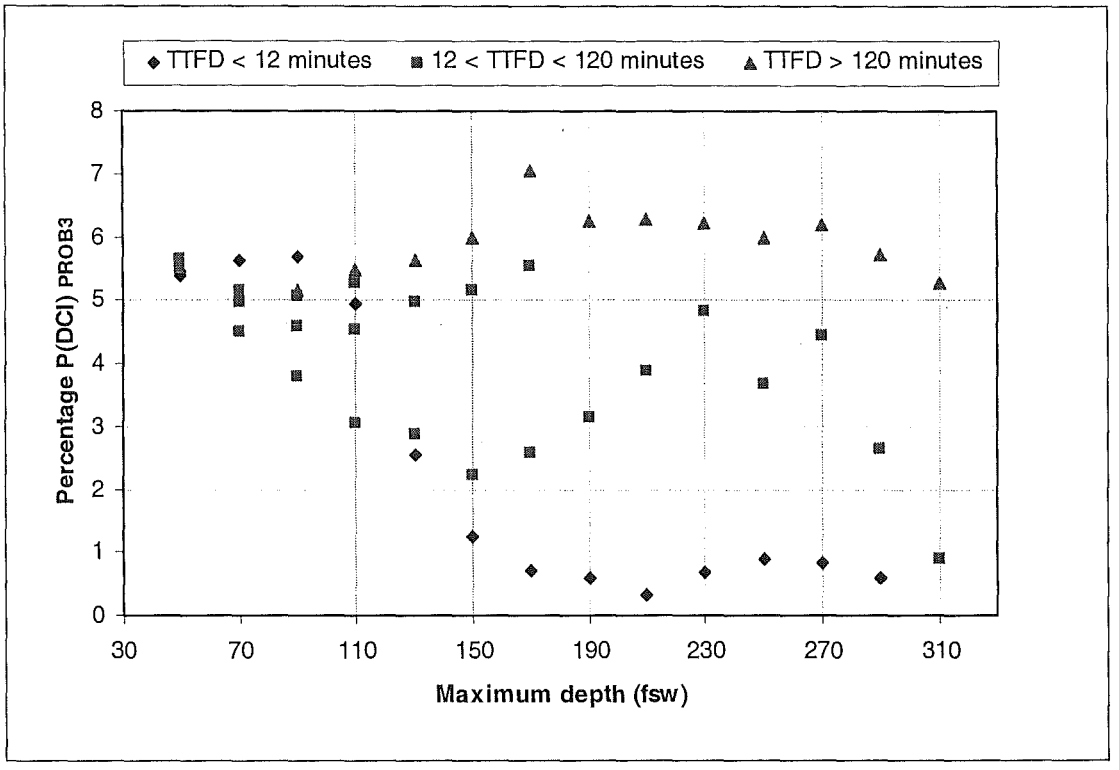

Figure 5.1 *The probability of decompression illness as calculated by PROB3 for fifty dive schedules in the US Navy 0.7 ata oxygen in helium tables.*

Another decompression method that is used for dives using oxygen in helium mixes is Bühlmann's ZH-L16A Model [Bühlmann, 1995]. To the authors knowledge the data used to develop this model was not from dives using a constant partial pressure of oxygen. At least half the dives used to develop the safe ascent criteria were based on deep saturation dives to between 260 and 1640 fsw. The tissue half times for helium are derived from those used for nitrogen and the difference in solubility of the two gases in the body tissues.

One implementation of the ZH-L16A Model is in the Proplanner Software [Bushell & Gurr, 1997]. Dives with the shortest and longest bottom times for each of the depths considered in Figure 5.1 were processed by Proplanner to give decompression schedules for a diver breathing a constant partial pressure of 0.7 bar oxygen in helium. The probability of decompression illness for each of these decompression schedules was then calculated using PROB3.

Figure 5.2 compares the total time for decompression given by the US 0.7 ata oxygen in helium tables and the Proplanner software with the estimated risk of decompression illness as given by PROB3. The data for the shortest bottom time dives for each maximum depth as given by the US 0.7 ata oxygen in helium tables are plotted.

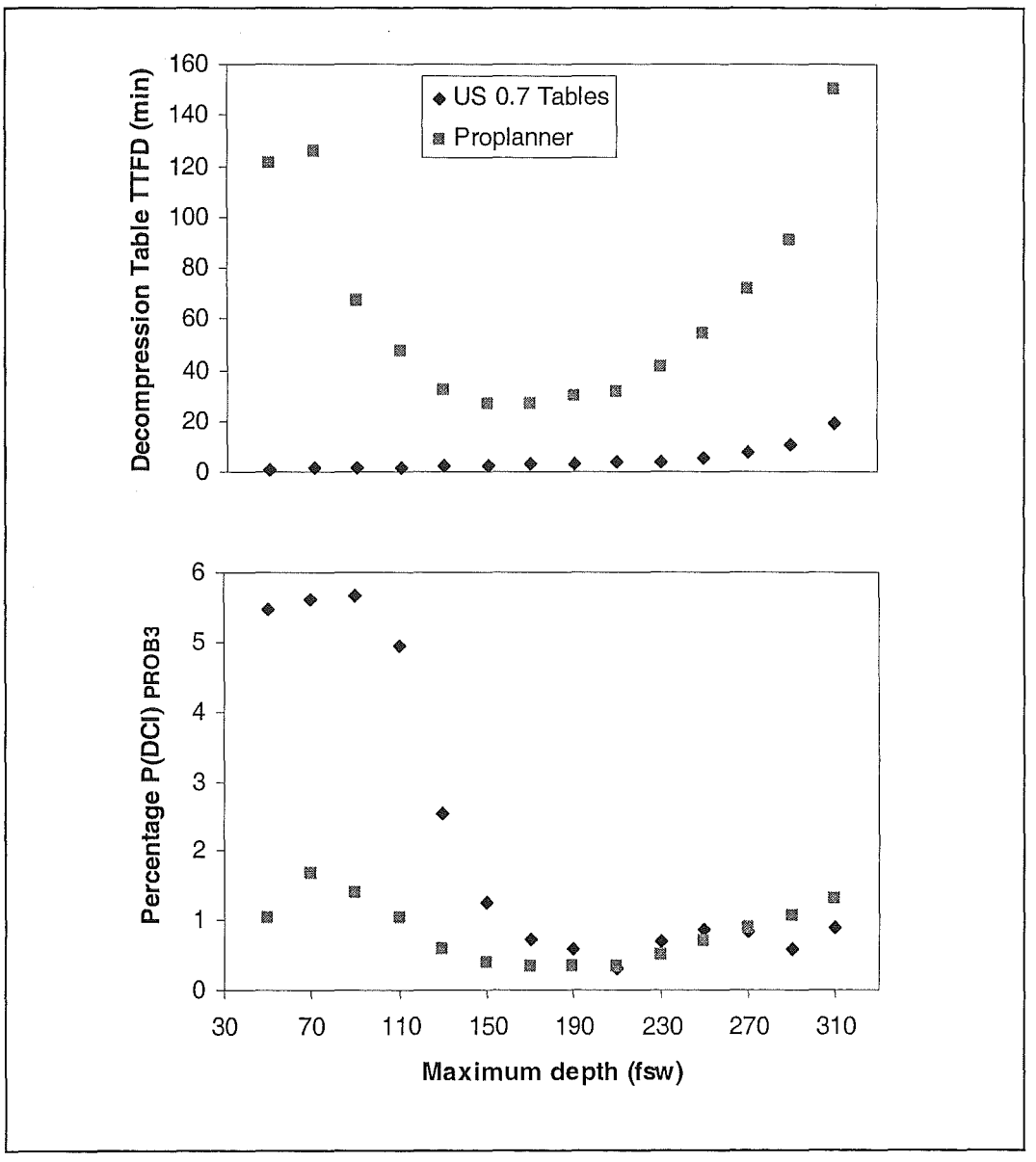

Figure 5.2 *Comparison of the total time for decompression (TTFD) and the probability of decompression illness as calculated by PROB3 ($P(DCI)_{PROB3}$) for no-stop or short decompression dives to between 50 fsw to 310 fsw taken from the US 0.7 ata oxygen in helium tables and Proplanner software.*

Proplanner generated schedules all have longer decompression stops than the US 0.7 ata oxygen in helium tables. Proplanner's significantly greater decompression times for shallower dives results in a useful decrease in the PROB3 risk of decompression illness.

The deeper dives to 200 fsw or more with bottom times close to 5 minutes do not follow this trend. The increased decompression stops generated by Proplanner result in the same or higher risk of decompression illness. This can be explained by considering the uptake and elimination of carrier in the body tissues. A short dive to a deep depth will mainly load the tissues with short gas exchange halftimes. These same tissues will eliminate the carrier quickly on ascent. If decompression stops are introduced to the ascent it is possible for the longer halftime tissues to initially be absorbing carrier on the ascent while the shorter halftime tissues are eliminating carrier. The carrier in the longer halftime tissues causes the higher risk of decompression illness even though more time is spent decompressing in the water.

In Figure 5.2 a diver using the Proplanner software to dive to 310 fsw would spend two hours more ascending in the water than a diver using the US 0.7 ata oxygen in helium tables for no reduction in risk of decompression illness. The Proplanner data shown in Figure 5.2 is an example of a decompression model being used for dives that are beyond the scope of the data originally used to generate the model.

A comparison of the total time for decompression for the longest bottom times listed as non-severe dives in the US 0.7 ata oxygen in helium tables was performed. For all of the dives considered the Proplanner schedules required five or more hours of decompression than the US tables for a reduction in risk of decompression illness from about six percent to one percent. However, the length of decompression time required by the Proplanner schedules means that they are unlikely to be used for rebreather diving.

5.3 Decompression advantages of higher partial pressures of oxygen in helium.

The US Navy 0.7 ata oxygen in helium decompression tables discussed in the previous section were designed and tested for rebreather apparatus with an oxygen set point of 0.7 ata. The purpose of this research is to develop tables suitable for a rebreather with an oxygen set point of 1.3 bar. Figure 5.3 shows the probability of decompression illness for the fifty US Navy 0.7 ata oxygen in helium table dives discussed in the previous section. The probability of decompression illness is given for dives breathing 0.7 bar and 1.3 bar oxygen in helium gas mixes.

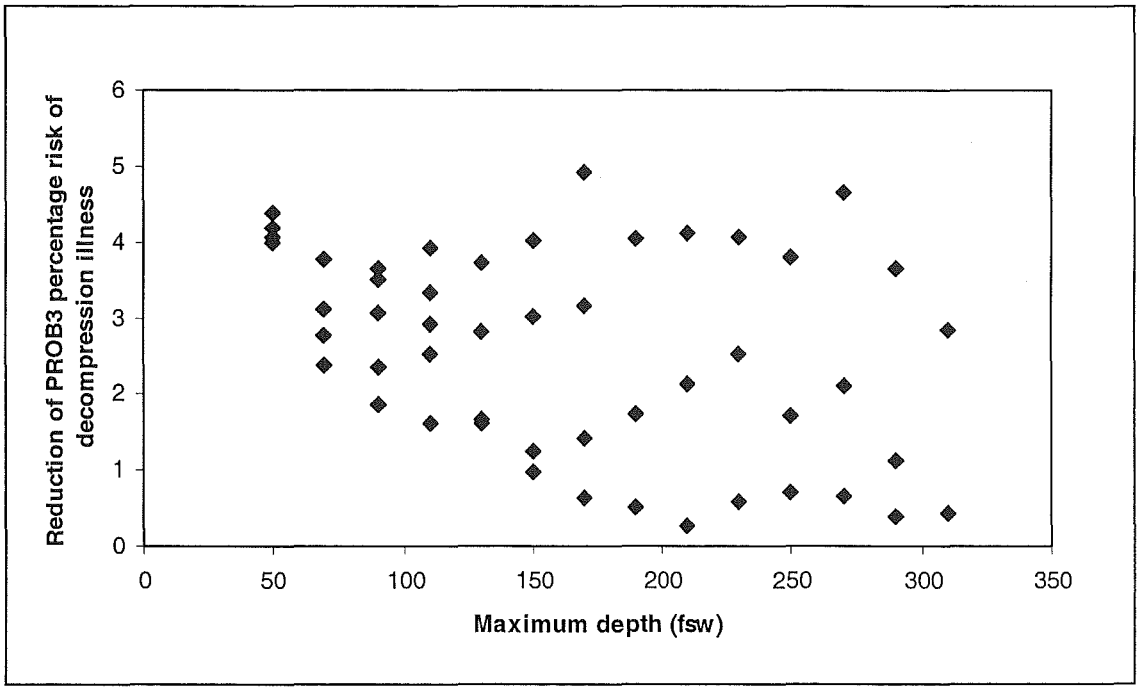

Figure 5.3 *Reduction in the PROB3 estimated risk of decompression illness for 50 dive schedules when Rebreather apparatus are set to 1.3 bar instead of 0.7 bar partial pressure of oxygen in helium.*

Figure 5.3 illustrates the possible reduction in the risk of decompression illness gained by breathing the higher partial pressure of oxygen. This reduction in risk spans across the range of depths and time for decompression covered by the fifty dives. All dives have a probability of decompression illness below 2.5% associated with them. Diving with apparatus using an oxygen set point of 1.3 bar as opposed to 0.7 bar has increased the safety of the dive.

An increase in the partial pressure of oxygen also means a longer bottom time can be taken for the same decompression time compared to dives using a smaller partial pressure of oxygen gas mix. For example, consider a set of bounce no-stop dives to 70 fsw (approximately 21 msw). A no-stop dive is one in which the diver ascends straight from the maximum depth to the surface. PROB3 was used to calculate the probability of decompression illness for no-stop dives to 70 fsw for a range of bottom times with the rebreather oxygen set point at 0.7 bar or 1.3 bar. The results are shown in Figure 5.4 and Table 5.1. The results in Table 5.1 were interpolated from the graph and verified using the PROB3 program.

$P(DCI)_{PROB3}$ (%)	Bottom Time (minutes)	
	PO_2 = 0.7 bar	PO_2 = 1.3 bar
1	26	56
2	34	84
3	44	116
4	56	150

Table 5.1 *The difference in bottom times with a given risk of decompression illness for a no-decompression dive to 70 fsw breathing 0.7 bar or 1.3 bar partial pressure of oxygen in helium.*

The results in Figure 5.4 and Table 5.1 clearly show advantage in reducing the decompression requirements by breathing a higher partial pressure of oxygen. At a one percent risk of decompression illness the 1.3 bar partial pressure of oxygen rebreather allows an increase in bottom time at a depth of 70 fsw by half an hour. This extension to the possible bottom time increases to one and a half hours at the higher risk level of four percent risk of decompression illness.

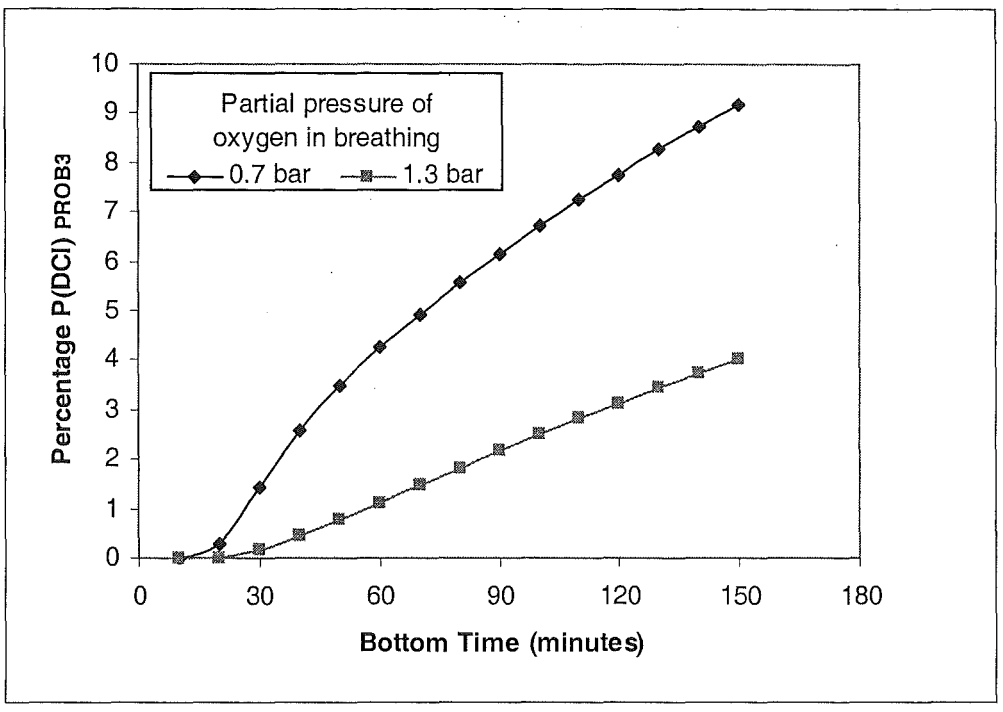

Figure 5.4 *Relationship between probability of decompression illness as calculated by PROB3 and bottom time for no decompression stop dives to 70 fsw breathing 0.7 bar and 1.3 bar partial pressure of oxygen in helium.*

A similar trend is observed for dives using decompression stops. The rebreather with an oxygen set point of 1.3 bar partial pressure of oxygen offers significant decompression time advantages over the 0.7 bar set point rebreather equipment as confirmed by a US Navy trial in 1998 [Survanshi et al., 1998].

Constraining the 1.3 bar equipment to be operated using the US 0.7 ata oxygen in helium tables is over conservative and subjecting divers to the increased dangers associated with the diver being in the water longer than needed during decompression.

5.4 Iso-probability decompression tables

Ideally, all the dive schedules in a decompression table should have an equal risk of decompression illness. Such a decompression table would be an iso-probability table. PROB3 analysis of published tables and decompression programs suggests that currently used decompression schedules are not optimised for the risk of decompression illness and there is no information given to the user about the relative risks of different dive schedules in a table.

5.5 What is an acceptable risk of decompression illness?

Iso-probability tables provide a series of dive schedules of equal risk. From a users perspective this gives the proportion of dives they expect to result in decompression illness. In comparison, current tables are classed as 'safe', even though it is known and accepted that some cases of decompression illness will occur.

Quantifying the risk leads to ethical questions of what is an acceptable incidence of decompression illness? The choice of level of risk can result in the tables not being used:

- If the risk is perceived to be too high, nobody will be willing to use such a decompression table because of the fear of the diver getting decompression illness.

- Set the risk at too low a level and divers will be spending more time in the water decompressing than required by decompression tables they know from experience to be 'safe'.

Sports dives are typically done in good conditions and for dive profiles where decompression stops are a few minutes. Dives often take place two or more hours from a compression chamber and appropriately trained medical staff. In this scenario, a slightly longer decompression in return for a lower risk of decompression illness could be acceptable.

Military divers who are diving with the back up of an on board compression chamber and associated medical staff, may be willing to use tables generated at a higher risk of decompression illness. The higher risk of decompression illness may be offset by lowering the risk to the diver of being in a hostile environment during decompression such as; strong currents, cold temperatures or explosions. The on board compression facilities would be able to provide prompt treatment of any problems that arise.

5.6 Conclusions

PROB3 estimates of decompression illness risk for two published decompression methods provide an example of the possible range of risk of decompression illness across different tables and across schedules within a table. An iso-probability table would be a safer option though the risk of decompression illness level must be decided.

A US Navy dive trial [Survanshi et al., 1998] and PROB3 analyses of dives breathing different constant partial pressures of oxygen have illustrated the decompression advantage that can be gained by breathing a higher partial pressure of oxygen. To use 0.7 bar oxygen in helium tables for 1.3 bar oxygen in helium breathing apparatus is overly conservative.

Chapter 6

Application of sequential quadratic programming to decompression optimisation

6.1 Notation

BT	Bottom Time	n	Number of design parameters
MDT	Maximum Dive Time	R	Estimate of risk of decompression illness (%)
$TTFD$	Total Time For Decompression	R_{acc}	Acceptable risk of decompression illness (%)
f	Objective function	$\bar{s}$	Search direction vector for design parameters $(s_1, s_2, \ldots, s_n)$
g_j	Inequality constraint function	$\bar{x}$	Design parameter vector $(x_1, x_2, \ldots, x_n)$
h_k	Equality constraint function	α	Scaling factor for design parameter update
H	Approximation of the Hessian Matrix	ξ	Allowable risk error
m	Number of inequality constraints	L, λ_i	Lagrangian Function and multipliers

6.2 Introduction

In the opening chapter of this thesis an optimised decompression profile was defined as:

A dive profile with the quickest ascent from maximum depth to the surface that will result in a specified risk of decompression illness.

This chapter will introduce how the sequential quadratic programming method (SQP) can be used to create optimised decompression profiles.

6.3 The general optimisation problem applied to decompression optimisation.

A general description of an optimisation problem is to find the real valued design parameters $\bar{x} = (x_1, x_2, \ldots, x_n)^T$ which

$$\min_{\bar{x} \in \Re^n} \quad f(\bar{x})$$

subject to constraints

$$g_j(\bar{x}) \leq 0 \quad j = 1, \ldots, m$$
$$h_k(\bar{x}) = 0 \quad k = 1, \ldots, m_e$$

and bounds $(\bar{x})_L \leq \bar{x} \leq (\bar{x})_U$ (6-1)

where $f(\bar{x})$ is the objective function to be minimised subject to the inequality constraints $g_j(\bar{x})$ and equality constraints $h_k(\bar{x})$ and lower and upper bounds on the design parameters [Fletcher, 1987].

Applying the above description to decompression optimisation, the objective function is the function which evaluates the total time for decompression (**TTFD**) of the dive:

$$f(\bar{x}) = \mathbf{TTFD}(\bar{x}). \tag{6-2}$$

The decompression optimisation problem provides inequality constraints in two areas; risk and dive duration.

The first constraint comes from physical limitations of the divers breathing apparatus. Rebreather apparatus have a finite duration of operation due to oxygen consumption by the diver and the ability of the chemical system to remove carbon dioxide from the breathing loop. For the purposes of this work, a total maximum dive time (**MDT**) will be imposed, where the dive time consists of the bottom time (**BT**) and the total time for decompression (**TTFD**),

$$g_1(\bar{x}) = \mathbf{BT} + \mathbf{TTFD}(\bar{x}) - \mathbf{MDT} \leq \mathbf{0}. \tag{6-3}$$

Depending on the choice of objective function for total time for decompression, this constraint may be linear or non-linear.

The remaining constraints come from the definition of decompression optimisation that states the risk of decompression illness should be a specified value. The value of risk for the purpose of this and following chapters will be calculated using the PROB3 program [Horn, 1999a] of the non-linear LEM model (Chapter 4). However, the formulation of the problem would easily allow other risk models to be substituted for the LEM model in future research.

The risk of decompression illness, $\boldsymbol{R}$, is defined as the percentage of man dives expected to result in decompression illness for the given dive profile. To optimise the dive, the risk of decompression illness, $\boldsymbol{R}$, should be less than or equal to a specified acceptable value, $\boldsymbol{R_{acc}}$, with a given margin of error, ξ,

$$R_{acc} - \xi \leq R(\bar{x}) \leq R_{acc}$$

that can be written as two non-linear inequality constraints of the form given by expression (6-1).

$$\begin{aligned} g_2(\bar{x}) &= R(\bar{x}) - R_{acc} \leq 0 \\ g_3(\bar{x}) &= R_{acc} - \xi - R(\bar{x}) \leq 0. \end{aligned} \tag{6-4}$$

In general, reducing the total time for decompression will increase the risk and only the upper bound risk constraint will be active during the optimisation. If deeper stops are shortened it is possible to reduce the total time for decompression at the same time as reducing the risk value. For this reason the lower bound risk constraint was included.

No equality constraints are used to describe the decompression optimisation. The lower and upper bounds of the design parameters will be dependent on the choice of function for the total time for decompression.

In summary, the decompression optimisation description becomes,

$$\min_{\bar{x} \in \Re^n} \quad \mathrm{TTFD}(\bar{x})$$

subject to

$$\begin{aligned} \mathrm{BT} + \mathrm{TTFD}(\bar{x}) - \mathrm{MDT} &\leq 0 \\ R(\bar{x}) - R_{acc} &\leq 0 \\ R_{acc} - \xi - R(\bar{x}) &\leq 0. \end{aligned} \tag{6-5}$$

6.4 Introduction to Sequential Quadratic Programming

The MATLAB program [MATLAB 2001] function '*fmincon*' was used to solve the constrained optimisation problem given by expression (6-5). Function *fmincon* uses a sequential quadratic programming algorithm to solve the optimisation problem in an iterative manner where the parameter values at the end of the $p+1^{th}$ iteration are

$$(\bar{x})_{p+1} = (\bar{x})_p + \alpha_p (\bar{s})_p. \tag{6-6}$$

The change in $\bar{x}$ is given by the search direction vector, $\bar{s}$, multiplied by a scaling factor α.

To encompass constraints into the minimisation problem, the constraints and the objective function are combined as a Lagrange function,

$$L(\bar{x},\bar{\lambda}) = f(\bar{x}) + \sum_{j=1}^{m} \lambda_j g_j(\bar{x}) \tag{6-7}$$

where λ_j are the Lagrange multipliers which give a measure of the rate of change in the objective function due to a change in the corresponding constraint value.

The objective function, $f(\bar{x})$, is iteratively minimised subject to constraints $g_j(\bar{x})$ using the method described in Figure 6.1.

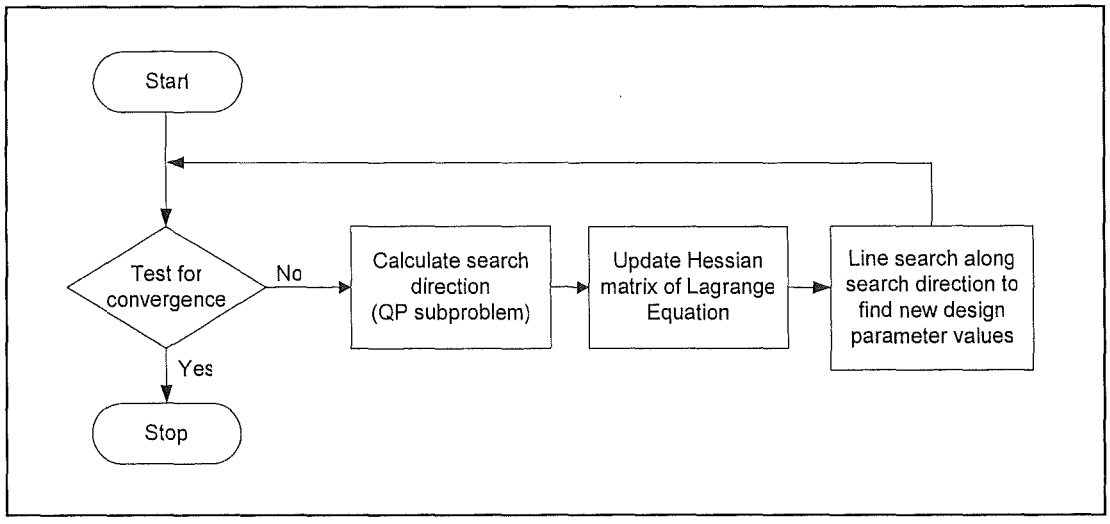

Figure 6.1 Summary of Sequential Quadratic Programming Method

At each iteration a numerical estimate of the Hessian of the Lagrange function is calculated using the Broyden [1970], Fletcher [1970], Goldfarb [1970] and Shanno [1970] (BFGS) method. The BFGS method estimates the new Hessian matrix, $\boldsymbol{H}_{p+1}$, from old Hessian matrix, $\boldsymbol{H}_p$, and gradients of the Lagrange function,

$$H_{p+1} = H_p + \frac{\bar{q}_p \bar{q}_p^T}{\bar{q}_p^T \bar{s}_p} - \frac{H_p \bar{s}_p \bar{s}_p^T H_p^T}{\bar{s}_p^T H_p \bar{s}_p} \tag{6-8}$$

where

$$\bar{s}_p = \bar{x}_{p+1} - \bar{x}_p$$

$$\bar{q}_p = \left[\nabla f(\bar{x}_{p+1}) + \sum_{j=1}^{m} \lambda_j \nabla g_j(\bar{x}_{p+1})\right] - \left[\nabla f(\bar{x}_p) + \sum_{j=1}^{m} \lambda_j \nabla g_j(\bar{x})\right]$$

where ∇ is the gradient operator such that $\nabla f = \left(\frac{\partial f}{\partial x_1}, \frac{\partial f}{\partial x_2}, \ldots, \frac{\partial f}{\partial x_n}\right)^T$.

The Hessian is initialised as the identity matrix and is modified during the calculations to maintain a positive definite matrix. The Hessian is kept positive definite if $\bar{q}^T \bar{s}$ is positive for each update. When $\bar{q}^T \bar{s}$ is not positive up to two modifications are made to $\bar{q}$.

Firstly the ith element of vector $\bar{q}$ corresponding to the most negative value of $q_i s_i$ is halved. This process is repeated until $\bar{q}^T \bar{s}$ is greater or equal to -10^{-5}.

If after this process $\bar{q}^T \bar{s}$ is still negative then a factor is added to $\bar{q}$,

$$\bar{q} = \bar{q} + \bar{v}\omega \tag{6-9}$$

where ω is a weight that starts at 10^{-2} and is repeatedly doubled until the $\bar{q}^T \bar{s}$ is positive or the weight becomes too large. v_i is zero unless $q_i . \omega < 0$ and $q_i s_i < 0$, when it is given by

$$v_i = \sum_{j=1}^{m} \frac{\partial g_j(\bar{x}_{p+1})}{\partial x_i} g_j(\bar{x}_{p+1}) - \sum_{j=1}^{m} \frac{\partial g_j(\bar{x}_p)}{\partial x_i} g_j(\bar{x}_p). \tag{6-10}$$

To calculate the search direction vector, $\bar{s}$, the minimisation problem (6-1) is transformed into a quadratic approximation of the objective function minimised by

the search direction. The second order Taylor Series for the objective function with a change in parameter values, $\Delta\bar{x}$, is given by

$$f(\bar{x}+\Delta\bar{x}) \approx f(\bar{x}) + \nabla f(\bar{x})^T \Delta\bar{x} + \tfrac{1}{2}\Delta\bar{x}^T H \Delta\bar{x}. \qquad (6\text{-}11)$$

If the scaling factor, α, from equation (6-6) is set to one, the change in parameter values become the search directions vector, $\bar{s}$. Substituting the approximation for the next guess of the objective function into expression (6-1), the minimisation problem becomes

$$\min_{\bar{s}\in\Re^n} \quad \tfrac{1}{2}\bar{s}^T H \bar{s} + \nabla f(\bar{x})^T \bar{s}. \qquad (6\text{-}12)$$

The second order constraint information is included in the Hessian matrix to ensure second order convergence of the solution [Fletcher, 1987, page 140]. The problem is further simplified by ensuring all the constraints are linear equations by transforming them using the linear approximation of Taylor's Series,

$$\nabla g_j(\bar{x})^T \bar{s} + g_j(\bar{x}) \le 0 \qquad j=1,\ldots,m. \qquad (6\text{-}13)$$

The MATLAB Optimisation Toolbox uses an active set strategy similar to that of Gill et al. [1991] to solve expressions (6-12) and (6-13) for the search direction, $\bar{s}$.

Once the search direction is known a scaling factor less than or equal to one is found that reduces a merit function of the form

$$f(\bar{x}) + \sum_{j=1}^{m} \lambda_j \cdot \max\left\{0,\ g_j(\bar{x})\right\} \qquad (6\text{-}14)$$

and reduces the maximum constraint violation if any constraints are violated. If all constraints are met and the objective function is positive, a step length must be chosen that also reduces the objective function value.

6.5 Convergence and stopping criteria

The MATLAB functions use a number of criteria for the solution of a minimisation problem with constraints. There are five user set values that control the termination of the algorithm;

- tolX: Tolerance on change in design parameters.
- tolFun: Tolerance on change in function value.
- tolCon: Tolerance on constraint violation.
- maxFunEvals: Maximum number of objective function evaluations.
- maxIter: Maximum number of iterations.

The choice of these user set values will relate to the choice of function for the ascent profile and constraint functions. The termination rules for the iterative process are summarised in Figure 6.2.

The diving optimisation problem given in Section 6.3 is unlikely to produce a risk constraint region that will coincide with a minimum of the objective function. This means that the problem is unlikely to converge using the checks for a function minimum as given in box 1 of Figure 6.2.

If the search direction steps become too small relative to the design parameter tolerance or the change in objective function due to the change in design parameters

$$f(\bar{x}+\bar{s}) - f(\bar{x}) \approx \nabla f(\bar{x})^T \bar{s} \tag{6-15}$$

becomes small compared to objective function tolerance { box 2 }, the solution has converged. If the constraint tolerances have been met then a local solution to the optimisation problem has been found.

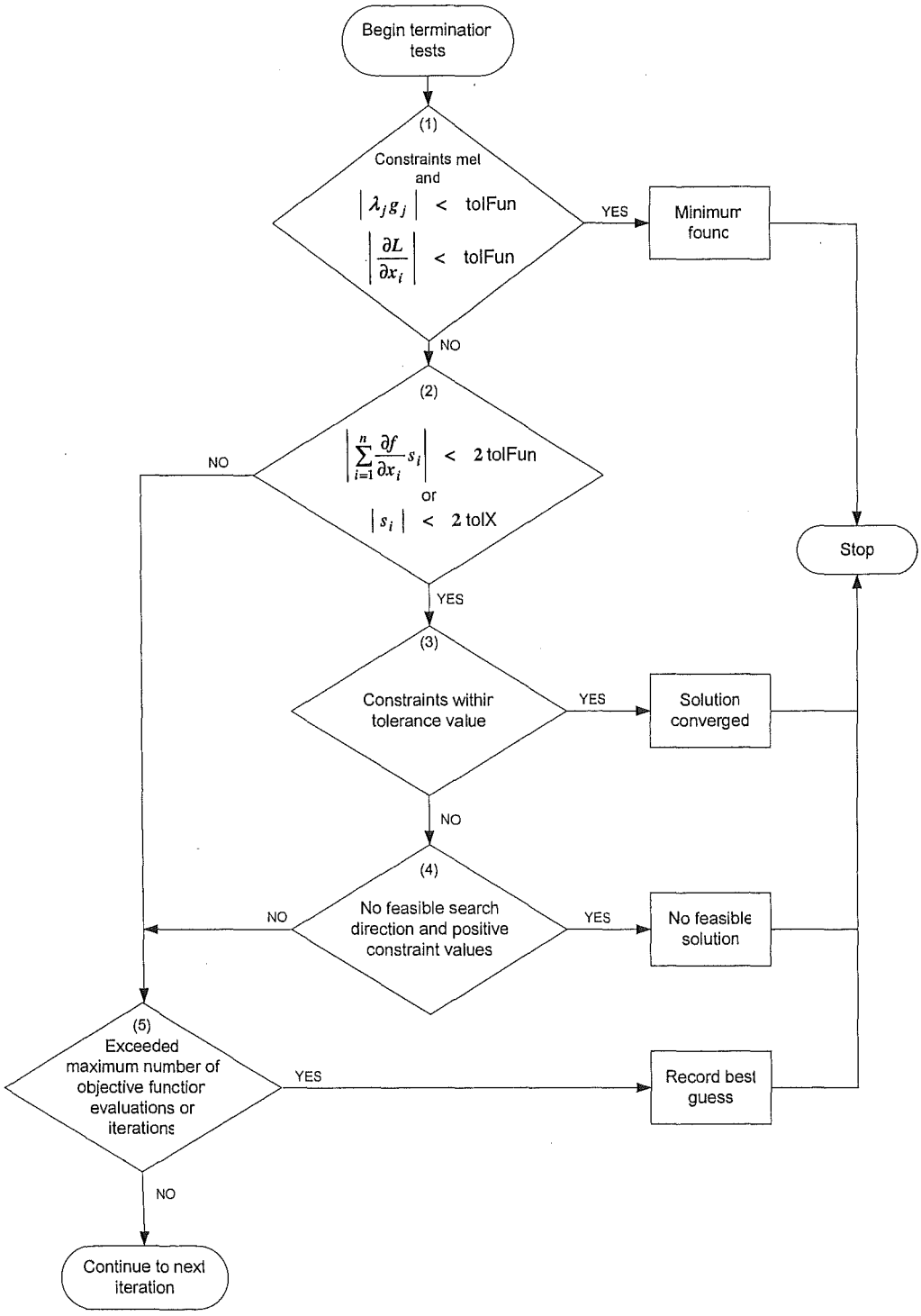

Figure 6.2 *Termination criteria for sequential quadratic programming method used in MATLAB function 'nlconst'.*

If the conditions of box 2 have been met and the quadratic programming problem given by expressions (6-11) and (6-12) is infeasible with the constraints not satisfied then no feasible solution can be found and the program is terminated { box 4}.

In all other cases the next iteration of the optimisation process will proceed unless the maximum number of function evaluations or iterations has been exceeded {box 5}. In this case the design parameter values, $\bar{x}$, which produced the minimum value of the objective function while satisfying the constraints are recorded as the solution.

These termination criteria do not guarantee a global solution to the optimisation problem. To test the ability of this method to find a global solution for the given problem, the method should be tested using a range of initial parameter values. The production of different solutions for different starting values will indicate alternative approaches would need to be applied to work towards locating a global solution to the optimisation problem.

6.6 Evaluation of Sequential Quadratic Programming schemes for diving optimisation

Traditionally decompression tables for open water diving ascend from the bottom depth to the surface in a series of steps called decompression stops. Decompression stops are easier for a diver in mid-water to implement than a continuous ascent. In most cases, the quickest continuous ascent is not a uniform rate of ascent. Since the beginning of decompression research in the early twentieth century [Hempleman, 1995] it has been known that it is possible to ascend at a faster rate at deeper depths than close to the surface.

Decompression stops are defined by the depths at which the divers pause their ascent and the time spent at these depths. UK Royal Navy dive profiles conform to the following constraints:

- The deepest stop depth (DSD) is a multiple of 3 msw (≈10 fsw).
- The distance between stop depths is 3 msw (≈10 fsw).

- The shallowest decompression stop is taken at 6 msw (≈20 fsw).

Given the above constraints, a stepped ascent is defined by the time spent decompressing at all possible stop depths. For a dive to 81 msw there are 25 possible decompression stops, requiring 25 parameter values to define them.

In Chapter 7 the ascent profile and total time for decompression is defined by the stop times that are the parameters to be optimised using sequential quadratic programming.

Decompression tables provide a limited number of schedules for a single maximum depth. For greater accuracy in tissue loading for multi-level bottom depths divers often wear wrist dive computers that calculate the tissue carrier loadings based on the actual time-depth profile of the bottom time. To fully optimise the decompression process, divers would require a working optimised decompression method to run in real time on a wrist worn dive computer.

To implement an optimisation scheme in real time it may be advantageous to reduce the number of parameters that need to be estimated. One way to reduce the number of parameters is to approximate the stepped ascent profile as a continuous curve defined by fewer parameters. Once the curve is defined, the curve could be converted to a stepped ascent for operational use.

Chapter 9 shows how using curves to describe the ascent profile during the optimisation process can generate optimised decompression schedules. For operational use in open water the ascent profile must be given as a series of stop times and depths. Chapter 8 describes a scheme to convert the curved ascent profile to a stepped profile

Seven dive profiles are used to evaluate the optimisation schemes in Chapters 7 and 9. These profiles were chosen to cover the range of ascent profiles that could be expected in 1.3 bar oxygen in helium rebreather decompression tables. The dive

profiles all have the same characteristics as given in Table 6.1 with maximum depth and bottom times given in Table 6.2.

Rate of descent (ROD)		150 fsw/min
Rate of ascent (ROA)		50 fsw/min
Shallowest stop depth (SSD)		20 fsw
Stop depth interval		10 fsw
Maximum dive duration		240 minutes
Gas Profile	0 → 33 fsw	0.75 bar oxygen in helium
	33 → MD → 13.1 fsw	1.3 bar oxygen in helium
	13.1 → 0 fsw	0.75 bar oxygen in helium

Table 6.1 Dive profile characteristics for optimisation test dives

Maximum depth (fsw)	**Bottom time (minutes)**
100	30
	80
	120
200	20
300	5
	15
	20

Table 6.2 Maximum depth and bottom time for optimisation test dives

6.7 Conclusions

This chapter has described the governing equations of the decompression optimisation problem and outlined the method of sequential quadratic programming as implemented in the MATLAB Software.

For a complete description of the algorithms used by the MATLAB software, refer to the Optimisation Toolbox Manual or the '*fmincon*' and related functions source code.

NOTE – The MATLAB functions; '*fmincon*' Revision 1.29 and '*nlconst*' Revision 1.35 were used for the results given in this thesis. Earlier issues of these functions contained code errors when used for non-linear constrained optimisation.

THIS PAGE IS INTENTIONALLY BLANK

Chapter 7

Decompression optimisation using decompression stop time design parameters

7.1 Notation

BT	Bottom time (min)	n	Number of stop times
fsw	Feet of sea water	q	Number of negative stop times
MD	Maximum depth (fsw)	R	Risk of decompression illness (%)
ROA	Rate of ascent (fsw/min)	$\bar{s}$	Search direction
$TTFD$	Total time for decompression (min)	L,λ_j	Lagrange function and multipliers
d_k	Depth at decompression stop k	$\bar{x}$	Vector of stop times
f	Objective function	α	Search direction scaling factor
g_j	Inequality constraint j		

7.2 Introduction

The stepped ascent from the Maximum Depth (***MD***) of a dive to the surface comprises a series of short ascents at a given constant rate of ascent (***ROA***) interspersed with decompression stops. A decompression stop is the time the diver stays at the same depth before continuing the ascent.

This chapter will evaluate the sequential quadratic programming optimisation method for minimising the total time for decompression, while yielding iso-probabilistic decompression schedules when the design parameters are stop times for all possible decompression stop depths.

7.3 Governing equations

In this formulation of the decompression optimisation problem the n design parameters $\bar{x}$ are the decompression stop times. The stop times must all be greater or equal to zero. If there is no decompression stop at a given stop depth, d_i, the value of x_i is set to zero.

The function to minimise, the Total Time for Decompression (***TTFD***), can be expressed in terms of the time spent ascending and the sum of the decompression stop times,

$$TTFD(\bar{x}) = \frac{MD}{ROA} + \sum_{i=1}^{n} x_i \qquad (7\text{-}1)$$

$$= \textbf{Direct ascent time} + \textbf{Sum of stop times}$$

The direct ascent time is independent of the choice of stop times, so can be dropped from the minimising objective function. The governing equations for the minimisation problem become;

$$\min_{\bar{x} \in \Re^n} \; f(\bar{x}) = \sum_{i=1}^{n} x_i \quad \text{with } x_i \geq 0 \quad \text{for } i = 1, 2, \ldots, n \qquad (7\text{-}2)$$

subject to one linear constraint; the maximum dive duration must be less than the maximum equipment duration of 240 mniutes,

$$g_1 = BT + \frac{MD}{ROA} + \sum_{i=1}^{n} x_i - 240 \leq 0 \qquad (7\text{-}3)$$

and two non-linear risk constraints

$$g_2 = R(\bar{x}) - R_{acc} \leq 0 \qquad (7\text{-}4)$$

$$g_3 = R_{acc} - \xi - R(\bar{x}) \leq 0.$$

The risk values were given in percentage units to provide better scaling against the time variables. The risk error, ξ, was set to 0.01%. Only one of the two risk constraints, g_2 and g_3 , can be active at each iteration.

Analytical first derivatives of the objective function and dive time constraint are unity. No second order information is provided by the objective function or dive time constraint. The Hessian matrix used to calculate the search direction (equation 6-8) is only updated using the risk constraint gradients.

7.4 MATLAB implementation

The algorithm was implemented using the MATLAB "fmincon" function [MATLAB 2001]. Functions were written to provide the values and derivatives of the objective function and the constraints for given stop times, x_i.

The gradients of the nonlinear risk constraints were calculated using the forward difference formula with the time interval h equal to six seconds.

$$\frac{\partial R}{\partial x_i} \approx \frac{R(\bar{x} + he_i) - R(\bar{x})}{h} \tag{7-5}$$

where e_i is the i^{th} column of the n x n identity matrix.

A six second interval h was chosen to be bigger than the two second update time for calculating the tissue gas exchange in PROB3.

Central or backwards difference formula could not be used because of the lower bound constraint on the stop times, x_i, to avoid negative stop times. Negative stop times are not physically possible and tissue carrier pressures cannot be calculated. Central or backwards difference formula cold have been used away from the zero stop times, but these were not implemented in the following analyses.

During early analyses, negative stop times were observed due to numerical errors in the representation of a zero stop time. To avoid this problem, the lower bound on x_i was set to 10^{-7} minutes and a check for negative values added to the MATLAB 'nlconst' function. The lower bound value was chosen to be small enough not to affect the risk and total time for decompression calculations.

7.5 Initial analyses

The MATLAB program has a number of termination criteria as given in Section 6.5; TolX, TolFun and TolCon. To test for suitable values of these criteria, the test dive profiles given in Section 6.6 were run using function values of,

TolX and TolFun : $1x10^{-5}$

TolCon : $1x10^{-3}$ and

MaxIter : 100.

The TolX and TolFun values were chosen to be very small so that the path of the design parameters could be observed and suitable bigger termination criteria chosen. The TolCon value was chosen to be smaller than the risk error value (equation 7-4) to ensure only one of the two risk constraint values was active at a time.

Three levels of risk were examined; 1%, 2% and 5% risk of decompression illness resulting from the dive. The 1% and 2% dives represent a level of risk that tables may be set to while the 5% risk level was chosen to observe the optimisation performance for higher risk dives. The stop time parameters were all initialised with a value of one minute.

The dive involving the least amount of carrier exchange in the tissues was the dive to 100 fsw for a bottom time of 30 minutes. The 5% risk profile resulted in a direct ascent to the surface from maximum depth while the 1% and 2% risk profiles both converged to a solution within 8 iterations. Table 7.1 shows the 2% risk stop times

for the eight iterations. The termination criteria are given in Table 7.2. The tolerances in ( ) in columns 4-7 of Table 7.2 indicate the termination values for these columns.

The stop times converge to give the longest stop times at the shallowest stop depths. The final solution has been found by the fifth iteration when the maximum constraint violation is less than TolCon, but the other termination criteria have still to be achieved. The small value of the Lagrangian gradient suggests that a local minimum for the total time for decompression has been found.

Iteration	Decompression stop times (minutes)							
	20 fsw	30	40	50	60	70	80	90
1	0.13	0.11	0.08	0.06	0.04	0.02	0	0
2	0.25	0.19	0.13	0.07	0	0	0	0
3	0.79	0.22	0	0	0	0	0	0
4	0.89	0.14	0	0	0	0	0	0
5	1.02	0	0	0	0	0	0	0
6	1.02	0	0	0	0	0	0	0
7	1.02	0	0	0	0	0	0	0
8	1.02	0	0	0	0	0	0	0

Table 7.1 *Decompression stop times at each iteration of the optimisation process for a dive with 2% risk of decompression illness, maximum depth of 100 fsw and bottom time of 30 minutes.*

Iteration	Number of function evaluations	$f = \sum_{i=1}^{n} x_i$	Maximum constraint violation (TolCon)	$\sum_{i=1}^{n} \frac{\partial f}{\partial x_i} s_i$ (2TolFun)	Max of $\left\|\frac{\partial L}{\partial x_i}\right\|$ or $\left\|\lambda_j g_j\right\|$ (TolFun)	$\max\|s_i\|$ (2TolX)
1	3	0.439	0.506	-7.560	0.408	1.000
2	5	0.639	0.227	0.200	0.884	0.117
3	7	1.013	0.017	0.374	1.800	0.541
4	9	1.037	5×10^{-17}	0.024	0.158	0.101
5	11	1.017	8×10^{-4}	-0.020	0.025	0.144
6	13	1.019	9×10^{-20}	0.002	0.001	0.002
7	15	1.019	3×10^{-6}	-1×10^{-4}	1×10^{-4}	1×10^{-4}
8	17	1.019	1×10^{-7}	5×10^{-6}	1×10^{-4}	1×10^{-5}

Table 7.2 *Termination criteria at each iteration of the optimisation process for a dive with 2% risk of decompression illness, maximum depth of 100 fsw and bottom time of 30 minutes.*

The longest bottom time for the 100 fsw dives of 120 minutes produced a dive that could not provide a decompression resulting in a 1% or 2% risk with a total dive time of 240 minutes. The risk and dive time constraints cannot both be satisfied and no solution is possible. The algorithm tried to solve the problem until the maximum number of function evaluations (800) was exceeded. After 14 iterations insignificantly small changes were made to the stop times, resulting in no change in suggested stop times for the remaining iterations. For automated table generation, tests would need to be incorporated to identify this scenario.

The one percent risk of decompression illness dives to 200 fsw for 20 minutes and 300 fsw for 5 minutes both produced results with the range of values in the Hessian matrix becoming as high as of the order 10^{29}. The MATLAB 'nlconst.m' function modifies the Hessian matrix to ensure it is positive definite as described in Section 6.4 even though the Hessian may not be positive definite at the solution. For these dive profiles the weighted adjustments to the Hessian matrix became excessively

large and no improvements to estimated solutions were found after the excessive weighting of the Hessian occurred.

The 300 fsw water dive for 5 minutes bottom time at a prescribed risk of 5% initially produced results that caused the Lagrange multipliers to become excessively large and the search direction small. On investigation, the risk of decompression illness associated with a direct ascent after a bottom time of 5 minutes at 300 fsw was 5.078%, so the solution to the problem is a very small total stop time. The algorithms in the PROB3 code included a check for direct ascents. The ascent is set to contain no stops if the total stop time was below a given value. Hence the risk gradient in the region of interest was set to zero or a very small number that caused the Lagrange multipliers to increase correspondingly. This problem was corrected by setting the direct ascent checking bound at a value of 0.02 minutes.

The last profile that failed to terminate correctly was the 300 msw dive for 20 minutes with 2% or 5% risk of decompression illness. In both these cases the first iteration tried to set most of the stop times to negative values except for the 80 and 90 fsw stops which had large positive stop times.

Even with a positive non-zero lower bound imposed, the MATLAB 'fmincon' functions still produced negative stop times. The function does not allow hard boundaries to be applied and it is not possible to calculate the risk of decompression illness, $\boldsymbol{R}$, for an ascent profile including negative stop times. To solve this problem a penalty function was incorporated into the risk constraint function to weight the risk and risk gradients associated with negative stop times.

When w of the stop times x_i are negative, where w is greater or equal to one, let $x_i \quad i = 1,\ldots,w$ be the set of w negative values and $x_i \quad i = w+1,\ldots,n$ be set of positive stop times. The risk cannot be calculated using negative stop times so an estimate of the risk, $\hat{R}$, is calculated setting the negative stop times to $+10^{-7}$ minutes.

The risk constraints including a penalty weight are defined by

$$g_2 = \left(1 + \sum_{i=1}^{w}(-x_i)\right)\hat{R} - R_{acc} \quad \text{and} \quad g_3 = R_{acc} - \xi - \left(1 + \sum_{i=1}^{w}(-x_i)\right)\hat{R} \qquad (7\text{-}6)$$

and the risk differentiated by x_i corresponding to a negative stop times are given by

$$\frac{\partial g_2}{\partial x_i} = -\hat{R} + \frac{\partial \hat{R}}{\partial x_i}\left(1 + \sum_{j=1}^{w}(-x_j)\right) \quad \text{and} \quad \frac{\partial g_3}{\partial x_i} = \hat{R} - \frac{\partial \hat{R}}{\partial x_i}\left(1 + \sum_{j=1}^{w}(-x_j)\right) \qquad i = 1,\ldots,w$$

$$\frac{\partial g_2}{\partial x_i} = \frac{\partial \hat{R}}{\partial x_i} \quad \text{and} \quad \frac{\partial g_3}{\partial x_i} = -\frac{\partial \hat{R}}{\partial x_i} \qquad i = w+1,\ldots,n.$$

The addition of the risk penalty for negative stop times produced good results. The 2% risk dive profile converged to a realistic schedule but the 5% risk level failed to produce feasible results for a different reason. The analysis stopped after four iterations because the elements of the search direction vector had become too small with the maximum constraint violation still too large. The third iteration gives zero stop times for all the stops apart from the deepest stop that has a stop time of 100 minutes. This is comparable to a dive to 300 fsw for 2 hours followed by a direct ascent to the surface that produces a high limiting risk of decompression illness. The risk constraint gradient at this point will be very close to zero because the risk cannot get much higher, causing small search direction vector elements that terminate the optimisation process.

The algorithm may need the initial choice of decompression stop times to be closer to the solution to avoid negative stop times being estimated in the first iterations. Alternative initial values for the stop times will be presented in the next section.

All the other dives terminated with a feasible solution with the longest decompression stops closest to the surface. If a range of body tissues can contribute to the risk of decompression illness, the stop times should increase with decreasing depth. The analyses resulted in cases where the series of stop times was irregular as shown in Table 7.3 for a dive to 300 fsw for 15 minutes at a risk of decompression illness of 5%.

Stop Depth (fsw)	100	90	80	70	60	50	40	30	20
Stop Time (min)	0.28	6.43	2.39	3.77	0.00	5.68	1.87	10.79	14.52

Table 7.3 *Decompression schedule for a dive to 300 fsw for 15 minutes at a 5% risk of decompression illness.*

Figure 7.1 shows the instantaneous risk (section 4.6) during a dive to 300 fsw associated with the three tissues of the LEM model. Recall that only positive risk contributes to the total risk of decompression illness for the dive. Tissue 3 with the slowest uptake of carrier into and elimination from the tissue contributes a low level of instantaneous risk to the risk of decompression illness for a long period after the diver surfaces. This will be only mildly affected by the distribution of stop times over the ascent. The faster carrier exchange tissues represented by tissues 1 and 2 control the individual stop times in this dive. Tissue 1 has the highest weighting to the overall risk of decompression illness and seems to be the main forcing factor to irregular stop times.

It is possible that if a physiological model with more tissues, or tissues that were more evenly weighted were used with the optimisation scheme, the stop times would be more regular. Though by the nature of trying to minimise the total time for decompression subject to a risk constraint the optimisation process will always fit tightly to the physiological model used.

When decompression illness knowledge reaches a level that can specifically model the tissues and vascular system to predict decompression illness, irregular ascent profiles may provide safer schedules than regularly increasing stop times with decreasing depth.

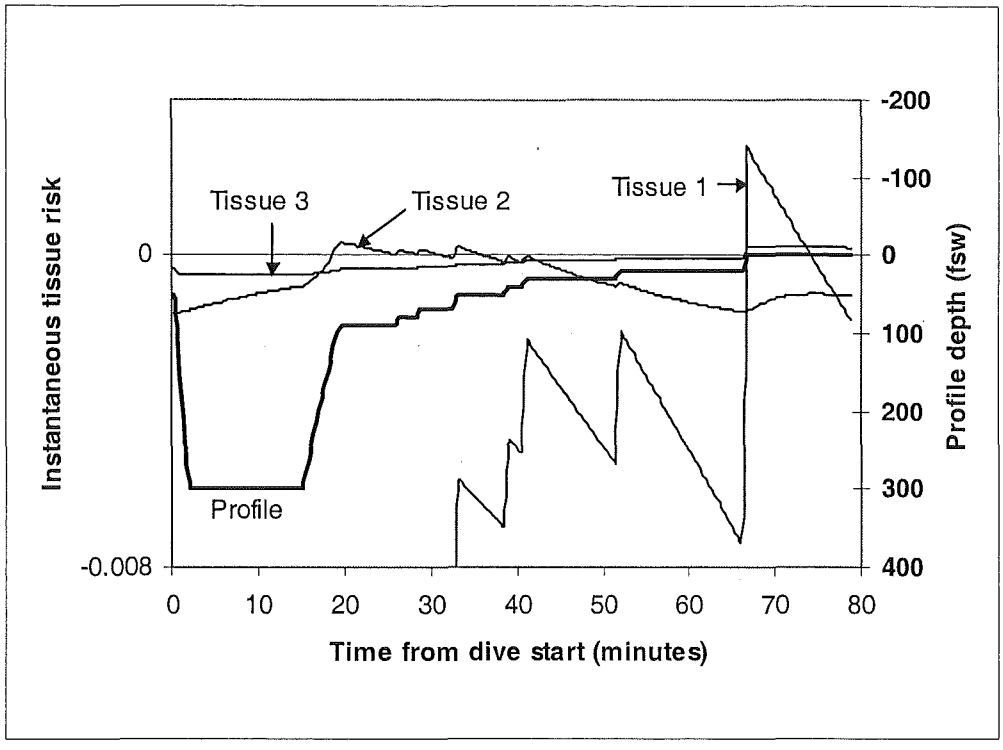

Figure 7.1 *Instantaneous risk for a 300 fsw dive for 15 minute bottom time with total risk of decompression illness of 5%.*

There are many possible solutions to the minimisation of the total time for decompression problem for a given risk of decompression illness. This is especially true for longer deeper dives where more carrier is absorbed into the body at maximum depth. Deeper dives also provide a larger number of possible decompression stops.

7.6 Convergence criteria

Table 7.4 shows the results that would be obtained if TolX and TolFun were set to 10^{-2}, 10^{-3} and 10^{-4} with TolCon set to $2x10^{-3}$. Apart from the short dives, the minimum of the Lagrangian function was not found and the optimisation process typically terminated when the change in objective function had converged.

In most cases the analyses resulted in many iterations of the algorithm that did not significantly change the stop times before termination criteria were achieved. The results in Table 7.3 show there is no advantage in setting TolX and TolFun to a value smaller than 10^{-3}. In all cases apart from the 300 fsw for 20 minute dive, a TolX value of 10^{-2} would have been acceptable. The choice of 10^{-2} over 10^{-3} for TolX provides a considerable reduction in iterations and function evaluations.

For example the dive to 100 fsw for 80 minutes would take 77 function evaluations with TolX=10^{-2} compared to 256 with TolX=10^{-3}. The difference in total stop times for the two dive profiles is 17 seconds which would be insignificant when the stop times would be rounded to complete minutes for use in decompression tables.

7.7 Sensitivity to initial choice of stop time values

This section evaluates the outcome of the sequential quadratic programming method to the choice of starting values of the design parameters, which in this case are the decompression stop times. The same dive profiles as discussed in the previous two sections were processed for two different sets of starting values.

Maximum depth (fsw)	Bottom time (minutes)	Risk (%)	$\sum_i x_i$			Number of iterations			Number of function evaluations		
			10^{-2}	10^{-3}	10^{-4}	10^{-2}	10^{-3}	10^{-4}	10^{-2}	10^{-3}	10^{-4}
100	30	1	4.38	4.38	4.38	9	10	12	19	21	25
		2	1.02	1.02	1.02	5	6	7	11	13	15
		5	DIRECT ASCENT								
	80	1	105.78	105.75	None	20	47	-	77	256	Exceeded
		2	70.11	70.03	None	18	29	-	36	146	Exceeded
		5	4.86	4.82	4.83	7	15	20	15	49	63
	120	5	48.9	45.44	45.46	10	22	27	21	82	96
200	20	1	None, best guess with TolCon=0.006 is *$f(x_i)$=77.87, at iteration 26.*								
		2	42.33	42.27	None	23	36	41	77	188	269
		5	15.13	→	15.13	10	→	17	27	→	45
300	5	1	7.28	7.28	None	9	10	Exceeded	19	21	-
		2	4.63	4.63	4.61	6	7	10	13	15	31
		5	0.09	→	0.09	5	→	6	11	→	13
	15	1	146.04	146.27	None	58	97	Exceeded	227	543	-
		2	100.05	99.60	99.60	49	87	89	206	504	530
		5	46.02	45.73	45.73	47	60	70	161	246	401
	20	1	214	→	208.71	13	→	101	79	→	1024
		2	→	→	174.11	→	→	67	→	→	682
		5	INFEASIBLE TERMINATION								

Table 7.4 *Comparison of performance of sequential quadratic programming optimisation for different termination tolerances. Design parameters are decompression stop times with initial values set to one. An arrow → indicates the termination criteria reduced straight to a termination value smaller than the value for this column.*

The first set, called the 'series' set has a constant increase Ω in stop time duration with decreasing depth. The deepest possible stop depth has an initial stop time of Ω, the second deepest stop depth has an initial stop time of 2Ω and so on until the 20 fsw is reached. Recall there is no 10 fsw stop. Or expressed as an equation,

$x_{n-l} = (l+1)\Omega \qquad l = 0, 1, \ldots, n-1$ where n is the number of possible decompression stop depths.

For this analysis Ω was set to a value of 0.25 to provide an initial total time for decompression of 107 minutes for a dive to 300 fsw.

The second set, called the 'quad' set fits a quadratic function to the initial stop times, with the aim of producing much shorter deep stops and longer shallow stops than the series set. The initial stop time x_i at stop depth d_i is given by

$$x_i = t_o\left(\frac{d_i^2}{MD^2} - \frac{d_i}{MD} + 1\right) \qquad \textbf{where} \quad t_o = \frac{MD}{20} \tag{7-7}$$

This choice of t_o provides an initial total time for decompression of 134 minutes for a dive to 300 fsw. Figure 7.2 shows the ones, series and quad starting dive profiles.

Six dives profiles from the previous section were chosen for a risk of decompression illness of 2%. The 100 fsw dive for a bottom time of 120 minutes was not considered because the dive had been proven to be infeasible with dive duration of less than 240 minutes. The termination criteria were set at TolCon, TolX and TolFun equal to 10^{-3}. The optimisation process for all the dives completed before the maximum number of iterations was reached.

The results are shown in Table 7.5 which compares the performance of the optimisation process for the three different sets of initial stop times.

Maximum depth (fsw)	Bottom time (minutes)	$\sum_i x_i$			Number of iterations			Number of function evaluations		
		ones	series	quadratic	ones	series	quadratic	ones	series	quadratic
100	30	1.02	1.02	1.02	6	13	9	13	41	25
	80	70.03	70.02	70.00	29	25	24	146	56	83
200	20	42.27	42.47	41.86	36	60	49	188	393	173
300	5	4.63	4.63	4.62	7	17	24	15	37	61
	15	99.6	101.27	102.28	87	96	84	504	1000	556
	20	174.2	164.43	179.60	58	97	77	382	456	631

Table 7.5 *Comparison of performance of sequential quadratic programming optimisation for different initial decompression stop times. TolX, TolFun and TolCon set to 10^{-3} and decompression illness risk set to 2%.*

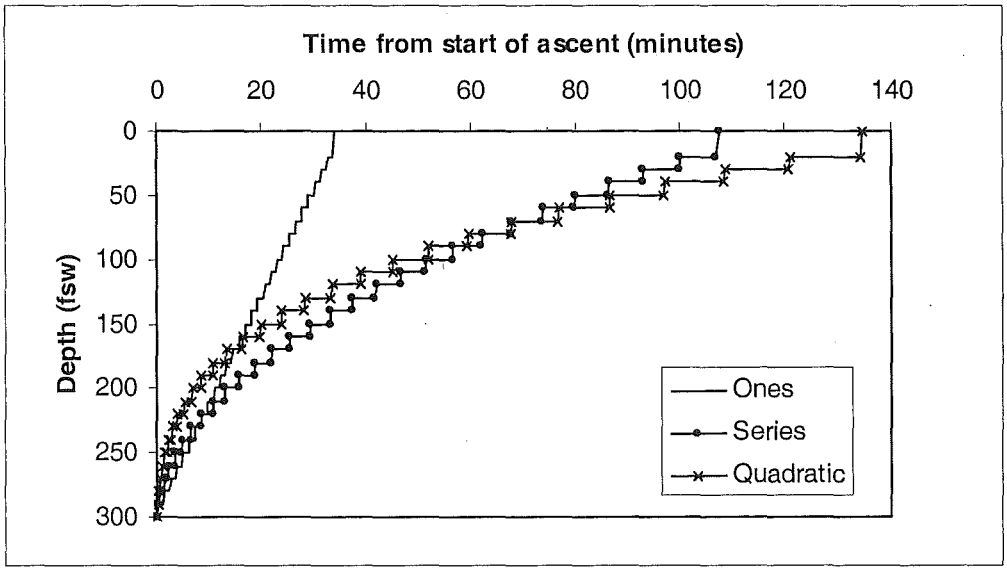

Figure 7.2 Initial ascent profiles for a dive to 300fsw.

Apart from the most extreme dives to 300fsw for 15 and 20 minutes, all the ascent profiles produced similar values for the total time for decompression. The computed ascent profiles were slightly different for the different starting values, confirming there are many local solutions to the problem. An example is given in Table 7.6 that shows the decompression schedules derived for the 200 fsw dive for a bottom time of 20 minutes.

Stop time starting values	Stop times (minutes) at given stop depths (fsw)							TTFD (min)
	20	30	40	50	60	70	80	
ones	30.83	3.28	1.91	3.41	1.48	1.06	0.29	42.27
series	30.32	1.75	5.49	0.46	3.10	0.10	1.24	42.47
quadratic	30.37	2.75	1.52	3.08	2.8	1.16	0.17	41.86

Table 7.6 Comparison of decompression schedules for ones, series and quadratic stop times applied to a 200 fsw dive for a bottom time of 20 minutes at a risk of decompression illness of 2%.

The 300 fsw dives with 15 and 20 minute bottom times have different total stop times for the different initial stop time values. There are no clear best initial values for the stop times. The ones set produces the best results for the 15 minute bottom time dive in terms of total stop time and number of function evaluations. For the 20 minute bottom time the series stop times produce results that reduce the total stop time by 10 minutes compared to the ones stop time results.

The ascent profiles for the 300 fsw dive for 20 minutes given the series and quadratic starting values for the stop times are shown in Figure 7.3. For table production, the difference in results suggests that more than one starting value should be tried, especially for deeper dives.

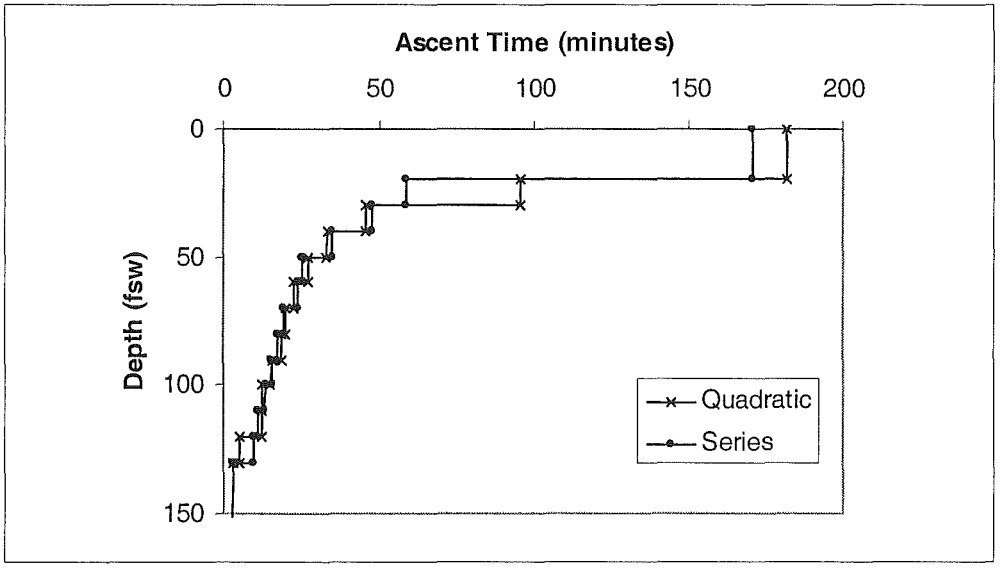

Figure 7.3 *Ascent profiles for a 300 fsw dive for 20 minute bottom times produced used quadratic and series stop times.*

The biggest variation in the performance of the optimisation process using different initial stop times is the number of iterations and function evaluations required as shown in Table 7.5. For the 200 fsw dive with a bottom time of 20 minutes, optimisation using ones and quadratic initial stop times requires 188 and 173 function evaluations compared to 393 required by the series stop times.

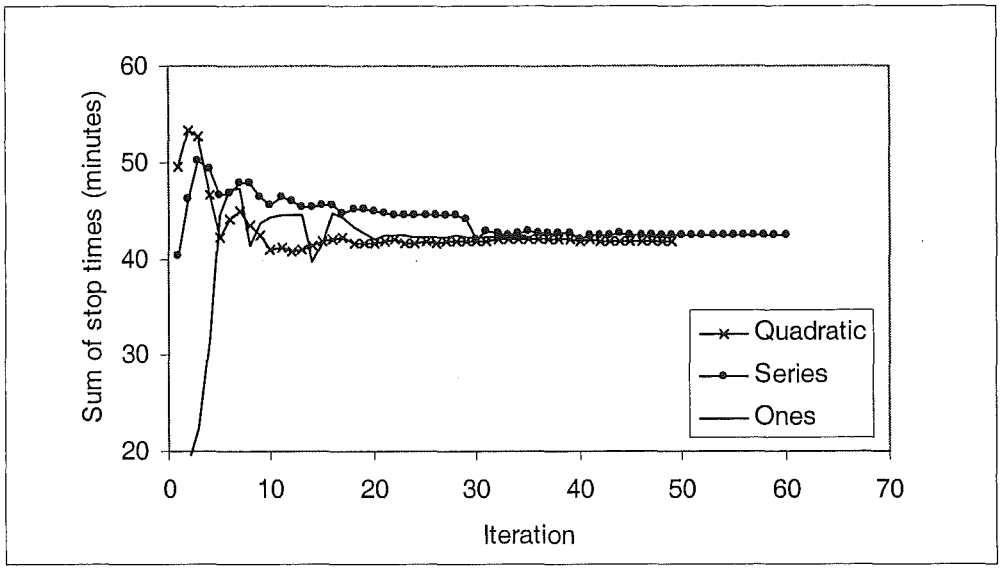

Figure 7.4 *Comparison of the total stop times for each iteration of the optimisation process started with ones, series and quadratic initial stop time values. 200 fsw dive for 20 minutes.*

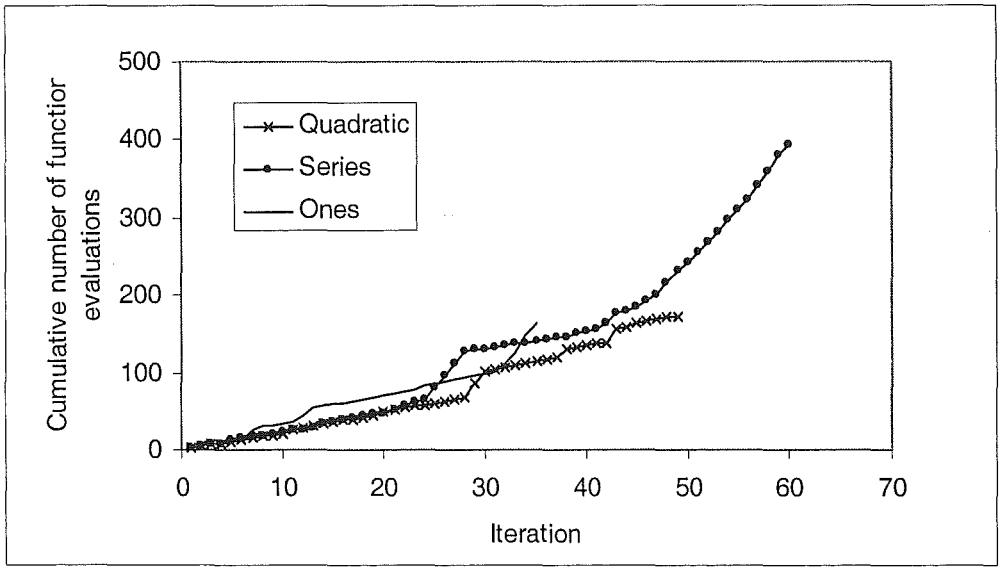

Figure 7.5 *Comparison of the cumulative number of function evaluations for each iteration of the optimisation process started with ones, series and quadratic initial stop time values. 200 fsw dive for 20 minutes.*

Figures 7.4 and 7.5 show the sum of the stop times and the cumulative number of function evaluations at each iteration of the 200 fsw dive. All the solutions have converged to close to the same total stop time by the 30th iteration, but require further iterations to meet the termination tolerances. Note that most of the function evaluations occur once the solution has almost converged. Recall the stop times $\bar{x}$ are updated by the formula

$$(\bar{x})_{p+1} = (\bar{x})_p + \alpha_p (\bar{s})_p \tag{7-8}$$

where $\bar{s}$ is the search direction vector. A line search is performed along the search direction to ensure the merit function given by equation 6-13 is reduced. This is done by repeatedly halving the scaling factor α until the merit function is reduced. Once the solution has almost converged, the acceptable scaling factor is very small and the merit function has been calculated many times. Each calculation of the merit function requires the function and constraints to be calculated. Relaxing the termination tolerances may reduce the number of function evaluations, but the results in Table 7.4 showed that this may not produce the best solution to the problem.

7.8 Adding weights to the objective function for total stop time.

In the previous analyses the objective function was set to the sum of the stop times,

$$f_1 = \sum_{i=1}^{n} x_i \tag{7-9}$$

An ideal decompression schedule would have most of the decompression stops close to the surface where the diver is closest to surface support and air to breathe should problems arise. In the previous sections, the fitting of the decompression stops to the three tissue model caused irregular stop times during the ascent which are unlikely to be acceptable to today's divers. These two reasons prompted the testing of two new objective functions of the stop times, x_i and the stop depths, d_i,

$$f_2 = \sum_{i=1}^{n} x_i \left(1 + \frac{d_i}{MD}\right)$$
$$f_3 = \sum_{i=1}^{n} x_i \frac{d_i}{MD}. \qquad (7\text{-}10)$$

The stop times were weighted, such that the deeper dives contributed more per minute to the objective function than the shallower functions. The second objective function was chosen such that the deepest stop was approximately double the weighting of the shallowest stop. The third function gives the deepest stop about 10 times the weighting of the shallowest stop.

The same six dive profiles were chosen as used in the previous section, with the risk of decompression illness set to 2% and TolCon, TolFun and TolX was set to 10^{-3}. Table 7.7 shows the performance of the optimisation scheme for the two weighted objective functions compared to the original non-weighted function.

The optimisation process using the third objective function increases the total stop time for most of the dive profiles compared to the non weighted objective function. The biggest increase of 20 minutes occurs for the 300 fsw dive for a 20 minute bottom time.

In two cases using the series initial stop times; 100 fsw for 30 minutes with f_2 and 300 fsw for 5 minutes with f_3, longer and irregular stop times were obtained at the termination tolerances. In both cases if the TolX values had been set to 10^{-5} results in line with the other objective functions would have been obtained.

The 300 fsw dive for 20 minutes optimised using the third objective function with ones as initial stop times did not terminate at TolX, TolFun equal to 10^{-3}. The best estimate in the 100 iterations with the constraint tolerance met gave a reasonable profile.

Table 7.9 shows the stops rounded to whole minutes for the three objective functions using 'ones' initial stop times for two dive profiles.

Maximum depth (fsw)	Bottom time (minutes)	Sum of stop times			Number of iterations			Number of function evaluations		
		f_1	f_2	f_3	f_1	f_2	f_3	f_1	f_2	f_3
100	30	1.02	1.02	1.02	6	5	6	13	11	13
	80	70.03	70.01	69.90	29	38	20	146	114	69
200	20	42.27	41.77	49.47	36	74	35	188	575	282
300	5	4.63	4.66	4.64	7	18	11	15	79	23
	15	99.6	101.87	108.05	87	95	69	504	713	353
	20	174.2	189.77	X	58	93	X	382	548	X

Table 7.7 *Comparison of optimisation performance for weighted and non weighted objective functions with ones initial stop times, risk set to 2% and TolCon, TolX and TolFun set to 10^{-3}.*

Maximum depth (fsw)	Bottom time (minutes)	Sum of stop times			Number of iterations			Number of function evaluations		
		f_1	f_2	f_3	f_1	f_2	f_3	f_1	f_2	f_3
100	30	1.02	3.59	1.02	13	6	12	41	16	25
	80	70.02	70.02	70.02	25	25	24	56	88	52
200	20	42.27	41.97	47.37	60	36	37	393	134	135
300	5	4.63	4.68	28.66	17	15	19	37	33	39
	15	101.27	100.93	116.41	96	57	72	1000	358	341
	20	164.43	177.2	185.53	97	67	54	456	413	344

Table 7.8 *Comparison of optimisation performance for weighted and non weighted objective functions with series initial stop times, risk set to 2% and TolCon, TolX and TolFun set to 10^{-3}.*

Dive	f_i	TTFD (min)	Stop times (minutes) at given stop depths (fsw)									
			110	100	90	80	70	60	50	40	30	20
200 fsw for 20 min	f_1	49	-	-	-	1	1	2	4	2	4	31
	f_2	47	-	-	-	-	2	2	3	3	2	31
	f_3	55	-	-	-	2	-	-	3	8	14	24
300 fsw for 15 min	f_1	108	3	2	3	3	2	3	2	2	8	74
	f_2	109	1	2	1	8	1	0	4	0	10	76
	f_3	116	-	-	1	1	2	8	1	7	6	84

Table 7.9 *Comparison of decompression schedules for different objective functions for two dives produced using ones intial stop times, TolX, TolFun and TolCon equal to 10^{-3} and 2% risk of decompression illness.*

The f_2 objection function produces a slightly better schedule than the non-weighted function for the 200 fsw dive, but both weighted objective functions produce more irregular series of stop times for the 300 fsw dive than the non-weighted function. These results are typical of the results obtained for the other dive profiles.

From these results the use of weighted objective functions of the form given by equation does not improve the decompression optimisation scheme and in some cases gives more irregular stop times.

7.9 Conclusions

This chapter has shown that it is feasible to use the sequential quadratic programming optimisation method to minimise the total time for decompression and yield iso-probabilistic schedules when the design parameters are the stop times for all possible decompression stop depths.

The results have shown that:

- The method produces results that generally give the longest stop times at the shallowest stops. However some of the decompression stops are irregular in length during the ascent due to over fitting the ascent to a three tissue model.

- Because of the underlying physiological and risk model the analyses have shown that there is large difference in stop times associated with small changes in the risk of decompression illness.

- There are many local solutions to the optimisation problem. The method produces similar results for the total time for decompression when starting with different initial stop times, though the stop times may vary. The exceptions being the highest tissue loading dives to 300 fsw for 15 and 20 minutes that have bigger differences in total stop time values.

- Setting the initial values of the stop times all equal to one provides feasible results with the exception of the longest bottom time for the deepest dive considered, 300fsw for 30 minutes. For this a set of stop times increasing with decreasing depths produced a feasible solution.

- In most cases the minimum of the Lagrangian function is not found and termination of the optimisation occurs due to convergence of the objective function value. A value of termination tolerances of TolX, TolFun and TolCon equal to 10^{-3} produces converged results in most cases. In two cases a stricter tolerance was required.

- The method does not identify infeasible solutions due to conflicting constraint violations. The termination criteria should be written to be more specific to the decompression optimisation problem.

- The use of a weighted objective function to encourage longer shallower stops did not reduce the irregularity of the stop times and produced no advantage over using the sum of the stop times for the objective function.

- The Hessian matrix is often not positive definite and the matrix has to be modified during the optimisation process. In some cases the modification becomes excessive and the solution becomes unreliable.

Areas that require further work if the approach were to be used in an automated process are:

- Incorporation of hard lower bounds for stop times to avoid negative stop times being calculated.

- Development of termination criteria specific to the decompression optimisation problem.

- Investigate alternative Hessian update procedures and search direction calculations.

- Investigate the effect of removing the lower bound risk constraint.

Decompression schedules generated using the non-weighted objective functions with initial stop times set to one are compared to a current 1.3 bar decompression table in Chapter 10.

THIS PAGE IS INTENTIONALLY BLANK

Chapter 8

Conversion of a continuous curve ascent profile to a stepped ascent profile

8.1 Notation

DSD	Deepest stop depth	d	Depth (msw or fsw)
MD	Maximum depth	*fsw*	Feet of sea water
$P(DCI)_{PROB3}$	Probability of decompression illness estimated by PROB3	*msw*	Meters of sea water
ROA	Rate of ascent	τ	Time from beginning of ascent (minutes)
TTFD	Total time for decompression	ω, ϕ, ν	Curve parameters

8.2 Introduction

One possible curve function that can approximate the stepped ascent of a dive from the maximum depth to the surface is given by the equation,

$$d = MD\left[1 - \nu \tanh\left(\omega \tau^{\phi}\right)\right] \tag{8-1}$$

where ω, ϕ and ν are parameters which control the shape of the curve. Parameters ϕ and ν are dimensionless and ω has time dimension $\mathrm{T}^{-\phi}$.

This chapter describes a scheme to convert an ascent given by equation 8-1 into an operationally useable stepped ascent. This technique will be applied in the curved ascent optimisation method in Chapter 9 to produce operationally acceptable stepped ascents.

8.3 Constraints on stepped ascents

The stepped ascent of a diver from the maximum depth of the dive to the surface is controlled by a number of operational constraints as well as the decompression requirements. These include:

- The deepest stop depth is a multiple of 3 msw or 10 fsw.
- The depth interval between decompression stops is 3 msw or 10 fsw.
- The shallowest decompression stop is 6 msw or 20 fsw.
- The maximum rate of ascent between stops and to the surface is set at a level dependent on the dive type and the breathing apparatus.

The fastest way for a diver to ascend to the surface is to ascend at a constant rate equal to the operational maximum rate of ascent. The total time for decompression (***TTFD***) must be greater or equal to the maximum depth (***MD***) divided by maximum rate of ascent (***ROA***).

$$TTFD \geq \frac{MD}{ROA} \tag{8-2}$$

When the diver ascends between stops or to the surface at a constant rate of ascent, this type of ascent will be called a *direct ascent*. The direct ascent is assumed to be at the maximum operational rate.

8.4 Possible shapes of ascent curves

The shape of the hyperbolic tangent curve given by equation 8-1 will vary depending on the choice of curve parameters; ω, ϕ and ν. Figure 8.1 shows a number of curve types that can be generated and compares them against a direct ascent. Each plot is of a time depth profile of a possible ascent. The time, τ, is the time from leaving maximum depth.

The ascents in Figure 8.1 plots A and B show curves that result in an ascent to the surface earlier than allowed by the maximum operational rate of ascent. Plot B initially starts to ascend at a rate slower than the maximum rate of ascent, but then ascends much faster resulting in a surfacing time earlier than the direct ascent.

Plot C gives an example where the curved rate of ascent is always slower than the maximum operational rate of ascent. A similar curve is shown in the second half of the curve in Plot D. Initially the curve ascends faster than the direct ascent. The curved rate of ascent then decreases allowing the two ascent profiles to cross over.

Figures 8.1 plots E and F show curves which have rates of ascent that are a combination of faster and slower than the operational ascent rate with no cross over with the direct ascent.

In the following sections, these curves will be used to explain and test the method for converting from a curved to a stepped ascent.

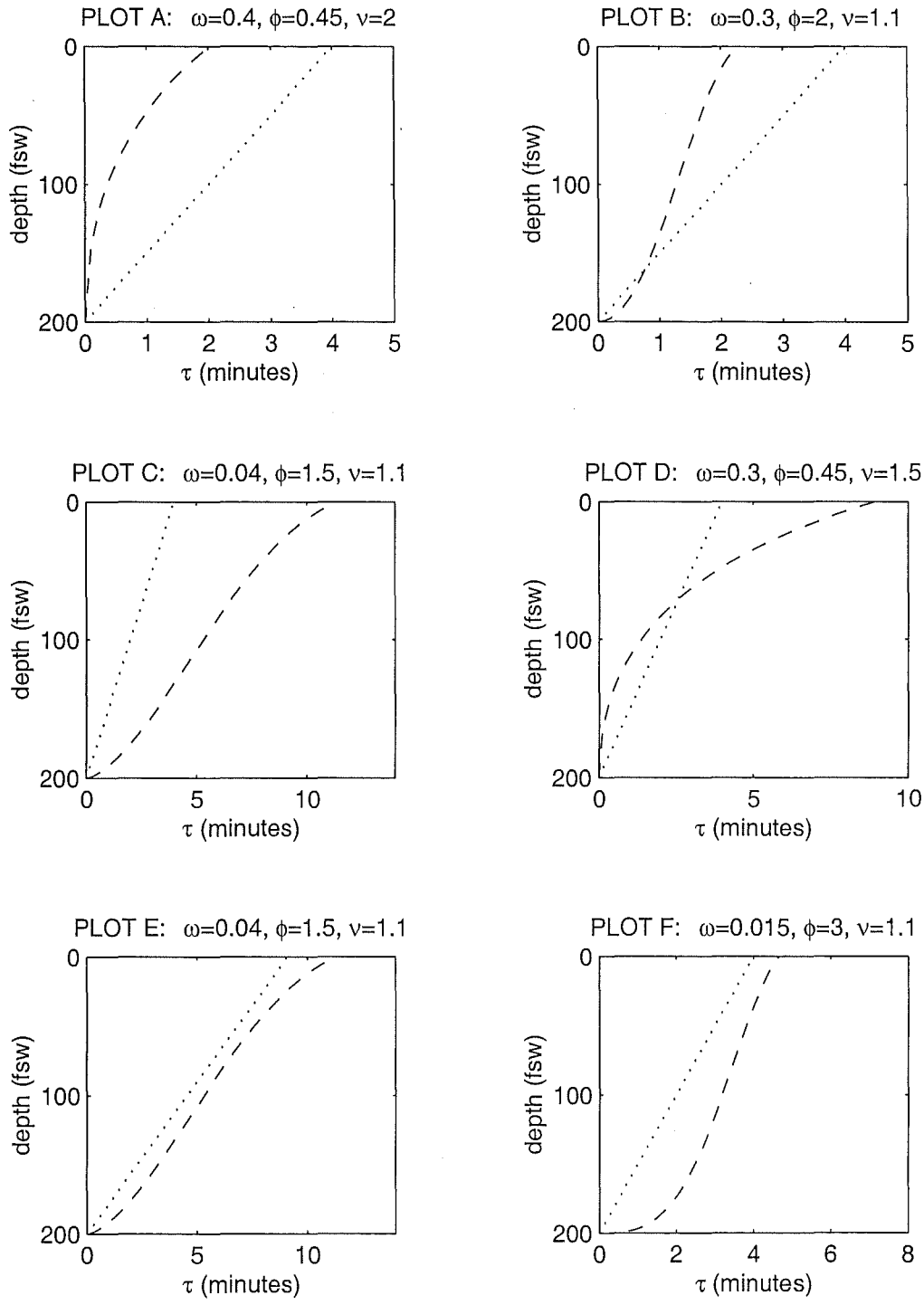

Figure 8.1 *Curved ascent profiles generated by equation 8-1 (dashed lines) in comparison to direct ascent profiles (dotted lines).*

8.5 A Method of converting a curved to a stepped ascent profile

Figure 8.1 showed the variety of curve profiles that can be generated by the hyperbolic tangent function given by equation 8-1. To automate the process of generating a stepped ascent profile from a curved one the following rules will be used:

1. When the total time for decompression of the curve ascent, $TTFD_{curve}$, is earlier than the total time for decompression given by the direct ascent, $TTFD_{da}$, the direct ascent will be used. This is shown in Figure 8.1 plots A and B.

2. When the total time for decompression of the curve ascent, $TTFD_{curve}$, is later than the total time for decompression of the direct ascent, $TTFD_{da}$, the total time for decompression will be set at the curve value.

3. The first ascent from maximum depth to the deepest possible stop depth, DSD, is taken along the direct ascent line. See area (◆) in Figure 8.2.

4. Between stop depths and from the shallowest stop depth to the surface the diver is assumed to ascend by a direct ascent.

5. When the curved profile reaches the next shallower stop depth earlier than a direct ascent would, the stepped ascent profile will use a direct ascent between the stop depths. See area (●) in Figure 8.2.

Using the above rules an algorithm was implemented in C-code, the logic of which is summerised in Figures 8.3 and 8.4. The numbers in { } in the following text relates to parts of the chart shown in Figure 8.4.

The algorithm first checks whether the dive will require any decompression stops {2,3}. If the curved ascent reaches the surface before the direct ascent no stops will be conducted {15}.

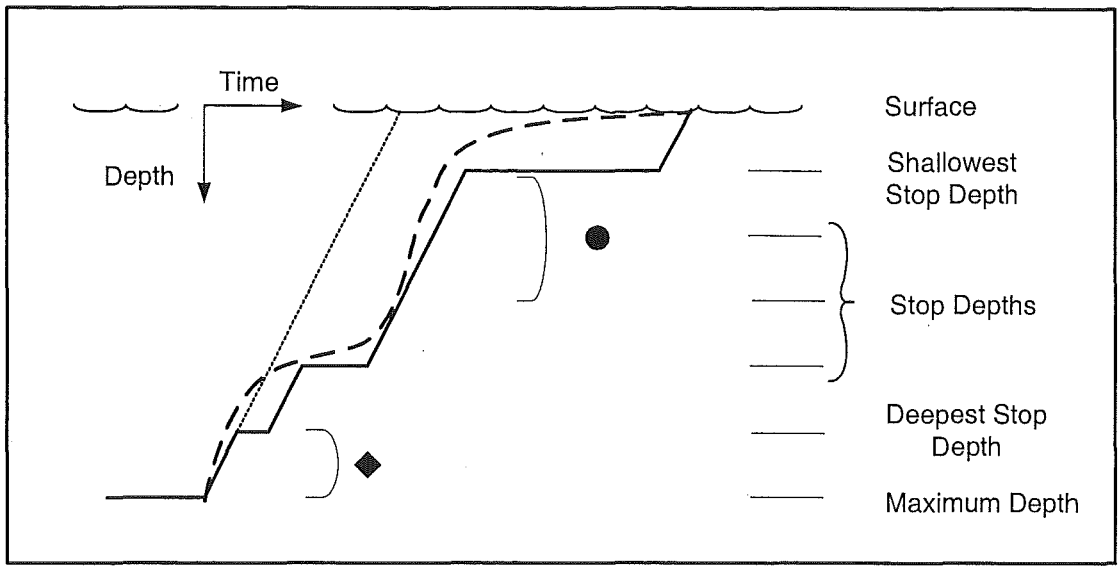

Figure 8.2 *Conversion of a curved ascent (dashed bold line) to a stepped ascent profile (solid bold line); (◆) direct ascent from maximum depth to deepest stop depth and (●) ascending at constant rate when the curved rate of ascent exceeds the operational rate of ascent.*

Once the need for decompression stops has been established, the dive ascent is broken down into a series of equal intervals in depth defining the stop depths. At the beginning of the ascent a direct ascent is made to the deepest possible stop depth, DSD {4,5}.

Following this, the algorithm enters the stepped ascent process. Consider the case when a diver has just reached a stop depth, d_k , at ascent time τ_k. To calculate the decompression stop time at the depth d_k, the following procedure is followed:

The time of intersection of the curve with the next shallowest stop depth, d_{k+1}, is calculated, τ_c {6}. The time coordinate τ_c relative to the time coordinate, τ_k, of reaching depth d_k, determines how the ascent will proceed up to the next shallowest stop depth, d_{k+1}. Starting from time τ_k the fastest the diver can ascend to the next shallower stop depth is by direct ascent rate.

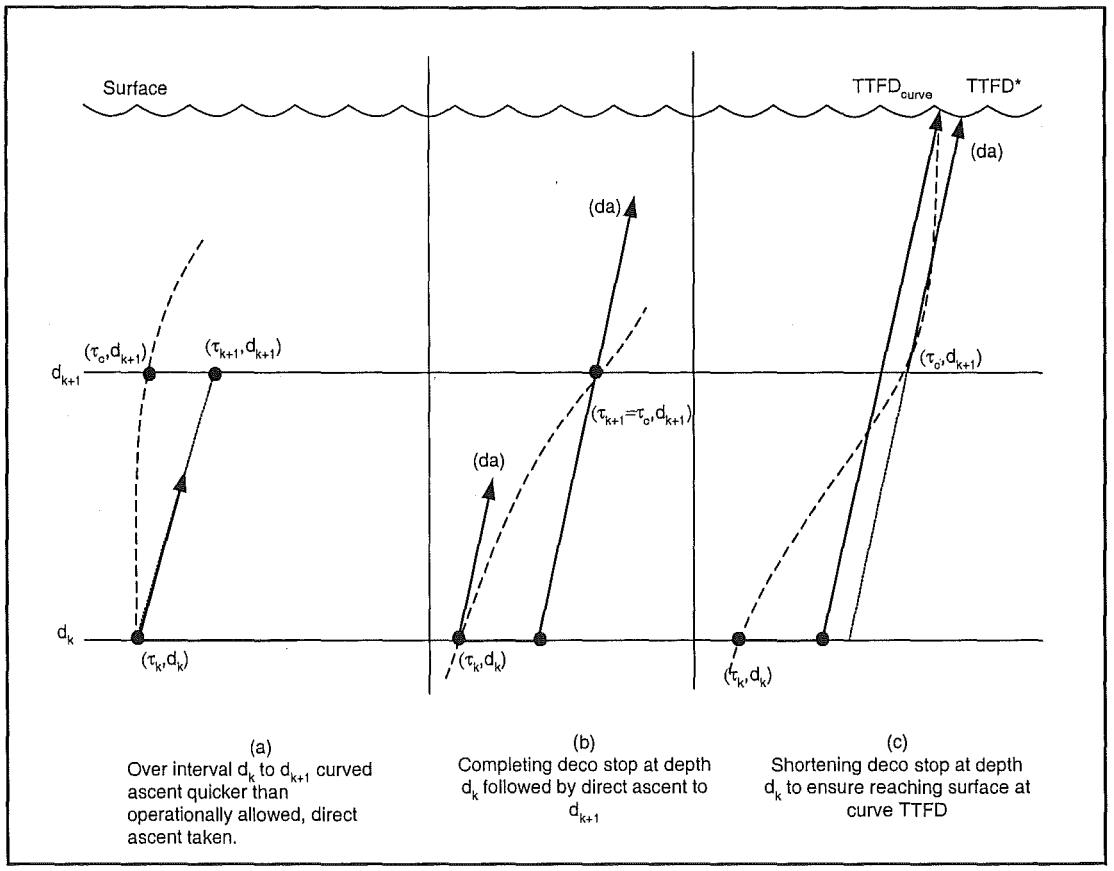

Figure 8.3 *Evaluation of decompression stop time at current stop time using the intersection of the curved ascent with next shallower stop depth.*

If the curve time coordinate τ_c is before or equal to the direct ascent time a direct ascent to depth d_{k+1} is taken {8}. If the curve time coordinate is after the direct ascent time then a decompression stop is calculated. The time coordinate of the end of the decompression stop at the stop depth d_k is calculated by removing the direct ascent time between the two stop depths, d_k and d_{k+1}, from the time τ_c {11}.

A check is made to see if a direct ascent to the surface can be made from the end of the decompression stop, before or at the same time as the curve total time for decompression {9,10}. If this is not possible the decompression stop time is reduced until this condition can be met and a direct ascent is made to the surface {14,15}.

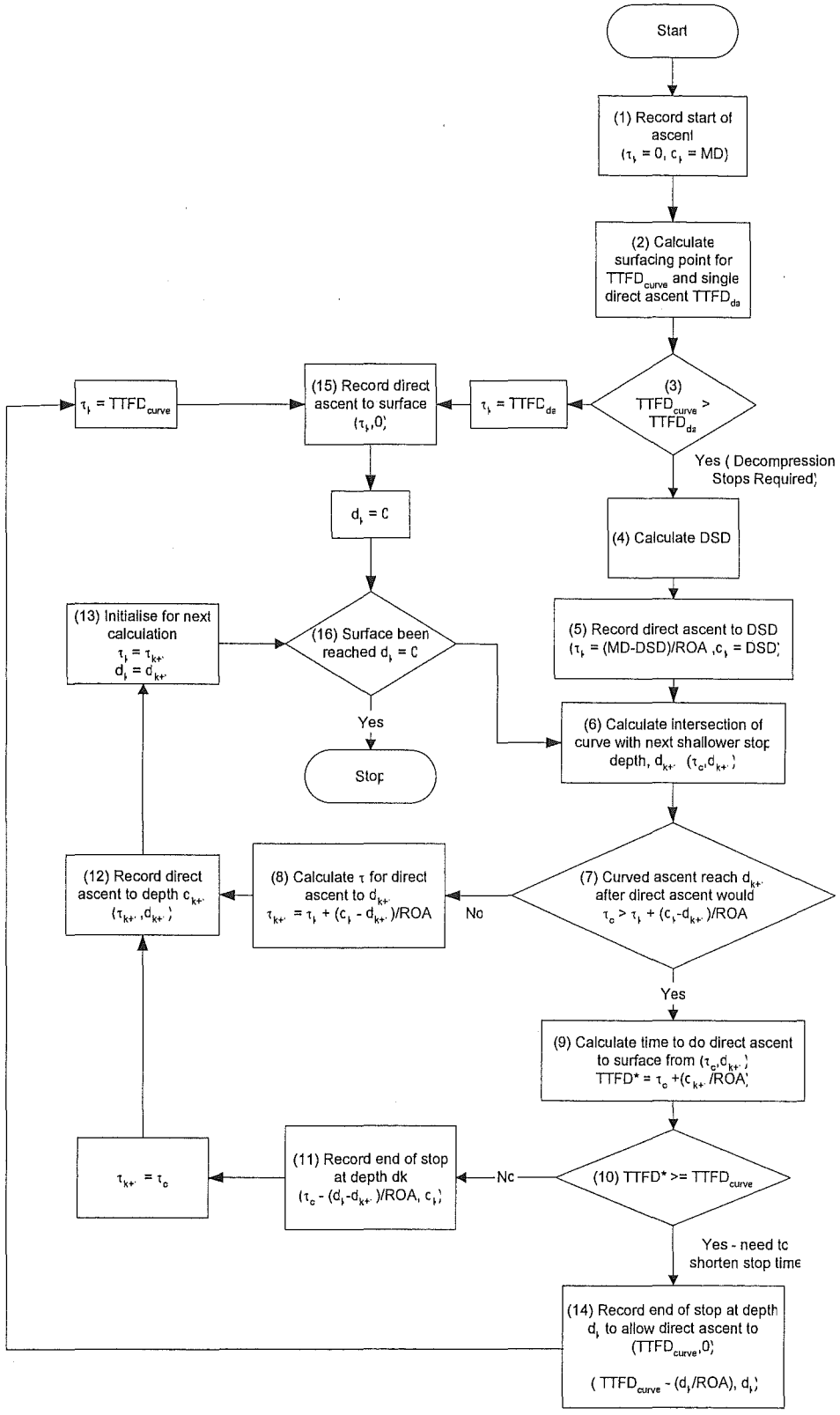

Figure 8.4 *Flow chart to show algorithm for converting a curved ascent profile to an operationally usable stepped profile.*

The process is repeated for each depth interval, d_k to d_{k+1} until the surface is reached {16}. At the end of each iteration, the next step is initialised by setting depth d_k equal to depth d_{k+1}. Note, the shallowest stop depth does not have to equal the depth interval between deeper stops.

8.6 Stepped ascent profiles generated from curved profiles

The algorithm described in Section 8.5 was used to fit stepped profiles to the curves shown in Figure 8.1. The resulting stepped profiles are plotted as solid lines in Figure 8.5 with the original curved profiles shown as dashed lines, and the direct ascent from maximum depth to the surface shown as a dotted line.

Plots A and B show direct ascents have been chosen to represent the curves. This is the correct ascent because the curve ascends to the surface faster then allowed by operational constraints.

The curve in Plot C always ascends at a rate slower than the direct ascent rate and decompression stops are calculated at all stop depths of the ascent.

Plot D shows how a direct ascent is taken from maximum depth until the curve ascent time becomes more than the direct ascent time at 80 fsw and decompression stops are calculated until the surface is reached. Similarly, the ascent in Plot E requires a direct ascent to be taken during the middle portion of the dive when the rate of curve ascent exceeds the direct ascent rate.

The final plot, Plot F shows how the stop at 190 fsw is shortened to ensure the ascent total time for decompression is equal to the curve total time for decompression, $TTFD_{curve}$, while adhering to the constraints of maximum ascent rate and positive decompression stop times.

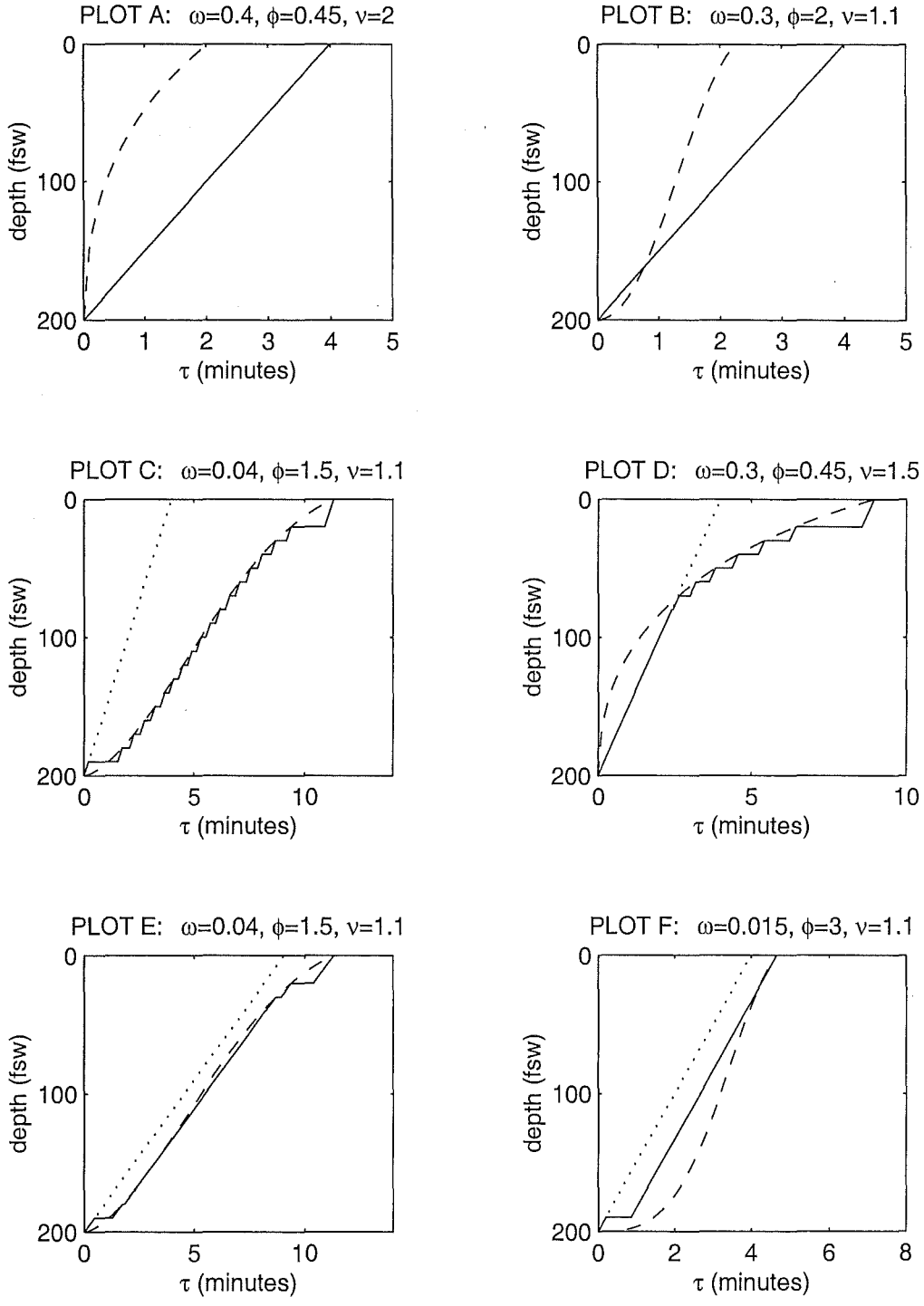

Figure 8.5 *Decompression stops (solid line) fitted to ascent curves (dashed line) for the curves plotted in Figure 8.1.*

To compare the PROB3 probability of decompression illness for the curved and stepped ascents a dive to 200 fsw for 10 minutes was considered. The diver is assumed to be breathing a 0.75 bar constant partial pressure of oxygen in helium gas mixture. The probabilities of decompression illness calculated by PROB3 for the two ascent types are given in Table 8.1.

The difference in risk of decompression illness for the curved and stepped ascent profiles given in Table 8.1 ranges from 0.18% to 1.48%. Five of the six ascent curves considered produced a higher estimate of decompression illness risk for the stepped ascent than the curved ascent. The difference can be explained by looking at the time spent at the deeper stop depths. This difference may be considered significant when trying to create tables with low risk values.

PLOT	ω	ϕ	ν	Maximum rate of ascent (fsw/min)	$P(DCI)_{PROB3}$ as %	
					Curved ascent	Stepped ascent
A	0.400	0.45	2.0	50	4.44	5.92
B	0.300	2.00	1.1	50	5.74	5.92
C	0.040	1.50	1.1	50	6.81	7.26
D	0.300	0.45	1.5	50	2.78	3.61
E	0.040	1.50	1.1	22	6.81	7.28
F	0.015	3.00	1.1	50	7.88	6.84

Table 8.1 *Comparison of risk of decompression illness, P(DCI), for curved ascent profiles and the comparable stepped ascents.*

The difference in risk between the curve and stepped ascent could be reduced by using a different curve fitting method. The above method was chosen to provide a simple, consistent method which would always produce a feasible ascent profile without using a numerical solution.

8.7 Conclusions

This chapter has described an algorithm to convert a curved ascent profile to a stepped profile suitable for operational open water use. The algorithm has been shown to reliably convert the curve to a useable stepped ascent profile for the range of possible curve shapes.

The constraints imposed on stepped ascents means the curved profile may be very different to the fitted stepped profile, resulting in different risk outcomes. A continuous set of curved profiles may not produce a continuous space of stepped ascent profiles. Correspondingly, the stepped ascent risk values may not produce a continuous space of risk values. This may have consequences when using the optimisation scheme in Chapter 9 to minimise the total time for decompression for a given risk value.

Chapter 9

Decompression optimisation using a curved ascent to define the stop times

9.1 *Notation*

BT	Bottom time	d	Depth
fsw	Feet of sea water	g_i	Inequality constraint
MD	Maximum depth	R	Estimated risk of decompression illness (%)
MDT	Maximum dive time	R_{acc}	Acceptable risk of decompression illness
ROA	Rate of ascent	η	Initial curve parameter
$TTFD$	Total time for decompression	κ	Risk penalty weight
$\#_{da}$	... direct ascent	τ	Time from beginning of ascent
$\#_{curve}$	... curved ascent	ω, ϕ, ν	Curve parameters

9.2 *Introduction*

Chapter 7 showed how it is possible to produce optimised iso-probabilistic tables using the stop times as the design parameters. This optimisation approach sometimes produced irregular series of stop times where the length of the stop time did not monotonically increase with decreasing depth.

To smooth out the irregular stop times caused by over fitting the decompression schedule to the three tissue model and to reduce the number of design parameters to be found curved ascents were investigated.

This chapter will evaluate the sequential quadratic programming method applied to the minimisation of the total time for decompression of ascents described by curves.

9.3 *Hyperbolic tangent curve ascent*

A curve function used to describe the decompression time-depth profile (τ,d) must have the following properties:

- At the start of the ascent, τ=0, the depth must equal the maximum depth (MD).
- The curve must cross the zero depth axis, otherwise the diver will never reach the surface.
- An initial fast ascent should be followed by longer stop times as the diver moves towards the surface. The curve needs to be able to have a steep gradient at the start of the dive followed by a decreasing gradient with decreasing depth.

One curve with the above characteristics is the three parameter hyperbolic tangent function that was introduced in Chapter 8,

$$d = MD\left[1 - \nu \tanh\left(\omega\tau^{\phi}\right)\right] \tag{9-1}$$

where d is the depth at ascent time τ. Here ϕ and ν are dimensionless curve parameters and ω is a curve parameter with time dimension $T^{-\phi}$. The units of ω depend on ϕ and will not be listed when presenting values of ω.

The form of equation 9-1 ensures that the start of the ascent is at the maximum depth, but the depth can only equal zero if ν is greater than one.

Figure 9.1 shows how the parameters ω, ϕ and ν affect the ascent profile. Some of the curves in Figure 9.1 cross the zero depth axis. This is the point at which the diver reaches the surface. The portion of the curve relating to negative depths is drawn solely for comparison of the curve shapes. For the diving scenario, the diver remains at zero depth for 24 hours following the dive that is processed by the PROB3 program.

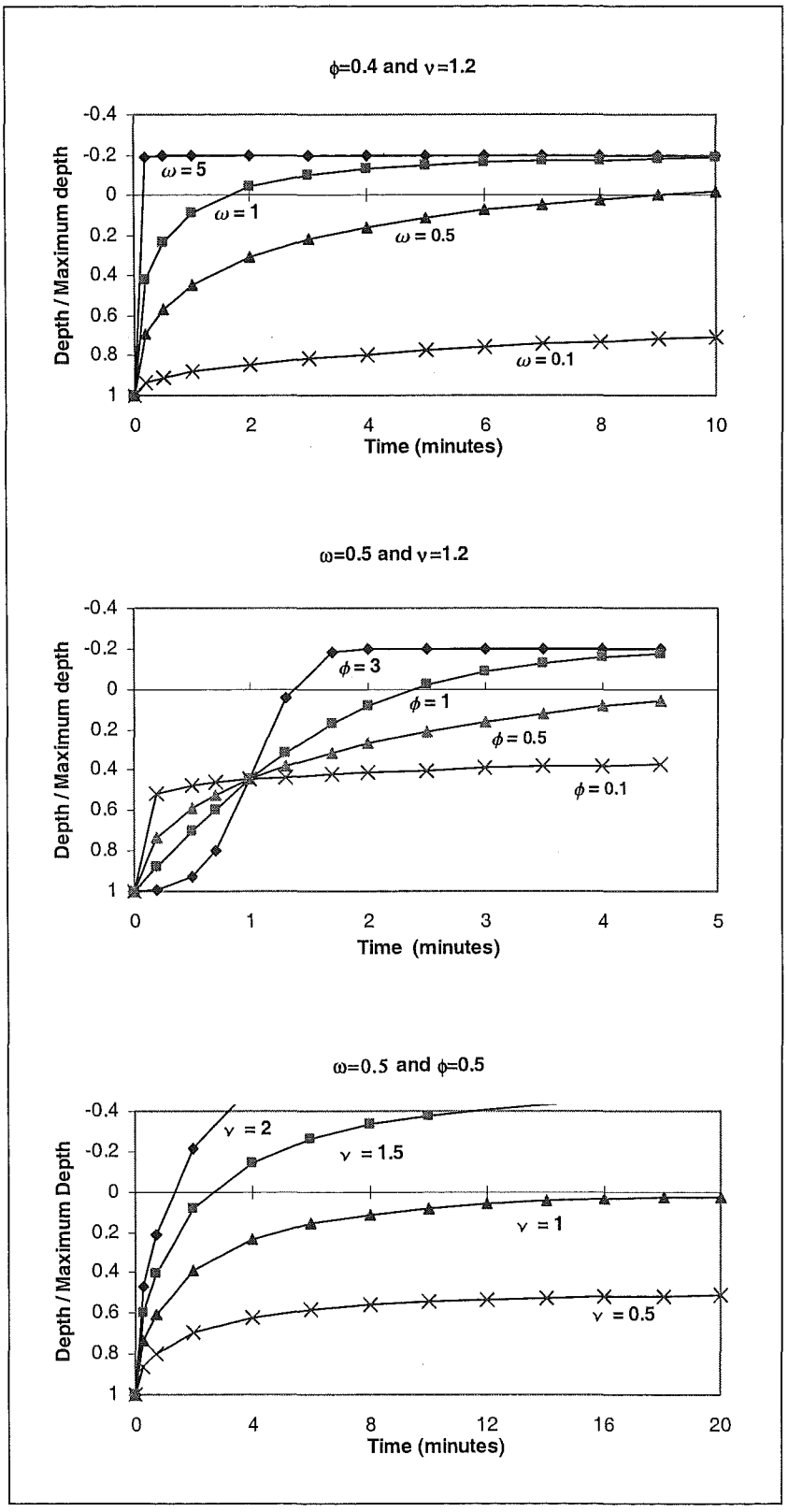

Figure 9.1 *The dependency of the depth-time profile defined by the hyperbolic tangent function on the curve parameters ω, ϕ and ν.*

The parameter ω controls how much of the hyperbolic tangent curve is used to describe the ascent profile. The parameter ϕ controls the curve shape and especially controls the initial part of the ascent curve. To mimic the uniform ascent rate usually seen at the start of an ascent the value of ϕ should be kept equal or less than one. The parameter ν controls how fast the curve approaches the surface.

Each of the plots in Figure 9.1 show at least one curve that will not reach zero depth in a calculable time frame. One example is the curve in the top plot given by the parameter values $\omega = 0.1$, $\phi = 0.4$ and $\nu = 1.2$.An analytical solution for the total time for decompression ($TTFD$) can be found from setting the depth equal to zero in equation 9-1 and rearranging to give,

$$TTFD = \left(\frac{\tanh^{-1}\left(\frac{1}{\nu}\right)}{\omega} \right)^{\frac{1}{\phi}} \quad . \tag{9-2}$$

From equation 9-2 and the curves in Figure 9.1 the following should be considered when choosing bounds to be applied to the hyperbolic tangent curve parameters;

- ω must be positive to avoid negative times.
- ϕ must be positive to ensure the depth decreases with increasing time.
- ω and ϕ must be large enough to avoid an excessively large total time for decompression.
- ν must be greater than one to ensure a zero depth can be reached and positive to avoid negative stop times.

From these rules the following lower bounds for the curve parameters will be used,

9.4 *Governing equations*

The curved ascent decompression optimisation problem is described by,

$$\min_{\omega,\phi,\nu} \quad TTFD = \left(\frac{\tanh^{-1}\left(\frac{1}{\nu}\right)}{\omega} \right)^{\frac{1}{\phi}} \qquad \omega > 0.01,\ \phi > 0.1 \text{ and } \nu > 1.01 \tag{9-3}$$

subject to two non-linear time constraints and two non-linear risk constraints. The first time constraint requires the ascent to be slower or equal to a direct ascent from maximum depth to the surface at the operational rate of ascent (**ROA**).

$$g_1 = \frac{MD}{ROA} - TTFD \leq 0 \ . \tag{9-4}$$

The second time constraint is the maximum dive duration due to equipment performance. This constraint was linear in the stop time optimisation scheme (section 7.3), but is now non-linear because the total time for decompression is a non-linear function.

$$g_2 = BT + TTFD - 240 \leq 0 \tag{9-5}$$

The two non-linear risk constraints are the same as described in section 7.3.

$$\begin{aligned} g_3 &= R - R_{acc} \leq 0 \\ g_4 &= R_{acc} - \xi - R \leq 0 \end{aligned} \tag{9-6}$$

The total time for decompression is optimised subject to the risk of decompression illness. The risk may be calculated for a diver following a curved ascent profile to the surface. The solution ascent profile would then have to be converted to a stepped ascent for operational use. Alternatively, at each iteration, the risk can be calculated for a stepped ascent that has been fitted to the curve.

Derivatives of the total time for decompression equation (9-2) are

$$\begin{aligned}
\frac{\partial TTFD}{\partial \omega} &= \frac{-TTFD}{\omega\phi} \\
\frac{\partial TTFD}{\partial \phi} &= \frac{-TTFD}{\phi} ln(TTFD) \\
\frac{\partial TTFD}{\partial \nu} &= \frac{TTFD}{\phi(1-\nu^2)tanh^{-1}(\frac{1}{\nu})}
\end{aligned} \tag{9-7}$$

where ***TTFD*** is given by equation 9-2. The risk gradients must be calculated using finite differences.

9.5 *MATLAB implementation*

The algorithm was implemented using MATLAB in the same manner as the stop time optimisation described in Chapter 7.

At each iteration the risk was calculated for a stepped ascent fitted to the curve ascent by the method described in Chapter 8. The curve was converted to a stepped ascent before calculation of the risk to avoid introducing an error in the risk of the final schedule. In the previous chapter Table 8.1 compared the risk of decompression illness for curved ascents and the corresponding stepped ascent. This table showed the stepped ascent could have a higher risk of decompression illness than the curved ascent.

The risk gradients $\frac{\partial R}{\partial \omega}, \frac{\partial R}{\partial \phi}$ and $\frac{\partial R}{\partial \nu}$ were calculated using the forward difference equation (7-5). The forward difference equation was used in preference to backwards or central difference methods to avoid violation of the lower bounds on the design parameters.

The fastest a diver can ascend to the surface is with no decompression stops and traveling at the operational rate of ascent. However, a hyperbolic tangent curve can ascend to the surface faster than the operational rate (Figure 8.1, plot A &B).

In all the analyses, the risk of decompression illness for a direct ascent profile was evaluated to check if decompression stops were required before any optimization took place. This guarantees that total time for decompression of the curve ascent must be greater than the direct ascent time. In the curve fitting scheme, all curves with a total time for decompression smaller than the operational direct ascent have the ascent set to a direct ascent for the risk calculation. In this region of the parameter space, the risk gradients will be zero.

To prevent a region of zero gradients an alternative risk function, $\hat{R}$, is used when the total time for decompression of the curve, $TTFD_{curve}$, is less than for the direct ascent, $TTFD_{da}$,

$$\hat{R} = \left[1+100\left(TTFD_{da}-TTFD_{curve}\right)\right]R\left(\text{direct ascent at ROA}\right). \tag{9-8}$$

9.6 *Initial analysis*

The MATLAB program termination criteria introduced in section 6.5 were set to:

- tolCon = $1\text{x}10^{-3}$ which is the same value used for the stop time optimisation described in Chapter 7.

- tolFun and tolX = $1\text{x}10^{-6}$ which is small enough to allow the changes in design parameters to be observed with each iteration of optimisation process and suitable termination tolerances chosen.

The initial parameter values were chosen to provide an ascent shape typical of current tables with the total time for decompression some multiple η of the time taken to do a direct ascent to the surface. The initial parameters were set to;

$$\omega = \frac{\tanh^{-1}\left(\frac{1}{\nu}\right)}{\left(\eta TTFD_{da}\right)^{\phi}}, \qquad \phi = 0.3 \quad \textit{and} \quad \nu = 1.3. \tag{9-9}$$

Ascent curves for different multiples of direct ascent time are given in Figure 9.2.

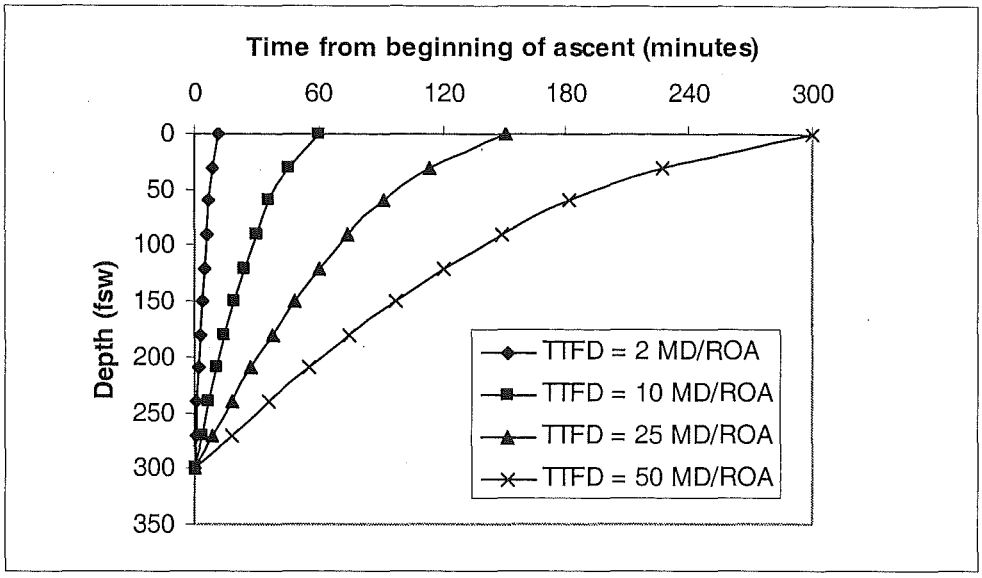

Figure 9.2 Curved ascent profiles used for initializing ω, ϕ and ν.

An initial set of test runs were performed on the dive profiles described in section 6.6. The risk of decompression illness was set at 2%. Two different initial curves were tested with η set to 2 and 25. The optimisation process was stopped for most of the dive profiles because the total time for decompression became too large.

For certain combinations of parameter values, small changes in parameter value can lead to large changes in total time for decompression. One example is given in Figure 9.3 which shows the contour plot of total time for decompression with contours at 40 minute intervals. For the fixed value of ν =1.1, it can be seen that reducing the values of ω and ϕ increases the rate of increase of total time for decompression. The largest contour plotted is 600 minutes but the value of total time for decompression for ω = 0.3 and ϕ = 0.15 is 5×10^4, increasing to 1×10^7 when ϕ further reduces to 0.1.

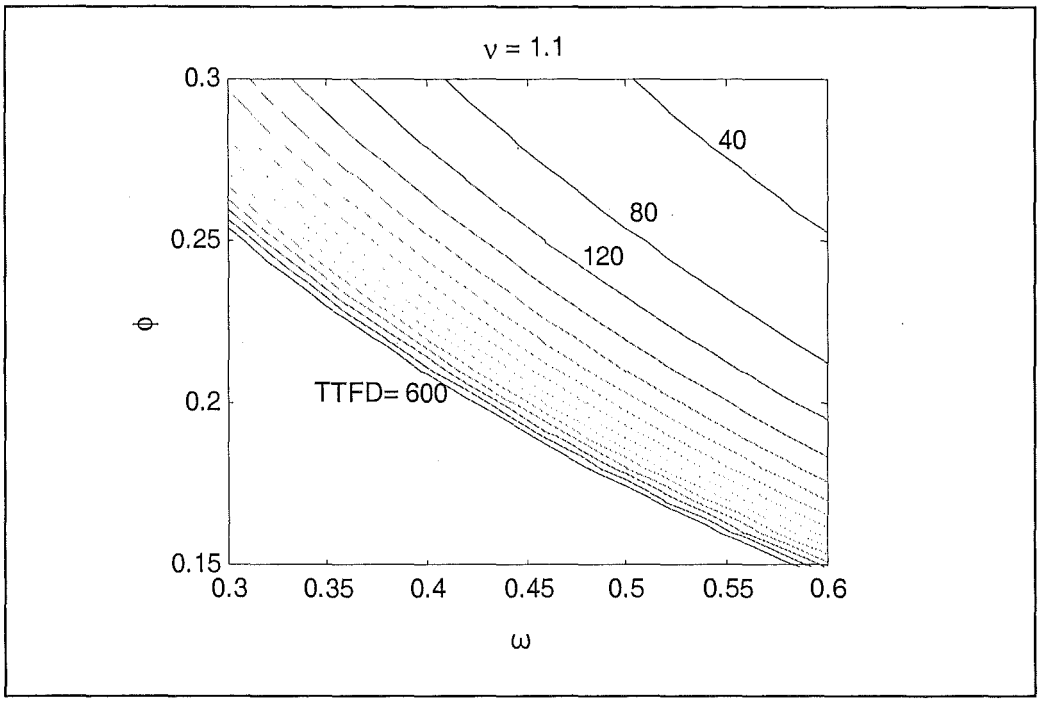

Figure 9.3 *Relationship between the total time for decompression and curve parameters ω and ϕ for a value of ν equal to 1.1. The contours of total time for decompression are at 40 minute intervals.*

For these analyses the maximum permissible total time for decompression was set to 2000 minutes. The risk is calculated from the tissue carrier pressures during the dive and for one day after the dive. Excessively long dives result in processing time that is excessively long. It will take more than a couple of hours to calculate a single risk value for a dive that is over 100 days long. The risk for dives that do not reach the surface cannot be calculated. Table 9.1 shows the total time for decompression at the solution or error terminated iteration for the 6 different dive profiles. The shaded boxes indicate the three cases where the optimisation completed successfully.

Only three of the twelve analyses resulted in a solution to the minimisation problem before the design parameters took values that produced large total time for decompression. It is not easy to provide a penalty function to each of the parameters separately to avoid large total time for decompression, because it is the combination of parameters in the hyperbolic tangent function that contribute to it's size.

Maximum depth (fsw)	Bottom time (minutes)	η=2		η=25	
		TTFD (minutes)	Termination iteration number	TTFD (minutes)	Termination iteration number
100	30	3.05	31	$5x10^6$	1
	80	$5x10^6$	2	$5x10^6$	1
200	20	$4x10^3$	2	52.01	31
300	5	$4x10^3$	5	11.36	40
	15	$3x10^{10}$	1	$5x10^6$	3
	20	NaN	1	$5x10^6$	18

Table 9.1 *Total time for decompression at the iteration the optimisation process was stopped. The successful minimisation outcome is indicated by the shaded cells.*

To encourage the solution to stay in the region of smaller total time for decompression an alternative risk function was used when the curve total time for decompression, $TTFD_{curve}$ was greater than twice the maximum allowable total time for decompression, $TTFD_{max}$,

$$TTFD_{curve} > 2\,TTFD_{max} = 2\,(MDT - BT). \tag{9-10}$$

Let $\breve{R}_{\omega}$ be the risk of decompression illness for a curved ascent with ϕ and ν fixed at the current iteration value and ω changed so the total time for decompression of the curve is twice the maximum allowable value. $\breve{R}_{\phi}$ and $\breve{R}_{\nu}$ are defined in the same way.

A weighted risk function that avoids calculating the risk for long total time for decompression times can be written

$$\breve{R} = \left(1 + \kappa - \frac{2(MDT - BT)}{TTFD_{curve}}\kappa\right)\left(\frac{\breve{R}_{\omega} + \breve{R}_{\phi} + \breve{R}_{\nu}}{3}\right) \qquad TTFD_{curve} > 2(MDT - BT)$$

where κ is a weight value set to 100 for the rest of the results in this thesis. This form of function was chosen to ensure continuity of risk at the boundary defined by $TTFD_{curve} = TTFD_{max}$.

The risk gradients $\frac{\partial \breve{R}_\omega}{\partial \omega}, \frac{\partial \breve{R}_\phi}{\partial \phi}$ and $\frac{\partial \breve{R}_\nu}{\partial \nu}$ are calculated using forward difference formula. Simplified risk gradients are then calculated using the follow estimate,

$$\frac{\partial R}{\partial x_i} \approx \left[1+\kappa-\frac{2(MDT-BT)}{TTFD_{curve}}\kappa\right]\frac{\partial \breve{R}_{x_i}}{\partial x_i} \qquad x_i = \omega, \phi \text{ or } \nu. \tag{9-12}$$

Incorporating the penalty function into the algorithm resulted in ten out of the twelve analyses in Table 9.1 successfully completing the optimisation. The dive to 100 fsw for 30 minutes with $\eta = 25$ tried a value of parameter ν which was less than one resulting in MATLAB producing a complex number for the total time for decompression. Recall that

$$\tanh^{-1}\left(\frac{1}{\nu}\right) \in \Re \quad \text{for} \quad \nu < 1.$$

Recall that MATLAB function '*nlconst*' treats parameters bounds as linear constraints, not hard bounds that can not be exceeded. If a new program was to be written hard bounds should be incorporated into the method.

The second dive that failed to terminate was the dive to 300 fsw for 20 minutes with $\eta = 2$. This time the optimisation stopped when all three parameter values became too small and the total time for decompression could not be calculated. Both these dives are at the extremes of the dive profiles considered and a successful optimisation occurred when the alternative starting curve that was closer to the final solution was used.

These analyses produced increasing stop times with decreasing depth. The curved ascent optimisation scheme has solved the problem of irregular stop times that was highlighted in Table 7.3 for the stop time optimization scheme. Table 9.2 shows the

decompression stop times produced by the curved ascent and the stop time optimisation schemes applied to a dive to 300 fsw for 15 minutes at a 5% risk level.

Optimisation scheme	TTFD (minutes)	Decompression stop times (minutes) at stop depths								
		100 fsw	90	80	70	60	50	40	30	20
Stop time	51.8	0.3	6.4	2.4	3.8	-	5.7	1.9	10.8	14.5
Curve	53	-	-	-	1.4	2.8	4	5.7	7.8	25.3

Table 9.2 *Comparison of decompression schedules for a dive to 300 fsw for 15 minutes at a 5% risk level produced by the stop time and curve optimisation schemes.*

The total time for decompression for the two schedules is the same to within two minutes, with the stop time scheme producing a slightly shorter schedule. Further comparison of schedules produced by the two optimisation schemes will be made in Chapter 10.

9.7 *Convergence criteria*

Six dive profiles were analysed with risk set points of 1%, 2% and 5%. Initial parameter values were set to $\phi = 0.3$, $\nu = 1.3$ and ω calculated to provide a total time for decompression of 2 and 25 times the direct ascent time. The total time for decompression and iteration information with η = 25 for different termination tolerances for either tolX or tolFun is given in Table 9.3. The convergence results for the analyses using the shorter initial total time for decompression, with η = 2, were similar to those for η=25.

Maximum depth (fsw)	Bottom time (minutes)	Risk (%)	$TTFD_{curve}$			Number of iterations			Number of function evaluations		
			10^{-2}	10^{-3}	10^{-4}	10^{-2}	10^{-3}	10^{-4}	10^{-2}	10^{-3}	10^{-4}
100	30	1	6.41	6.38	6.39	7	9	20	23	27	60
		2	Failed due to $\nu < 1$			1			3		
		5	DIRECT ASCENT								
	80	1	110.28	110.21	110.21	9	11	19	33	37	83
		2	75.36	74.25	74.06	9	23	32	33	88	127
		5	7.40	6.84	6.83	17	38	53	43	114	169
200	20	1	90.08	86.79	86.06	8	24	37	34	93	139
		2	48.93	47.50	47.43	13	20	26	54	73	128
		5	→	→	19.40	→	→	43	→	→	218
300	5	1	13.38	13.33	13.33	17	29	30	114	185	189
		2	26.05	10.69	10.68	14	25	33	33	69	88
		5	→	→	6.09	→	→	23	→	→	98
	15	1	→	153.33	153.69	→	17	23	→	58	81
		2	→	115.38	114.83	→	20	30	→	96	171
		5	Best guess 53.00			Exceeded 100					
	20	1	→	218.9	218.88	→	76	77	→	509	512
		2	182.74	179.75	177.48	15	24	36	65	90	185
		5	→	→	94.83	→	→	98	→	→	510

Table 9.3 *Comparison of performance of sequential quadratic programming optimisation for different termination tolerances and risk of decompression illness. Design parameters are ω, ϕ and ν with initial total time for decompression set to 25 times the direct ascent time. The → indicates the termination criteria reduced straight to a termination value smaller than the value for this column.*

A comparison of the total time for decompression values across termination tolerances of 10^{-2}, 10^{-3} and 10^{-4} for tolX and tolFun shows the value 10^{-2} does not always provide a converged minimum for the total time for decompression. The biggest difference occurs for the dive to 300 fsw for 5 minutes at a 2% risk level, where the total time for decompression drops from 26 minutes at the 10^{-2} termination tolerance to 11 minutes at the 10^{-3} termination tolerance. Some of the dive profiles provided slighter smaller total for decompression at the 10^{-4} termination tolerance, but for many more function evaluations.

In future analyses the termination tolerances will be set to 10^{-3} for tolX, tolFun and tolCon.

For most of the analyses summarised in Table 9.3 the optimisation process terminated soon after reaching a converged value. The 300 fsw dive for 20 minutes with a 1% risk level took a large number of iterations before a solution with a total time for decompression of 219 minutes was found. This solution is very close to the maximum allowable total time for decompression of 220 minutes for a dive with a 20 minute bottom time. The first 68 iterations were spent with curve parameters that produced a total time for decompression greater than the maximum 220 minutes. The parameters continually changed until the maximum dive time constraint was satisfied at iteration 68. Once this point was reached, the optimisation process located a solution in the following 10 iterations.

9.8 *Sensitivity of schedules to choice of initial curve parameter values and optimisation scheme*

The initial curve parameter values were defined by equation 9-9. This section will further investigate the sensitivity of the optimised total time for decompression value to the initial parameter values. The results from the optimisation process using $\eta = 2$ and $\eta = 25$ are compared in Table 9.4. These results were generated for a 2% risk of decompression illness. For comparison purposes the results from the stop time optimisation scheme using initial stop times equal to one are also given in Table 9.4.

Maximum depth (fsw)	Bottom time (minutes)	*TTFD* (minutes)	$TTFD_{curve}$ (minutes)		Number of iterations			Number of function evaluations		
		Ones	$\eta = 2$	$\eta = 25$	ones	$\eta = 2$	$\eta = 25$	ones	$\eta = 2$	$\eta = 25$
100	30	3.02	3.02	X	6	11	X	13	40	X
	80	72.03	74.27	74.25	29	14	23	146	87	88
200	20	46.27	47.73	47.50	36	21	20	188	182	73
300	5	10.63	10.69	10.69	7	23	25	15	90	69
	15	105.6	124.76	115.38	87	12	20	504	55	96
	20	180.1	X	179.75	76	X	24	682	X	90

Table 9.4 *Comparison of performance of curved ascent sequential quadratic programming optimisation for two different initial decompression times and the stop time optimisation using initial stop times set to one. TolX, TolFun and TolCon set to 10^{-3} and decompression illness risk set to 2%.*

The results produced by the curve optimisation scheme are dependent on the choice of starting values for the short and shallow and deep and long dives. As discussed in section 9.6, if the starting curve is too far from the solution curve the optimisation algorithm may try curve parameter values outside the lower bounds of the curve parameters. This occurs in the 100 fsw dive for 30 minutes and the 300 fsw dive for 20 minutes, indicated by an X in Table 9.4.

There is also a difference of 10 minutes in the total time for decompression values for the 300 fsw dive for 15 minutes across the two different initial curves.

The remaining dives give total time for decompression values independent of the starting values. However, the ascent curves vary slightly for the different starting ascent profiles. To provide optimum decompression tables using the curved ascent optimisation scheme multiple starting values should be considered.

Comparison of the curved and stop time optimisation scheme results in Table 9.4 shows there is good agreement in the total time for decompression across the two schemes. The exception being the 300 fsw for 15 minute dive, where the stop time scheme generates a shorter decompression time by 10 minutes.

For the deeper dives and higher tissue carrier loadings at bottom time there are more possible ascent routes to surface at a given risk of decompression illness. Imposing a curve profile reduces the number of possible ascent paths that can be taken in comparison to optimising over the stop times and in some cases limits the minimum value of the total for decompression that can be found.

The number of iterations and function evaluations required by each of the two optimisation schemes varies for different types of ascent profile. The 100 fsw dive for 30 minutes and the 300 fsw dive for 5 minutes require only a few short decompression stops. For these profiles the stop time optimisation scheme is most efficient. For the remaining dive profiles resulting in longer and/or more decompression stops the curve optimisation scheme is more efficient.

9.9 *Conclusions*

This chapter has evaluated the ability of the sequential quadratic programming method with a curved ascent profile to minimise the total time for decompression for a dive and produce iso-probabilistic schedules.

The following has been observed:

- A three parameter hyperbolic tangent function can successfully be used to define dive ascent profiles which are conceptually acceptable to divers.

- The curve optimisation scheme requires a risk penalty function to be used when the total time for decompression becomes too large to avoid excessively long computation time to determine the risk of decompression illness for a dive. The penalty function reduces processing requirements and reduces the number of iterations required for a solution. An alternative curve function may reduce the sensitivity of the total time for decompression on the curve parameters and remove the need for a penalty function.

- The optimisation scheme is sensitive to the starting values for long deep dives and short shallow dives. In some cases a solution will not be found if the initial curve is too far from the solution. Multiple initial curves should be used for schedule generation.

- The curve optimisation scheme produces decompression stops that increase with decreasing depth and are not irregular as observed in the stop time optimisation decompression schedules.

- The curve optimisation scheme has better convergence behaviour than the stop time optimisation scheme for dives involving more than a couple of decompression stops.

THIS PAGE IS INTENTIONALLY BLANK

Chapter 10

Comparison of optimised decompression schedules with QinetiQ 90 Table

10.1 Introduction

This chapter compares decompression schedules generated by the stop time and curve optimisation schemes against the latest 1.3 bar oxygen in helium tables generated by QinetiQ Alverstoke. The ability of the two optimisation schemes to produce decompression tables and real time dive decompression schedules for use in a dive computer are also assessed.

10.2 QinetiQ 90 Decompression Tables

The QinetiQ 90 table [Evans & Anthony 2003] was generated by QinetiQ Alverstoke for rebreather dives with a constant 1.3 bar oxygen in helium gas mix. The UK Royal Navy have adopted these tables for 80 msw oxygen in helium diving.

The schedules are generated from a Haldanian, parallel tissue model using 9 tissue compartments (Figure 2.4a) and non-probabilistic safe ascent criteria. The carrier motion between the tissues and vascular system was described by the linear-exponential kinetics used in the LEM physiological model.

The model was calibrated using trials data and the PROB3 program used to ensure all decompression schedules had close to or less than a 2% operational risk of decompression illness.

Over 500 chamber and open-water dives were conducted to test the QinetiQ 90 decompression tables. One case of decompression illness for a dry chamber attendant

was reported during the trials. Doppler ultrasound equipment was used to detect bubbles in the blood stream of divers following the completion of the dive. Some of the dives resulted in high number of bubbles detected [T.G. Anthony, pers. comm.].

10.3 Generation of optimised schedules for QinetiQ dive profiles

Decompression schedules were generated for dives to 18 msw, 39 msw, 60 msw and 81 msw. For each depth three bottom times were chosen from the QinetiQ tables to span the range of bottom times that resulted in decompression stops.

The stop time optimisation scheme described in section 7.3 was used with tolX, tolFun and tolCon set to 10^{-3}. The initial values of the stop times were all set to a value of one.

The curved ascent optimisation scheme described in Chapter 9 was used with tolX, tolFun and tolCon also set to 10^{-3}. The dives were optimised using initial curve parameter values that resulted in total time for decompression equal to twice and twenty five times the direct ascent total time for decompression. The shortest decompression produced by the two initial starting curves was chosen as the decompression schedule. Each of the initial curves produced half of the final schedules.

The optimised decompression schedules generated by the stop time and curved ascent schemes gave decompression stops in minutes to a number of decimal places. Decompression schedules used by the Navy in open water require the stop times to be rounded to whole minutes.

The optimised stop times were rounded to whole minutes by rounding down if the fraction of a minute is less than or equal to one quarter. The stop time was rounded up to the next biggest complete minute if the fraction of a minute was more than a quarter.

The range of optimised values of the curve parameters ω, ϕ and ν for the dive profiles considered were as follows,

$$\mathbf{0.37 < \omega < 0.83, \quad 0.19 < \phi < 0.53 \quad and \quad 1.04 < \nu < 1.5.} \qquad (10\text{-}1)$$

10.4 Comparison of decompression schedules

Tables 10.1 to 10.3 show the decompression schedules generated by the optimisation schemes compared to the QinetiQ tables.

The schedules in the above tables show the effect on the risk of decompression illness from rounding the stop times to whole minutes is insignificant apart from dives with only a few minutes of stops such as the dive to 81 msw for 6 minutes.

The stop time and curved ascent optimisation schemes produced decompression schedules with similar total time for decompression, but different ascent profiles. The stop time scheme produced smooth schedules for the dives to 18 msw and 39 msw, but irregular stop times for the deeper dives to 60 and 81 msw which resulted in stop times greater than a couple of minutes.

The schedules produced by the curved ascent optimisation were smooth, but in some cases took a couple more minutes for the diver to surface. For one dive to 60 msw for 40 minutes the curved ascent optimisation produced a shorter schedule.

In all cases except one the optimisation schemes produced the same or shorter total time for decompression than the QinetiQ 90 table. The exception is the dive to 18 msw for 170 minutes. The QinetiQ schedule results in a risk of 2.047%, compared to the longer optimised schedules with 1.98% risk. In diving terms this difference is insignificant.

In some cases such as the dives to 39 msw for 20 and 80 minutes, the reduction in total time for decompression from using the optimised schemes may be due to the QinetiQ 90 schedule corresponding to a smaller risk of decompression illness. However, the QinetiQ and optimised schedules for a dive to 39 msw for 50 minutes have the same risk outcome, with the optimised schedules being 6 minutes shorter. A similar example is the 81 msw dive for 15 minutes where at least 22 minutes of decompression can be saved using the optimised schedule.

Maximum depth (msw)	Bottom time (min)	Stop times (min) at given depths (msw)					TTFD (min)	PROB3 % risk of DCI	Schedule Source
		18	15	12	9	6			
18	140	-	-	-	-	5	7	1.868	Q 90
		-	-	-	-	1	3	1.995	Stop time
		-	-	-	-	1	3	1.995	Curve
	170	-	-	-	-	15	17	2.047	Q 90
		-	-	-	-	17	19	1.982	Stop time
		-	-	-	1	17	20	1.962	Curve
	200	-	-	-	-	31	33	1.949	Q 90
		-	-	-	-	30	32	1.981	Stop time
		-	-	-	2	28	32	2.003	Curve
39	20	-	-	-	1	9	13	0.757	Q 90
		-	-	-	1	2	6	1.848	Stop time
		-	-	-	1	2	6	1.848	Curve
	50	-	4	5	10	52	74	1.992	Q 90
		-	2	2	2	59	68	1.988	Stop time
		-	1	3	6	56	69	1.991	Curve
	80	3	10	11	16	114	157	1.707	Q 90
		1	2	2	2	122	132	1.992	Stop time
		1	2	4	10	115	135	1.998	Curve

Table 10.1 *Decompression schedules from QinetiQ 90 (Q 90), stop time and curved ascent optimisation schemes for dives to 18 msw and 39 msw.*

Maximum depth (msw)	Bottom time (min)	Stop times (min) at given depths (msw)												TTFD (min)	PROB3 % risk of DCI	Schedule Source
		39	36	33	30	27	24	21	18	15	12	9	6			
60	9	-	-	-	-	-	-	-	-	1	1	2	7	15	1.866	Q 90
		-	-	-	-	-	-	-	-	-	-	1	1	6	1.900	Stop time
		-	-	-	-	-	-	-	-	-	-	-	2	6	1.892	Curve
	25	-	-	-	1	2	2	3	5	5	5	7	53	87	1.983	Q 90
		-	-	-	-	2	-	2	2	3	1	3	57	74	1.969	Stop time
		-	-	-	-	1	1	2	2	3	5	8	50	76	1.966	Curve
	40	-	-	1	5	5	5	5	5	10	11	18	119	188	1.661	Q 90
		-	-	1	3	-	-	-	10	17	-	9	25	169	1.928*	Stop time
		-	-	1	1	2	3	4	5	8	11	19	104	162	1.961	Curve

Table 10.2 *Decompression schedules from QinetiQ 90 (Q 90), stop time and curved ascent optimisation schemes for dives to 60 msw. (*: Optimisation did not terminate successfully, best estimate of ascent profile is given.)*

Maximum depth (msw)	Bottom time (min)	Stop times (min) at given depths (msw)															TTFD (min)	PROB3 % risk of DCI	Schedule Source
		48	45	42	39	36	33	30	27	24	21	18	15	12	9	6			
81	6	-	-	-	-	-	-	-	-	1	1	-	1	2	2	7	20	0.594	Q 90
		-	-	-	-	-	-	-	-	-	-	-	-	-	1	2	9	1.866	Stop time
		-	-	-	-	-	-	-	-	-	-	-	-	-	1	3	10	1.403	Curve
	15	-	-	-	1	2	2	2	2	3	2	3	5	5	9	52	94	1.955	Q 90
		-	-	-	-	-	-	-	2	1	5	3	2	3	2	44	68	1.984	Stop time
		-	-	-	-	-	-	1	1	1	2	3	4	5	8	41	72	1.938	Curve
	25	1	3	2	2	2	3	4	5	5	5	8	10	13	19	129	217	1.582	Q 90
		-	-	-	5	1	-	1	1	8	2	2	14	8	11	114	173	1.948*	Stop time
		-	-	-	-	-	1	2	3	4	5	8	11	17	25	105	187	1.950	Curve

Table 10.3 *Decompression schedules from QinetiQ 90 (Q 90), stop time and curved ascent optimisation schemes for dives to 81 msw. (*: Optimisation did not terminate successfully, best estimate of ascent profile is given.)*

10.5 Rounding decompression stops to complete minutes

The integer decompression stops given in Tables 10.1 to 10.3 were found by rounding down stop times with fractions of a minute less than or equal to a quarter of a minute and rounding up stop times with fractions of a minute over a quarter. Consider the 81 msw dive for 6 minutes at maximum depth as given in Table 10.3. Table 10.4 shows the estimated risk of decompression illness of the original un-rounded stop times and each of the possible rounding options.

	Stop times (min) at given depths (msw)			PROB3 % risk of DCI
	12	9	6	
Stop time	-	1.04	1.69	2.000
Curve	0.10	0.70	1.90	1.999
Rounding	-	2	2	1.420
	1	1	2	1.464
	-	1	2	1.875
	-	-	2	2.430
	-	1	1	2.420
	-	-	1	3.045

Table 10.4 *PROB3 estimated risk of decompression illness for stop times rounded to full minutes compared to optimised stop times for a dive to 81 msw for 6 minutes.*

Table 10.4 shows that the risk of decompression illness values are affected by the rounding of stop times to integer values. Choosing to round down below the quarter of a minute fraction and round up otherwise provides the closest risk value to 2%. The same result could have been obtained with a half minute cut off point, but using the quarter minute rule will help bias the risk to stay below the acceptable value.

The best rounding option could be found by comparing all the possible combinations of rounding the stop times. But each combination considered would require the calculation of risk for a dive profile and increase the computation required for a

solution with little gain to the diver in the final result compared to the simple quarter minute rule.

10.6 Consideration of optimisation schemes being applied to real time computing

If an optimisation scheme is to be incorporated into a real time system such as a dive computer the algorithm must reliably find the solution schedule in a short time frame. Figure 10.1 compares the number of iterations and function evaluations performed to locate a solution to the optimisation problem.

The stop time optimisation scheme did not converge to a solution after 100 iterations for the 60 msw dive to 40 minutes and the 81 msw dive for 25 minutes. These two dives correspond to dives with the greatest carrier loading at maximum depth out of the dives considered. These two dives are not plotted in Figure 10.1 for the stop time optimisation scheme.

The performance of the two optimisation schemes is comparable for the 18 msw dives and shortest dives to the deeper depths. However, for the remaining dives the stop time optimisation scheme requires many more function evaluations and iterations than curved ascent optimisation. The number of iterations increasing with the amount of carrier gas absorbed in the body tissues.

The number of iterations is more stable for the curved ascent optimisation and only starts to increase for the deepest longest dives considered.

The curve optimisation scheme should be used for future production of optimised decompression tables because of the fast and stable convergence to an ascent profile that will conceptually be accepted by divers.

For a dive computer to work in real time, the algorithms detailed in this thesis may not process fast enough. The LEM physiology-risk model currently takes up the greater portion of the processing requirements. If an acceptable simpler model could be developed the optimisation method would take a much shorter time.

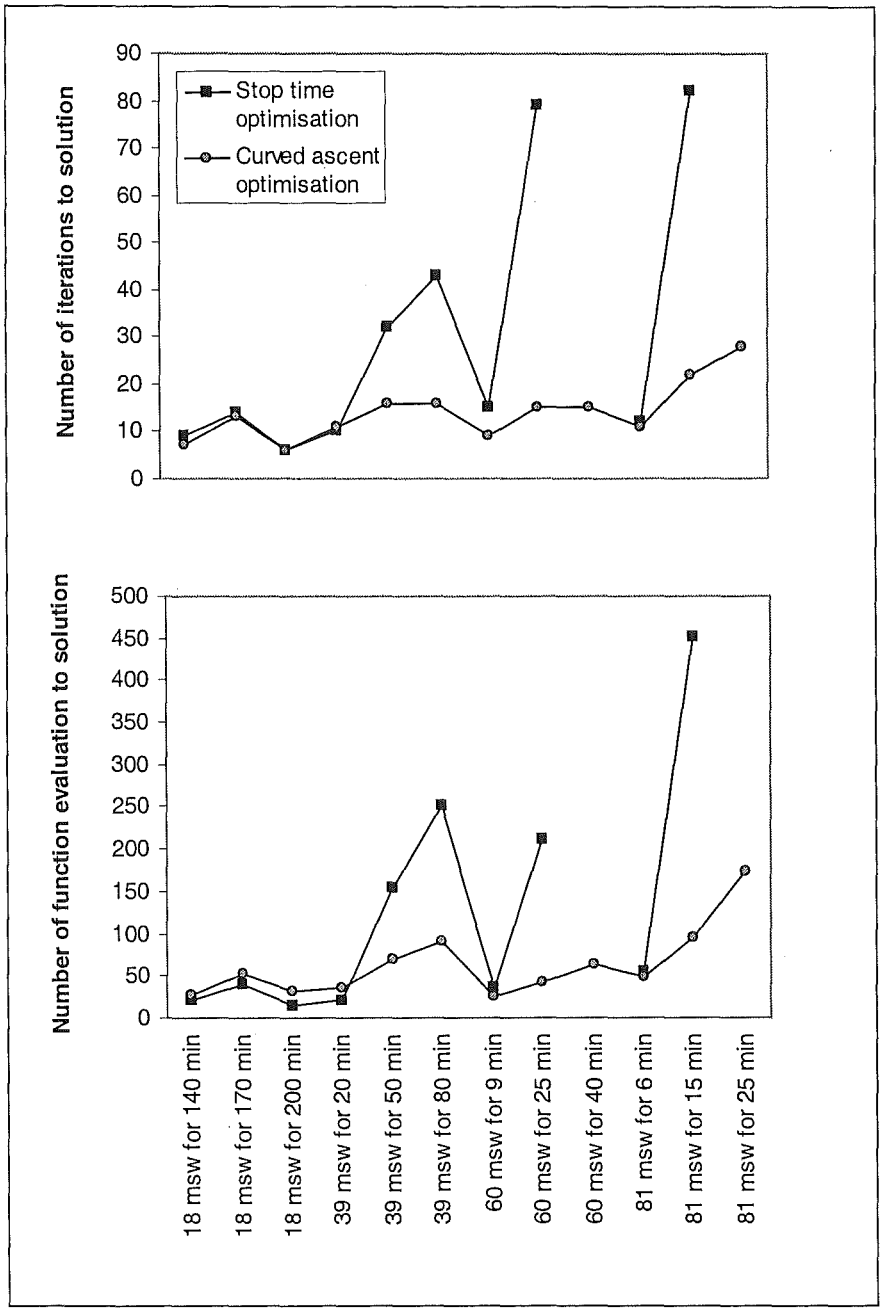

Figure 10.1 Performance of stop time and ascent curve optimisation applied to QinetiQ 90 dive profiles.

The convergence of the optimisation may be improved by choosing an initial curve close to the solution. This could be achieved by using a look up iso-probabilistic table matching depth and carrier tissue loading to the start of ascent.

Alternatively, the ascent could be calculated at regular intervals throughout the bottom time of the dive and each new optimisation could use the last known ascent curve as the initial curve.

10.7 Conclusions

The QinetiQ 90 decompression table was generated using PROB3 to ensure the schedules had a risk of decompression illness close to 2%.

The optimisation schemes described in Chapters 7 and 9 have been used to produce decompression schedules that cover the range of depths and bottom times covered by the tables; depths of 18 to 81 msw and bottom times of 6 to 200 minutes.

Comparison of decompression schedules has shown the optimised schedules provide the benefit of shorter total time for decompression than the QinetiQ tables. The biggest difference is 30 minutes for the dive to 81 msw for 25 minutes.

The curved ascent optimisation scheme can be used to produced optimised decompression tables, but further work on convergence and reducing the processing time is required to implement the optimisation in a real time system such as a dive computer.

Chapter 11

Conclusions

11.1 Research aim

This research has shown that it is feasible to produce optimised iso-probabilistic decompression schedules that are operationally practical given an acceptable physiology-risk model.

11.2 The Linear-Exponential Multi-gas decompression model

The US LEM model and parameters programmed into the PROB3 software provides an indication of the risk of decompression illness for dives. The model predicts the risk of decompression illness of grouped trials data well for dives shallower than 200 fsw. For deeper dives with bottom times of greater than 30 minutes the LEM model tends to over predict the risk of decompression illness.

A sensitivity study was conducted for the risk of decompression illness given by the LEM model for dives using a constant partial pressure of oxygen or a cyclic partial pressure characteristic of rebreather apparatus. For partial pressures of oxygen of 0.7 bar and above the constant partial pressure of oxygen assumption does not significantly affect the risk of decompression illness. The overshoot in oxygen partial pressure that occurs on descent may become significant if the LEM model parameters are altered to incorporate greater carrier oxygen levels.

The LEM model has not been tested by manned trials and should only be used as an indicator of risk until it is tested.

The LEM model was used to show there is a variation in risk of decompression illness across decompression tables and schedules within the same tables. This variation in risk is not visible to the diver using the decompression tables.

11.3 Sequential Quadratic Programming optimisation

The sequential quadratic programming method can be used to solve the constrained optimisation of decompression. The minimum of the total time for decompression (***TTFD***) is found subject to the maximum dive time (***MDT***) achievable with the breathing apparatus and risk of decompression illness (***R***) constraints;

$$\min_{\bar{x} \in \Re^n} \quad TTFD(\bar{x})$$

subject to

$$\begin{aligned} \mathrm{BT} + \mathrm{TTFD}(\bar{x}) - \mathrm{MDT} &\leq 0 \\ R(\bar{x}) - R_{acc} &\leq 0 \\ R_{acc} - \xi - R(\bar{x}) &\leq 0 \end{aligned}$$

where R_{acc} is the acceptable risk of decompression illness, ξ is acceptable risk error and $\bar{x}$ are the design parameters. There are many local solutions to this constrained minimisation problem and a small change in risk of decompression illness can result in large changes in the total time for decompression and stop times.

Two approaches to the optimisation have been taken:

1. The total time for decompression is described as the sum of the stop times plus the ascent time, with the stop times set as the design parameters. This scheme produces optimised decompression schedules. Some of the schedules for dives deeper than 40 msw have an irregular series of stop times that do not monotonically increase with decreasing depth. The dives with the largest loadings of carrier

gas at maximum depth also did not reach the termination tolerances before a maximum number of iterations of 100 was reached.

2. The ascent curve and total time for decompression can be described as a three parameter hyperbolic tangent equation. This scheme also produced optimised decompression schedules. However, the series of stop times produced by this scheme monotonically increase with decreasing depth making the schedules conceptually acceptable to divers. The number of iterations required to solve the optimisation problem is generally smaller than the stop time scheme and more stable. The ascent curve scheme is sensitive to the initial ascent curve used to start the optimisation, suggesting the use of multiple starting values.

Both of these methods required risk penalty functions to be applied to keep the parameters away from infeasible ascent profiles.

11.4 Iso-probabilistic decompression schedules

The curved ascent optimisation scheme described in Chapter 9 can be used to generate optimised iso-probabilistic decompression tables for 1.3 bar oxygen in helium rebreather dives.

In comparison to QinetiQ Table 90, the optimised schedules gave a reduction in the total time for decompression for a dive. The biggest reduction of 30 minutes occurred for the deepest, longest dive tested; a dive to 81 msw for 25 minutes.

11.5 Recommendations for moving towards real time decompression optimisation

For an optimisation method to perform in real time, the method must reliably converge to a solution and complete calculations within the bounds of the processing power of an embedded processor suitable for a dive computer. To use the curve optimisation scheme in real time further work needs to done. To improve the reliability of the method the following areas should be addressed:

- The modification of the Hessian in the MATLAB function 'nlconst' (Chapter 6, page 90) to ensure it is positive definite caused some excessive weighting of the Hessian matrix. Alternative Hessian update or modification methods should be investigated.

- The convergence criteria are not aimed at problems that have many local solutions that may not occur at the minimum of the objective function for total time for decompression. Decompression specific convergence criteria need to be developed. Such criteria may also improve the termination performance of the stop time optimisation scheme.

- The MATLAB code does not impose hard boundaries on the design parameter values. The algorithm should be altered to keep boundaries from being violated.

- The use of a lower and upper bound constraint on the risk of decompression illness may overly constrict the path of the optimisation process. The use of only an upper bound risk constraint should be investigated as a possible way to improve convergence.

- Dives which are not feasible because the maximum dive time is too short for a given dive risk, are not recognised by the algorithm. The algorithm just keeps trying to solve the optimisation problem. A diver at the maximum depth of their dive needs an ascent profile to follow. They cannot be told that it is not possible to get to the surface! The optimisation scheme would need to give the

next best ascent option within the time constraint. A warning could be given to the diver to say they have exceeded their proposed risk level.

To improve the speed at which a solution can be found the following areas should be investigated:

- With further optimisation of decompression schedules it would be possible to gain information on the range of the curve parameters for the dives and equipment being considered. Restricting the parameter space should help to reduce the number of iterations required to find a solution and produce more reliable results.

- The PROB3 calculation of the risk of decompression illness takes the most processing during optimisation. A simpler physiology-risk model that involves only analytical solutions and requires less processing would speed up the optimisation process considerably.

- The curved ascent optimisation scheme is dependent on the choice of initial curve parameters. A decrease in the number of iterations to a solution may occur of the initial ascent curve is closer to the solution curve. This could be achieved in two ways:

    1. Use a set of iso-probabilistic reference ascent curves that could be matched to the current dive by the tissue carrier loading and maximum depth.

    2. Optimise the ascent at regular intervals during the bottom time and ascent. For each solution use the previous solution as the initial ascent curve.

With some or all of the above modifications it should be possible to implement an optimised decompression algorithm for use in a dive computer.

THIS PAGE IS INTENTIONALLY BLANK

References

Anthony, T.G. and Horn, B.J. *Mine countermeasure / explosive ordinance disposal life support equipment interim decompression tables,* DERA Alverstoke, UK. Report DERA/SSES/TR961011/2.0.

Bailey, R.C. and Homer, L.D. (1977) *An analogy permitting maximum likelihood estimation by a simple modification of general least squares algorithms.* Naval Medical Research Institute, Maryland, US. Report 77-55.

Ball, R. et al (1995) Does the time course of bubble evolution explain decompression sickness risk. *Undersea hyperbaric med.* **22** (3), 263-280.

Bennet, P.B. and Elliott, D.H. (1995) *The physiology and medicine of diving.* Fourth Edition, W.B. Saunders Company, London, ISBN 0-70201589-X.

Berghage, T.E., Woolley, J.M. and Keating, L.J. (1974) The probabilistic nature of decompression sickness. *Undersea Biomed. Res.* **1**(2), 189-196.

Bert, P. (1878) *Barometric Pressure : Researches in Experimental Physiology.* Translated by M.A. Hitchcock & F.A. Hitchcock, Undersea Medical Society.

Broyden, C.G. (1970) The convergence of a class of double rank minimisation algorithms, *J. Inst. Math. Applic.* **6**, 76-90.

Bühlmann, A.A. (1995) *Tauch Medizin*, Fourth Edition, Springer Verlag, Berlin.

Burkard, M.E. and Van Liew, H.D. (1995) Effects of physical properties of breathing gas on decompression sickness bubbles. *J. Appl. Physiol.* **79** (5), 1828-1836.

Bushell, N. and Gurr, K. (1997) Pro-dive decompression Software – Rebreather edition. Version 7.

Curtis, H. and Barnes, N.S. (1989) *Biology,* Fifth Edition, Worth Pub. ISBN 0-87901394-X.

Donald, K.W. (1955) Oxygen bends. *J. Appl. Physiol.* **7**, 639-644.

DRA Alverstoke - Notes from DRA Alverstoke Trimix Trials.

Eatock, B.C. and Nishi, R.Y. (1986) *Procedures for doppler ultrasonic monitoring of divers for intravascular bubbles.* Defence and Civil Institute of Environmental Medicine, Ontario, Canada. Report 86-C-25.

Elliott, D.H. and Moon, R.E. (1995a) 'Manifestations of the decompression disorders.' In: *The physiology and medicine of diving.* Fourth Edition, Eds: P.B. Bennet and D.H. Elliott, W.B. Saunders Company, London, ISBN 0-70201589-X, pp 481-505.

Elliott, D.H. and Moon, R.E. (1995b) 'Long term health effects of diving' In: *The physiology and medicine of diving.* Fourth Edition, Eds: P.B. Bennet and D.H. Elliott, W.B. Saunders Company, London, ISBN 0-70201589-X, pp 585-604.

Evans, M.A. and Anthony, T.G. (2003) *QinetiQ decompression tables 90, 91, 92 and 93.* QinetiQ Alverstoke, UK, Report QINETIQ/KI/CHS/CR030606/1.0.

Fletcher, R. (1970) A new approach to variable metric algorithms. *Comp. Journal* **13**, 317-322.

Fletcher, R. (1987) *Practical methods of optimisation.* 2nd Edition, John Wiley & Sons, ISBN: 0471494631.

Flook, V. (1997) The effect of exercise on decompression bubbles: A theoretical study. *Diving and Hyperbaric Med. Proc. 23rd EUBS Congress (Bled, Slovenia), pp55-61.*

Flynn, E.T. and Parker, E.C. (1998) *A proposed emergency decompression procedure for constant 1.3 ATA oxygen in helium diving.* Naval Medical Research Institute, Maryland, Report (last known to be in preparation).

Folkow, B. and Neil, E. (1971) *Circulation.* New York: Oxford University Press.

Foster, P.P. et al (1998) Role of metabolic gases in bubble formation during hypobaric exposures. *J. Appl. Physiol.* **84** (3), 1088-1095.

Foster,P.P. et al (2000) Predicting time to decompression illness during exercise at altitude based on the formation and growth of bubbles. *Am. J. Physiol.: Regulatory Integrative Comp. Physiol.* **297**, R2317-R2328.

Francis, T.J.R. and Gorman, D.F. (1995) 'Pathogenesis of decompression disorders.' In: *The physiology and medicine of diving.* Fourth Edition, Eds: P.B. Bennet and D.H. Elliott, W.B. Saunders Company, London, ISBN 0-70201589-X, pp 454-480.

Gault, K.A. (1992) *Prediction of bubble formation in divers using the method of maximum likelihood.* Physics Dept. University of Waterloo, Canada, Technical Report.

Gay, L.A. et al (1997) *Mine countermeasure / explosive ordinance disposal life support equipment for RN use: manned production proving trial.* DERA Alverstoke, UK, Report DERA/SSES/CR971024/1.0.

Gill, P.E., Murray, W. and Wright, M.H. (1991) *Numerical linear algebra and optimisation,* Vol. 1, Addison Wesley.

Goldfarb, D. (1970) A family of variable metric updates derived by variational means. *Math. Comput.* **24**, 23-26.

Hempleman, H.V. (1995) 'History of decompression procedures.' In: *The physiology and medicine of diving.* Fourth Edition, Eds: P.B. Bennet and D.H. Elliott, W.B. Saunders Company, London, ISBN 0-70201589-X, pp 342-375.

Hennessy, T.R. (1974a) *No-stop dives on mixed gases.* Royal Naval Physiological Laboratory, Alverstoke, UK, Report 7/74.

Hennessy, T.R. (1974b) The interaction of diffusion and perfusion in homogeneous tissue. Bul. Math. Biol. **36**, 505-526.

Horn, B.J. (1999a) *Oxygen, nitrogen and helium probabilistic decompression software PROB3.* Dept. of Math. & Stat. University of Canterbury, NZ.

Horn, B.J. (1999b) *How many dives? An ideal world solution for a single dive profile.* Tech. Memo to T.G. Anthony, DERA Alverstoke, UK. August 1999.

Horn, B.J. (1998) *Doppler monitoring of divers during the MCM EOD LSE production proving trial.* Defence Evaluation and Research Agency, Alverstoke, UK, Report DERA/CHS/PPD/TR980110/1.0.

Hosmer, D.W. and Lemeshow, S. (1989) *Applied logistic regression.* John Wiley & Sons, ISBN 0-47161553-6.

Kleinbaum, D. (1996) *Survival Analysis: A self learning text.* Springer, New York. ISBN 0-38794543-1.

Leffler, C.T. (2001) Effect of ambient temperature on the risk of decompression sickness in surface decompression divers. *Aviat. Space. Environ. Med.* **72** (5), 477-483.

McCallum, R.I. and Harrison, J.A.B. (1995) 'Dysbaric Osteonecrosis.' In: *The physiology and medicine of diving.* Fourth Edition, Eds: P.B. Bennet and D.H. Elliott, W.B. Saunders Company, London, ISBN 0-70201589-X, pp 563-584.

Marquardt, D.W. (1963) An algorithm for least squares estimation of non-linear parameters. *J. Soc. Ind. Appl. Math.* **11**, 431-441.

MATLAB (2001) Software, Version 6.1.0.1989a, Release 12, Oct 2001, The Mathworks Inc, including the Optimisation Toolbox Version 2.1.

NMRI (1995) Correspondence from U.S. Naval Medical Research Institute, ABCA-10EP meeting, Palm Beach, 21 June 1995.

NMRI (1996) Correspondence from U.S. Naval Medical Research Institute, ABCA-10EP meeting, 26 January 1996.

Nishi, R.Y. and Lauckner, G.R. (1984) *Development of the DCIEM 1983 decompression model for compressed air diving.* Defence and Civil Institute of Environmental Medicine, Ontario, Canada. Report 84-R-44.

Nishi, R.Y. (1987) *DCIEM HeO_2 Decompression Model, Version 1 development.* Defence and Civil Institute of Environmental Medicine, Ontario, Canada. Report B10-87-11.

Nishi, R.Y. and Warlow, M. (1997) *Development of CUMA HeO_2 decompression tables.* Defence and Civil Institute of Environmental Medicine, Ontario, Canada. Report 97-R-68.

Parker, E.C. et al. (1992) *Statistically based decompression tables VIII: Linear Exponential Kinetics.* Naval Medical Research Institute, Bethesda, US. Report 92-73.

Parker, E.C., Survanshi, S.S. and Thalmann, E.D. (1994) Developing the new US Navy tables. *Aqua Corps* **8**, 54-60.

Parker, E.C. et al (1998) Probabilistic models of the role of oxygen in human decompression sickness. *J. Appl. Physiol.* **84** (3), 1096-1102.

Schreiner, H.R. and Kelly, P.L. (1971) A pragmatic view of decompression. *Underwater Physiol.* Ed: C.J. Lambertson. Philadelphia: Academic Press.

Shanno, D.F. (1970) Conditioning of Quasi Newton Method for function minimisation. *Math. Comput.* **24**, 647-656.

Stubbs, R.A. and Kidd, D.J. (1965) *A pneumatic analogue decompression computer.* Defence and Civil Institute of Environmental Medicine, Ontario, Canada. Report 65-RD-1.

Survanshi, S.S., Thalmann, E.D. and Weathersby, P.K. (1994) *Controlled risk decompression meter.* US Patent: US5363298, 8 Nov 1994.

Survanshi, S.S. et al (1998) *Human decompression trial with 1.3 ATA oxygen in helium.* Naval Medical Research Institute, Maryland, US. Report 98-09.

Suunto (1994) Suunto Solution-α dive computer instruction manual.

Thalmann, E.D. (1985) *Development of a decompression algorithm for constant 0.7 ATA oxygen partial pressure in helium diving.* Navy Experimental Diving Unit Report 1-85, US.

Thalmann, E.D. et al. (1997) Improved propabilistic decompression model risk predictions using linear-exponential kinetics. *Undersea Hyperbaric Med.* **24** (4), 255-274.

Tikuisis, P., Nishi, R.Y. and Giry, P. (1985) *Modelling the uptake of inert gas in anesthetized rabbits under hyperbaric conditions.* Defence and Civil Institute of Environmental Medicine, Ontario, Canada. Report 85-R-50.

Tikuisis, P., Weathersby, P. and Nishi, R.Y. (1991) Maximum likelihood analysis of air and HeO_2 dives. *Aviat. Space. Environ. Med.* **62**, 425-431.

US Navy (1996a) *US Navy Diving Manual Volume 1: Air Diving.* Best Publishing Comp. ISBN 0-94133218-7.

US Navy (1996b) *US Navy Diving Manual Volume 2: Mixed Gas Diving.* Best Publishing Comp. ISBN 0-94133222-5.

Van Liew, H.D. and Burkard, M.E. (1993) Density of decompression bubbles and competition for gas among bubbles in tissue and blood. *J. Appl. Physiol.* **75** (5), 2293-2301.

Weathersby, P.K., Homer, L.D. and Flynn, E.T. (1984) On the likelihood of decompression sickness. *J. Appl. Physiol (Environ. Exercise Physiol.)* **57** (3), 815-825.

Weathersby, P.K. et al. (1985) *Statistically based decompression tables II – equal risk air diving decompression schedules.* Naval Medical Research Institute, Bethesda, US, Report 85-17.

Wienke, B.R. (1989) Equivalent multi-tissue and thermodynamic decompression algorithms. *Int. J. Biomed. Comput.* **24**, 227-245.

Workman, R.D. (1965) *Calculations of decompression tables for nitrogen-oxygen and helium-oxygen dives.* Navy Experimental Diving Unit, Washington, US. Report 6-65.

THIS PAGE IS INTENTIONALLY BLANK